The Institute of Paper Chemistry

Appleton, Wisconsin

Doctor's Dissertation

Nucleophilicity of Hydroxide, Hydrosulfide, and Anthrahydroquinone Ions Toward Saturated and Unsaturated Carbon Centers at High Temperatures

Gregg Arthur Reed

June, 1988

NUCLEOPHILICITY OF HYDROXIDE, HYDROSULFIDE, AND ANTHRAHYDROQUINONE IONS TOWARD SATURATED AND UNSATURATED CARBON CENTERS AT HIGH TEMPERATURES

A thesis submitted by

Gregg Arthur Reed

B.S. 1982, University of Wisconsin-Green Bay
M.S. 1984, Lawrence University

in partial fulfillment of the requirements
of The Institute of Paper Chemistry
for the degree of Doctor of Philosophy
from Lawrence University,
Appleton, Wisconsin

Publication rights reserved by
The Institute of Paper Chemistry

June, 1988

TABLE OF CONTENTS

SUMMARY

Chemical pulping processes use various reagents to selectively remove lignin from wood and minimize carbohydrate degradation. Removal of lignin enables wood fibers to be separated and formed into a suitable paper sheet.

Key reactions to lignin removal are: (1) nucleophilic addition to extended carbonyl carbon (or unsaturated carbon) centers in quinonemethide intermediates, and (2) nucleophilic displacement at saturated carbon centers of β-aryl ethers through a neighboring group mechanism. Two model compounds were chosen to study nucleophilicities of pulping ions toward unsaturated and saturated sites at high temperatures in water.

Reactions at unsaturated carbon centers were modeled using *cis*-cinnamic acid. Nucleophilic addition under alkaline conditions at 195°C was followed by monitoring the isomerization rate to *trans*-cinnamic acid. Addition products of *cis*-cinnamic acid were synthesized and found to rapidly convert to *trans*-cinnamic acid upon heating in alkali. Anthrahydroquinone ion was two times more reactive than hydroxide ion, while hydroxide and hydrosulfide ions were similar in nucleophilic strength.

Since hydroxide ion is known to be a strong base at 170°C, abstraction of an olefinic hydrogen atom could possibly result in isomerization. Therefore, the reactions of α,β-dideutero-*cis*-cinnamic acid were investigated. The rate of isomerization for the deuterated compound was 1.07 times slower than that of the nondeuterated compound, indicating proton abstraction is not the rate-determining step. Initial production of α,β-dideutero-*trans*-cinnamic acid was also observed. The α-deuterium of α,β-dideutero-*cis*-cinnamic acid,

however, was rapidly exchanged for an α-hydrogen atom in alkali at 195°C without loss of the *cis*-geometry. It was concluded that isomerization resulted from addition-elimination rather than proton abstraction.

Reactions at saturated carbon centers were modeled using 3-[3′-(α,α,α-trifluoromethyl)phenoxymethyl]benzoic acid. Under alkaline conditions at 195°C, nucleophilic displacement of the phenolic group attached at the benzyl carbon resulted in formation of various primary products which were independently synthesized and heated in alkali to determine their stability. Hydrosulfide ion was 20 times more reactive than hydroxide ion, while anthrahydroquinone ion was 17 times more reactive.

Extension of these results to pulping systems suggests that anthrahydroquinone ion would be very effective in additions to quinonemethides, while sulfur species would be very effective in displacement of β-aryl ethers.

INTRODUCTION

The kraft pulping process is the dominant method of pulp production, accounting for over 75% of the pulp produced in the United States.[1] Kraft pulping replaced soda pulping as the dominant process earlier this century. Both of these processes are alkaline pulping methods, using hydroxide ions. The kraft process also employs reactive hydrosulfide ions. Advantages of the kraft process over the soda process include greater pulping rate, higher pulp yield and quality, and lower production cost.[2]

The advantages of kraft pulping were apparent earlier this century. The chemistry responsible for the enhanced reactivity of the kraft process, however, was not investigated until recently. Theories for alkaline degradation of carbohydrates[3,4] and lignin[5,6] were proposed using soluble model compounds to simulate reactions of these insoluble components of wood. These model compound studies appeared to give a good understanding of overall mechanisms.

In the past 10 years, a new additive, anthraquinone, was introduced to enhance pulping processes.[7] Use of anthraquinone and related compounds improved pulp yield and quality, and reduced chemical and energy consumption. Lower capital costs were projected, and the release of malodorous sulfur-containing compounds was diminished. Investigations were then launched to understand the chemistry by which anthraquinone enhanced pulping reactions. The potential for finding new additives renewed interests into understanding the chemistry behind pulping reactions.

Detailed knowledge of alkaline delignification reactions is needed to enhance lignin removal and to propose improved processes. A number of

chemical factors may be critical to the effectiveness of hydrosulfide and anthraquinone ions during delignification. Greater knowledge of these factors will expand the theory underlying pulping reactions. One such critical factor is knowing the nucleophilicities of pulping reagents. In the following section, nucleophilicity will first be defined, and various effects which alter nucleophilic order will be described. Our current understanding of alkaline delignification will then be discussed.

NUCLEOPHILICITY

Reactions of nucleophilic agents serving as pulping reagents is an important consideration which led to formulation of the conventional mechanism of kraft delignification. A closer examination of nucleophilicity is necessary to better understand delignification reactions.

A nucleophile is defined as a species having a free electron pair which is able to form a new bond to a substrate having an electron-deficient site. A leaving group is usually involved in the reaction and is defined as a portion of the substrate that is cleaved during reaction. The leaving group removes an electron pair to maintain no net charge change. Nucleophilicity is the rate of reaction of one nucleophile relative to another during substitution reactions under similar conditions. Nucleophilic order is dependent on the nature of the attacked substrate, the leaving group, the solvent, and the reaction temperature.[8]

Four principles are believed to govern the reaction rate:[8]

1. A nucleophile with a negative charge will be more nucleophilic than its conjugate acid.

2. Nucleophilicity is related to basicity when comparing elements of the same row in the periodic table.

3. Nucleophilicity increases when moving down the same column in the periodic table. This is true even though basicity decreases.

4. The less associated the nucleophile, the more reactive the nucleophile. The nucleophile may be associated with the solvent or be part of an aggregation which can either capture or free the nucleophile.

Solution Phase Studies

Swain and Scott have developed the following linear free-energy relationship to quantitatively correlate relative reaction rates:[9]

$$\log (k/k_0) = sn + s'e \qquad (1)$$

where k = measured rate constant of reaction between the substrate and the nucleophile

k_0 = measured rate constant of reaction between the substrate and water

s = substrate constant which measures the discrimination of the substrate to react with the nucleophile

s' = substrate constant which measures the discrimination of the substrate to react with the electrophile (electron-seeking species)

n = nucleophilic constant which measures the reactivity of the nucleophile

e = electrophilic constant which measures the reactivity of the electrophile

In aqueous solutions, water is defined as the electrophilic species so that e = 0; thus, Eq. (1) becomes:

$$\log (k/k_0) = sn \qquad (2)$$

Using methyl bromide as the standard substrate (s = 1.00, in pure water at 25°C), Swain and Scott developed a set of nucleophilic constants.[9] These values are shown in a set expanded by Wells[10] in Table 1.

Table 1. Nucleophilic constants[9,10]

Nucleophile	n	Nucleophile	n
$HPSO_3^{2-}$	6.6	C_5H_5N	3.6
$S_2O_3^{2-}$	6.36	Br^-	3.53
CN^-	5.1	$C_6H_5O^-$	3.5
SO_3^{2-}	5.1	HCO_2^-	2.75
HS^-	5.1	$CH_3CO_2^-$	2.72
I^-	5.04	Cl^-	2.70
$C_6H_5NH_2$	4.49	SO_4^{2-}	2.5
SCN^-	4.41	$HOCH_2CO_2^-$	2.5
HO^-	4.20	$ClCH_2CO_2^-$	2.2
$(NH_2)_2CS$	4.1	$2,4,6\text{-}(NO_2)_3C_6H_2O^-$	1.9
N_3^-	4.00	NO_3^-	1.03
$H_2PO_4^-$	3.8	H_2O	0.00
HCO_3^-	3.8		

Good agreement in nucleophilic constants is observed when the substrate is varied except in the case of hydroxide ion, which reacted abnormally fast with carbonyl carbons. Swain and Scott hypothesized that the increased reactivity was due to the "nakedness" of the negative charge on the hydroxide ion.[9] While other nucleophiles can distribute the negative charge within its molecule, hydroxide ion must react with another substrate, such as the partially positive carbon atom of a carbonyl group, in order to distribute

the negative charge. This stabilization of the negative charge in the transition state results in hydroxide ion having an abnormally high reactivity relative to other anions.

Edwards and Pearson discussed the effects of basicity, polarizability, and alpha effect on the reactivity of nucleophiles.[11] The reactivities of some substrates depend almost entirely on the basicity of the nucleophile, while the reactivities of other substrates depend on the polarizability of the nucleophile.

The following reaction rate order was observed for reactions at a saturated carbon center: $C_4H_9S^- > C_6H_5S^- > S_2O_3^{2-} > SC(NH_2)_2 > I^- > NC^- > NCS^- > HO^- > N_3^- > Br^- > C_6H_5O^- > Cl^- > C_5H_5N > CH_3COO^- > H_2O$.[11] The polarizability of the nucleophile paralleled its reactivity. For example, malonate ion reacted several times faster than the ethoxide ion even though ethoxide is 500 times more basic.

The following reaction rate order was observed for reactions at a carbonyl carbon atom: $HOO^- > ClO^- > HO^- > C_6H_5O^- > NC^- > CO_3^{2-} > C_5H_5N > F^- \approx S_2O_3^{2-} > CH_3COO^- > H_2O$.[11] Here, the basicity of the nucleophile paralleled its reactivity.

Nucleophiles which contain an electronegative atom having one or more pairs of unbonded electrons adjacent to the nucleophilic atom react more rapidly with substrates than expected; this is called the alpha effect.[11] Notable reagents of this class are hydrogen peroxide and anions of peroxides.

In general, substrates having a high positive charge and a low number of electrons in the outer orbitals of the central atom respond more to the basicity of nucleophile. Substrates having a low positive charge and

many electrons in the outer orbitals of the central atom respond more to polarizability. All substrates are influenced by the alpha effect.

Pearson classified acids and bases using a system of "hard" (high electronegativity and low polarizability) and "soft" (high polarizability and low electronegativity) (HSAB principle).[12] A classification scheme is shown in Table 2. In general, hard acids prefer to bond with hard bases, while soft acids prefer to bond with soft bases. It is possible, however, for a soft base, sulfide ion, to bind strongly to hydrogen ion, a hard acid.

Table 2. Hard and soft acids and bases.[8,12]

	Hard	Borderline	Soft
Bases	H_2O HO^- F^- AcO^- SO_4^{2-} Cl^- CO_3^{2-} NO_3^- ROH RO^- R_2O NH_3 RNH_2	$ArNH_2$ C_5H_5N N_3^- Br^- NO_2^-	R_2S RSH RS^- HS^- I^- R_3P $(RO)_3P$ CN^- RCN CO C_2H_4 C_6H_6 H^- R^-
Acids	H^+ Li^+ Na^+ K^+ Mg^{2+} Ca^{2+} Al^{3+} Cr^{2+} Fe^{3+} BF_3 $B(OR)_3$ $AlMe_3$ $AlCl_3$ AlH_3 SO_3 RCO^+ CO_2 HX (H-bonded molecules)	Fe^{2+} Co^{2+} Cu^{2+} Zn^{2+} Sn^{2+} Sb^{3+} Bi^{3+} BMe_3 SO_2 R_3C^+ NO^+ GaH_3 $C_6H_5^+$,	Cu^+ Ag^+ Pd^{2+} Pt^{2+} Hg^{2+} BH_3 $GaCl_3$ I_2 Br_2 CH_2 carbenes

Reactivities associated with the HSAB principle were attributed to (1) ionic-covalent σ-bonding effects, (2) π-bonding effects, (3) electron correlation effects, and (4) solvation effects.[12] Hard acids bind to bases with primarily ionic forces, while soft acids bind to bases with primarily covalent forces. Soft acids and bases are able to develop additional attractions through π-bonds. London or van der Waals dispersion forces enhance reactivity if both groups are polarizable. Solvation will generally lessen the reactivity of hard acids and bases and enhance the reactivity of soft

substances. Hard solvents dissolve hard solutes well, and soft solvents dissolve soft solutes well.[12] The solubility of the acid or base will also affect its reactivity.

Klopman described chemical reactivity using a quantum mechanical method.[13] In this study, nucleophilicity was related to the HSAB principle. He calculated the following nucleophilic orders under their respective conditions; these orders agreed with experimental results:

1. Toward a peroxide oxygen atom (a very soft electrophile),

   $HS^- > I^- > NC^- > Br^- > Cl^- > HO^- > F^-$

2. Toward a saturated carbon atom (a moderately soft electrophile),

   $HS^- > NC^- > I^- > HO^- > Br^- > Cl^- > F^-$

3. Toward a carbonyl carbon atom (a hard electrophile),

   $HO^- > NC^- > HS^- > F^- > Cl^- > Br^- > I^-$

Hard-hard interactions are charge-controlled and depend mainly on the ionic interaction of the species.[13] Charge-controlled reactions tend to occur between highly charged species. These species are strongly solvated and small in size.

Soft-soft interactions, on the other hand, tend to be frontier-controlled reactions.[13] Strong electron transfer occurs between nucleophiles of low electronegativity and electrophiles of high electronegativity. These species are easily polarized and have low solvation energies.

Solvents having different dielectric constants also cause variations in nucleophilic order. Solvents having high dielectric constants enhance

reactions between species with high polarizability and low solvation energies.[13]

A number of properties have been postulated as affecting nucleophilicity, such as polarizability, orbital energies, hardness and softness, and solvation energies. These properties, however, do not fully describe the reactivity of species.[14] The concept of hardness/softness was criticized since there is no precise definition of hardness/softness, and this property cannot be analyzed quantitatively. Determinations of polarizability and orbital energies are not possible in the solution phase. In general, solvation energies for species of interest are not available.

One possible source of information which can be determined and related to nucleophilicity is the standard electrode potential of the species. Ritchie found there was a linear relationship between log $\underline{k}$ and the one-electron oxidation potential for a series of second row nucleophiles for the reaction with the Pyronin cation.[14] Pearson, however, found there was no correlation between reactivity and one-electron oxidation potential for nucleophilic reactions with methyl iodide.[15]

Nucleophilic reactions have been studied in both protic and dipolar aprotic solvents. Protic solvents, such as water, methanol and ammonia, are strong hydrogen-bond donors. Dipolar aprotic solvents, such as dimethyl sulfoxide and dimethylformamide, have polarities similar to protic solvents, but are very weak hydrogen-bond donors.

Reactions typically proceed much faster in dipolar aprotic solvents than in polar solvents. The reactant anion is much more solvated by protic solvents than by dipolar aprotic solvents. Hydrogen bonding effects, disper-

sion forces, ion-dipole and dipole-dipole interactions, and solvent structure contribute to the solvation of the reactant anion, the substrate, and the transition state.[16] Solvation of the nucleophile, however, is the most important factor.

Nucleophilic orders were altered when the type of solvent system was changed.[16] In protic solvents, an order toward methyl iodide of $I^- > NCS^- \approx NC^- > N_3^- \approx Br^- > Cl^- > AcO^-$ is observed. In aprotic solvents, the order becomes $NC^- > AcO^- > Cl^- \approx Br^- \approx N_3^- > I^- > NCS^-$.

Small anions tend to be strong hydrogen-bond acceptors and, thus, are more solvated in protic solvents than large anions. The reaction rate of small anions will be much greater in dipolar aprotic solvents than in protic solvents. If the negative charge is dispersed by electron-withdrawing groups or if the charge is present on a large anion, the species tends to be a weak hydrogen-bond acceptor and is not significantly more solvated by protic solvents than by dipolar aprotic solvents. The reaction rate of these species, thus, will not be greatly affected when the solvent system is changed.

The structure of the solvent is also important. Large anions fit poorly into highly structured small molecule solvents. Such solvents strongly solvate small anions which can be more easily incorporated into the solvent matrix.

Nucleophilic order, up to this point in the discussion, has been investigated near room temperature. The character of the solvent and the relative degree of solvation of various ions may be different at elevated temperatures. The following studies by Gilbert, Blythe, and Smith address the effects of temperature on nucleophilicity and basicity.

Gilbert and Blythe investigated the reaction rates of methyl α-*D*-glucopyranoside with various nucleophiles at 170°C. Gilbert reported hydroxide ion cleaved the oxygen-aglycone bond about three times faster than iodide ion.[17] Blythe found hydrosulfide ion was found to be eleven times stronger as a nucleophile than hydroxide ion in cleavage of the oxygen-aglycone bond.[18] Hydrosulfide ion, however, was only 1.6 times as strong as hydroxide ion in cleavage of the glycosyl-oxygen bond.[18]

At room temperature, Swain and Scott reported both iodide and hydrosulfide ions were about seven times stronger as a nucleophile than hydroxide ion.[9] The reactivity of iodide ion decreased relative to hydroxide and hydrosulfide ions. This must be due to a decreased solvent cage surrounding the hydroxide and hydrosulfide ions; the nucleophilicity of hydroxide ion increased with increasing temperature because it became less solvated at high temperatures.

Smith studied the high temperature reactions of HO^- with various organic acids and phenols.[19] Hydroxide ion was found to be about 18 orders of magnitude stronger as a base at 170° than at room temperature. Trianions and possibly tetraanions of the tested substrates were generated. The reactions of sodium sulfide at 170° was also studied. Sulfide ion was completely dissociated to hydroxide and hydrosulfide ions in water, but the latter does not contribute to the basicity of the solution.

Gas Phase Studies

Studies of nucleophilic reactions in the gas phase have made it possible to investigate reactions without the influence of the solvent. Nucleophilicity and leaving group ability are not intrinsic properties;

nucleophilicity is dependent on the substrate, while leaving group ability is dependent on the nucleophile.[20] Nucleophilicity has no meaning unless given in the context of a specific reaction. The character of the solvent at pulping temperatures is largely unknown. At the elevated temperatures, pulping ions may be less solvated such that changes in nucleophilic order may occur. Gas phase reactions, therefore, were reviewed in order to better understand relationships between solution phase, especially high temperature, nucleophilicity and gas phase nucleophilicity.

Gas phase nucleophilic substitution reactions were investigated by Bohme, *et al.*[21] and by Brauman, *et al.*[22] Both found the following nucleophilic order toward methyl bromide, a saturated carbon center: $HO^- > F^- \approx CH_3O^- > CH_3S^- >> Cl^- > NC^- > Br^-$. Nucleophilic order is affected by the methyl cation affinity for the nucleophile (similar to a measure of bulk phase basicity) and by charge concentration (the more localized the charge, the better the nucleophile).[22] Polarizability is important in the solution phase, but not in the gas phase.

Nucleophilic orders are reversed when reactions done in a protic solvent (such as water) are compared to reactions done in an aprotic solvent or in the gas phase.[22] Leaving group order is similar in all three cases ($I^- > Br^- > Cl^- > F^-$). Most importantly, rates are much slower in a protic solvent due to solvation of the nucleophile.

Displacement reactions at carbonyl carbons display the following nucleophilic order in the gas phase: $CH_3O^- \geq F^- > NC^- \approx HS^- > Cl^-$.[23] A similar order was found for the same reactions studied in a protic solvent. The observed nucleophilic order parallels the basicities of the anions. The transition state for carbonyl additions has ionic character similar to that of

the attacking nucleophile. Thus, the effect of solvent change on relative reactivity is minimal.[23]

In contrast, nucleophilic substitution reactions at saturated carbons display a great difference in order when the medium is changed from a protic solvent to an aprotic solvent or gas phase.[23] The saturated carbon center under attack is only weakly polar and thus, the strength of attachment between the carbon and the nucleophile is weaker than the nucleophile-solvent bond strength. This results in a large desolvation energy which is responsible for a major part of the activation energy.

Techniques which imitate solvation effects in the bulk phase have been developed to measure nucleophilicities of solvated ions in the gas phase.[24] Hydration of hydroxide ion with up to three water molecules causes a drop in reactivity with methyl bromide of 4 orders of magnitude. There is a further difference of 12 orders of magnitude between the hydrated (three water molecules) gas phase and solution phase cases. The energy barrier resulting from the differential solvation of the reactants and the transition state accounts for low reactivity in solution phase reactions. This effect is observed as soon as two water molecules are added to a hydroxide ion.

In summary, nucleophilic order depends on the type of substrate under attack, the type of solvent used in the reaction, the leaving group, and the reaction temperature. Nucleophilicity is not an intrinsic property, and any reaction order must be given with respect to the reaction conditions so that the results of the investigation can be interpreted. The challenge is to relate this property to our current understanding of pulping.

MECHANISMS OF ALKALINE DELIGNIFICATION

Lignin is a complex, cross-linked, amphorous polymer. The basic structural unit of the lignin polymer is the phenylpropane unit. These units are principally linked together by carbon-oxygen bonds. Prominent linkages are illustrated in Fig. 1. Their proportions in spruce and birch lignins are shown in Table 3.[25] The most important bond is the *β-O*-4 ether bond (type A in Fig. 1) which constitutes about 50% of the linkages between monomeric units in native lignin. In order to successfully remove lignin during chemical pulping, this bond must be broken to produce soluble lignin fragments.

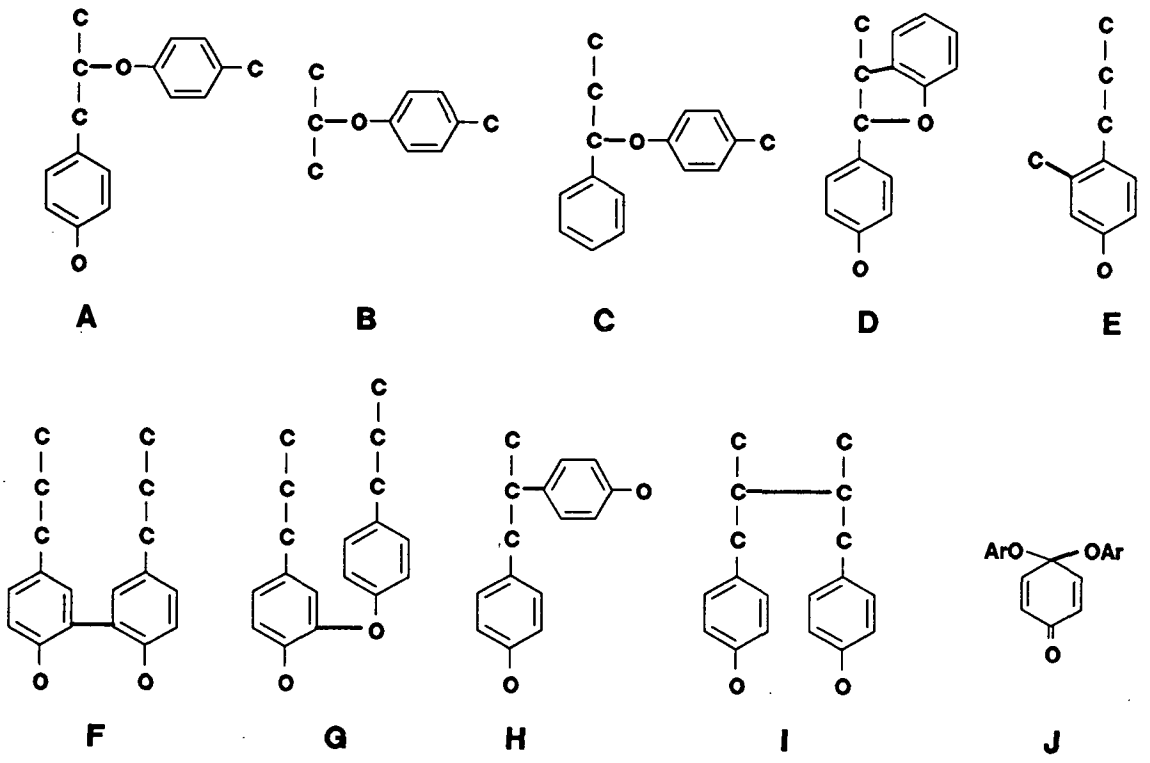

Figure 1. Types of bonds which link phenylpropane units in lignin.[25]

Table 3. Frequency of bonds between phenylpropane units.[25]

Bond type	Proportions (%) Spruce	Birch
Arylglycerol-β-aryl ether (A)	48	60
Glyceraldehyde-2-aryl ether (B)	2	2
Noncyclic benzyl aryl ether (C)	6-8	6-8
Phenylcoumaran (D)	9-12	6
Condensation at 2- or 6-positions (E)	2.5-3	1.5-2.5
Biphenyl (F)	9.5-11	4.5
Diphenyl ether (G)	3.5-4	6.5
1,2-Diarylpropane-1,3-diol (H)	7	7
β–β Linked structures (I)	2	3
Quinone ketal (J)	trace	

Delignification during pulping is generally thought to occur through nucleophilic addition and displacement reactions.[6] Many of these reactions occur through highly reactive quinonemethide intermediates (Fig. 2). A free phenolic hydroxyl group is necessary to form a quinonemethide. Following ionization of the phenolic hydroxyl, cleavage of the α-substituent occurs through formation of the quinonemethide. This reaction has been proposed to be the rate-determining step in during the initial phase of delignification.[26,27] Quinonemethides have centers of low electron density and are subject to nucleophilic attack. The addition products (adducts) may cause subsequent degradation of the lignin polymer. Attack is preferentially at the α-carbon which restores the aromaticity of the phenyl ring.

Quinonemethides undergo several types of competing reactions, including enolization, reverse aldol reactions, and nucleophilic addition, shown in Fig. 3 as pathways A, B, and C, respectively.[6] The β-hydrogen atom can be abstracted by hydroxide ion which results in formation of a stable vinyl ether structure (pathway A). Abstraction of the hydrogen atom from a γ-hydroxyl group, followed by reverse aldol condensation and elimination of formaldehyde also results in formation of a vinyl ether structure (pathway B).

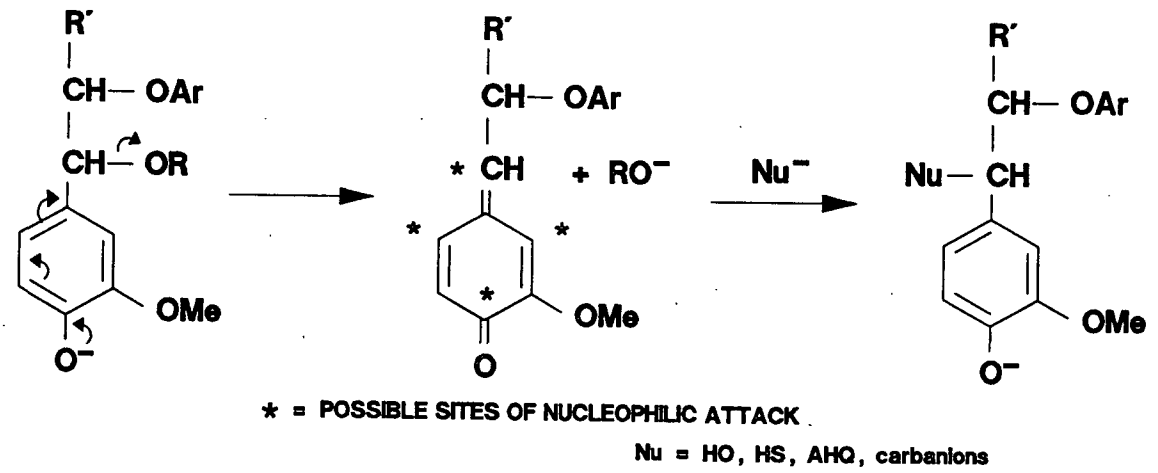

Figure 2. Nucleophilic attack of quinonemethide intermediates under alkaline conditions.[6]

Nucleophilic attack at the α-carbon atom gives rise to an adduct (pathway C). The driving force behind nucleophilic addition and competing reactions is aromatization of the quinonemethide. The balance between nucleophilic attack and competing reactions is dependent on the basic and nucleophilic character of each of the pulping reagents. Use of superior nucleophiles will favor nucleophilic addition and subsequent degradation of the lignin over competing reactions which tend to stabilize the lignin toward further degradation.[6]

Gierer claims that the nature of the pulping reagent used will determine the reactions of the quinonemethide.[6] Hydroxide ion can react as a base and convert quinonemethides into stable vinyl ether structures. Hydroxide ion can also add to the quinonemethide to produce benzyl alcohols which then undergo epoxide formation and cleave the β-aryl ether. This reaction, however, is considered minor for phenolic end units in the kraft system.[6] Hydrosulfide ion is considered a much weaker base than hydroxide ion,[19] and does not participate in acid-base reactions. Hydrosulfide ion can react as a nucleophile to produce benzyl mercaptans which will form episulfides and

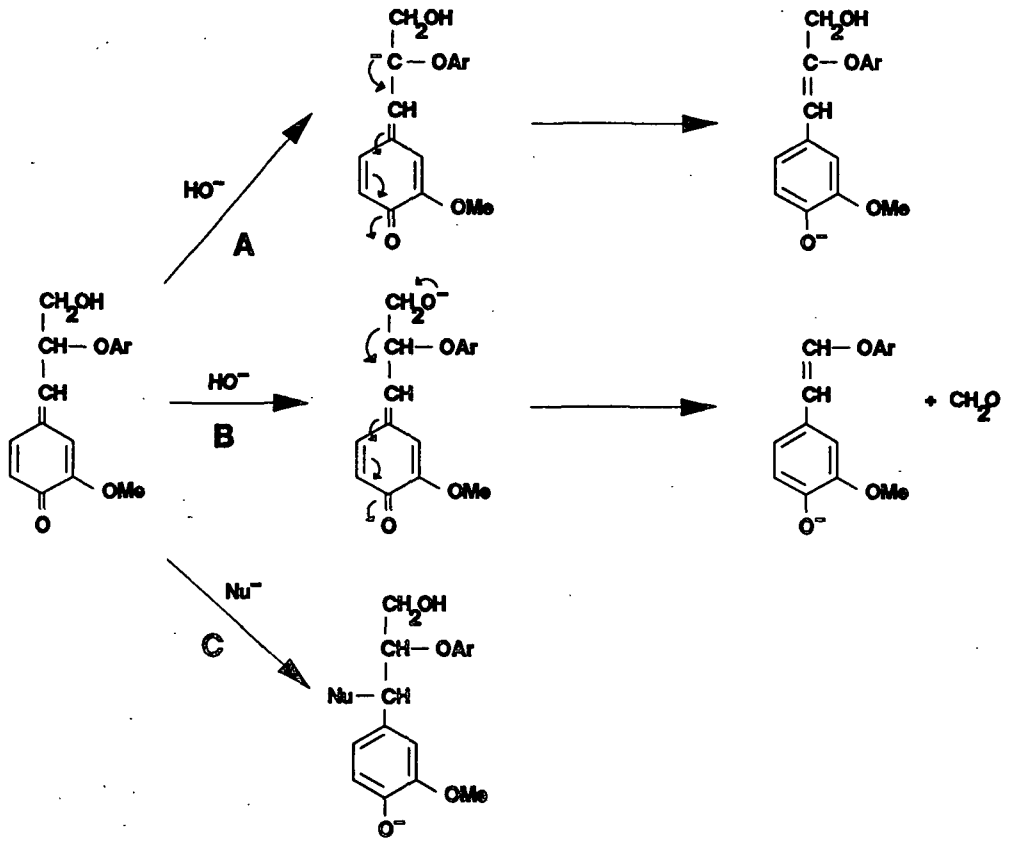

Figure 3. Reactions of quinonemethide intermediates.[6]

cleave the β-ether. The increased rate and extent of delignification in the kraft process can be explained by the possible superior nucleophilicity of hydrosulfide ions in comparison to hydroxide ion.[6]

Much of the lignin polymer is fragmented through reactions of quinonemethides. In soda or kraft pulping, little or no cleavage of the β-aryl ether bond is observed by direct substitution of the nucleophile on the β-carbon atom. Rather, cleavage of the β-aryl ether bond occurs through nucleophilic reactions of neighboring groups, specifically via participation of α-OH and α-SH groups (shown in Fig. 4).[6] The adduct is ionized by the surrounding basic medium and then undergoes nucleophilic attack of the β-carbon atom. The result is formation of a three-membered ring intermediate

as well as cleavage of the β-aryl ether as a phenoxide ion. The released phenoxide ion may then undergo a similar set of reactions, leading to extensive loss of polymer end groups and dissolution of the lignin component. The three-membered ring intermediates are not end products but will further degrade via several possible reactions.

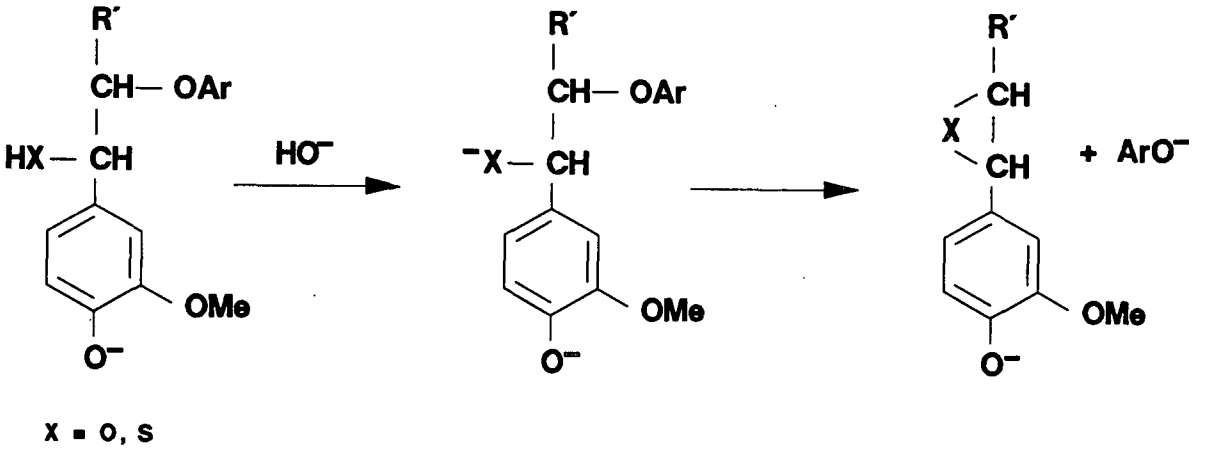

Figure 4. Neighboring group mechanism to cleave β-aryl ether bond during soda and kraft delignification.[6]

The bridging ability of the deprotonated α-sulfhydryl group versus α-hydroxyl group may also be an important step in delignification. Factors affecting the efficiency of this reaction include the acidity of the proton attached to the heteroatom, the nucleophilicity of the ionized α-substituent, and the ease of formation of the cyclic product or intermediate.[28] Formation of the cyclized product is influenced by bond lengths. Typical bond lengths for sp^3-C to sp^3-Y are 1.81 Å when Y = S and 1.41 Å when Y = O.[8] Bond lengths will be somewhat shorter when Y is ionized. Because episulfide formation results in a less strained intermediate than epoxide formation, reactions involving the episulfide are likely to dominate if factors other than bond length are equal.

Condensation reactions, the formation of new carbon-carbon bonds, also occur during chemical pulping. Heteroatom nucleophiles compete with carbanions for addition to the α-carbon atom of the quinonemethide (Fig. 5). Carbanions arise from phenolate structures formed during pulping reactions and can react with quinonemethides to produce condensation products.

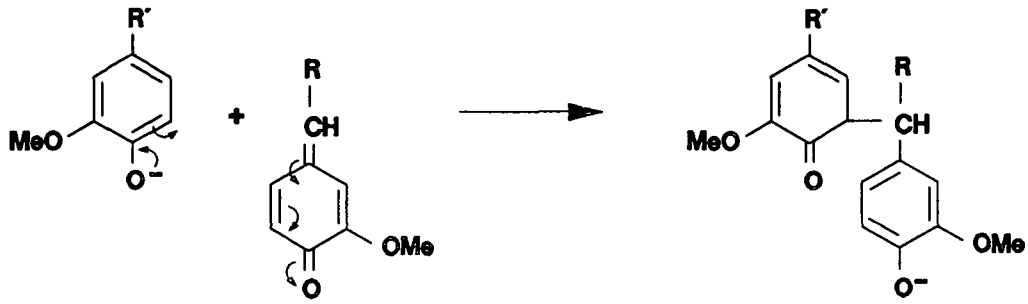

Figure 5. Reaction of carbanions with quinonemethides to form condensed lignin.[6]

The extent of condensation depends on the ability of the heteroatom nucleophiles to compete with carbanions for addition sites.[6] Heteroatom nucleophiles are thought to only retard but not prevent condensation reactions. Structural aspects of the reactive species present also influence the extent of condensation.[6] While fragmentation reactions are predominant in structures having β-ethers, structures without β-ethers are more likely to yield condensation products due to the reversibility of nucleophilic addition and the irreversibility of condensation product formation.

The reaction rate of carbanions with quinonemethides has been determined in order to estimate the rate of condensation. Hydrosulfide ion was found to be 13 times more reactive than 2,6-xylenol which was used as a condensing species.[27] Gierer and Ljunggren proposed the following order for competing reactions: β-proton abstraction < quinonemethide formation << formaldehyde elimination < carbanion addition < hydrosulfide addition.[27]

Cleavage of the α- and β-aryl ethers from structures containing free phenolic hydroxyl groups occurs during the initial phase of kraft pulping.[29] In the initial phase, reaction rates appear to be diffusion controlled, not chemically controlled; reaction conditions, such as temperature and the concentrations of hydroxide and hydrosulfide ions, have no effect on the amount of lignin remaining at the end of the cook.[30]

Alkaline cleavage of β-aryl ethers from non-phenolic units occurs during the bulk phase of pulping. The rate of lignin removal in the bulk phase is chemically controlled.[29] Cleavage of β-aryl ethers from non-phenolic end units requires neighboring group participation of an ionized hydroxyl or sulfhydryl group in the α- or γ-position, shown in Fig. 6.[6] Cleavage of the β-aryl ether may liberate new phenolic end units which can then undergo reactions via quinonemethides and cause further cleavage of α- and β-aryl ether bonds. These fast reactions do not influence the overall degradation rate, but have a great influence on the extent of lignin degradation. Increasing the bulk phase temperature will slightly decrease the amount of residual lignin remaining. Changes in the concentration of hydroxide ion do not affect residual lignin unless there is a drastic lowering in the hydroxide concentration; this causes condensation reactions and precipitation of lignin. Increasing the level of hydrosulfide ion, however, causes a substantial decrease in residual lignin.[30]

An analogous delignification mechanism to kraft pulping has been proposed for the reactions of anthraquinone with lignin (Fig. 7). Anthrahydroquinone (AHQ), the reduced form of anthraquinone, can act as a nucleophile and add to a quinonemethide to produce an adduct. In this case, however, the resulting adduct degrades through an electron shift to eliminate

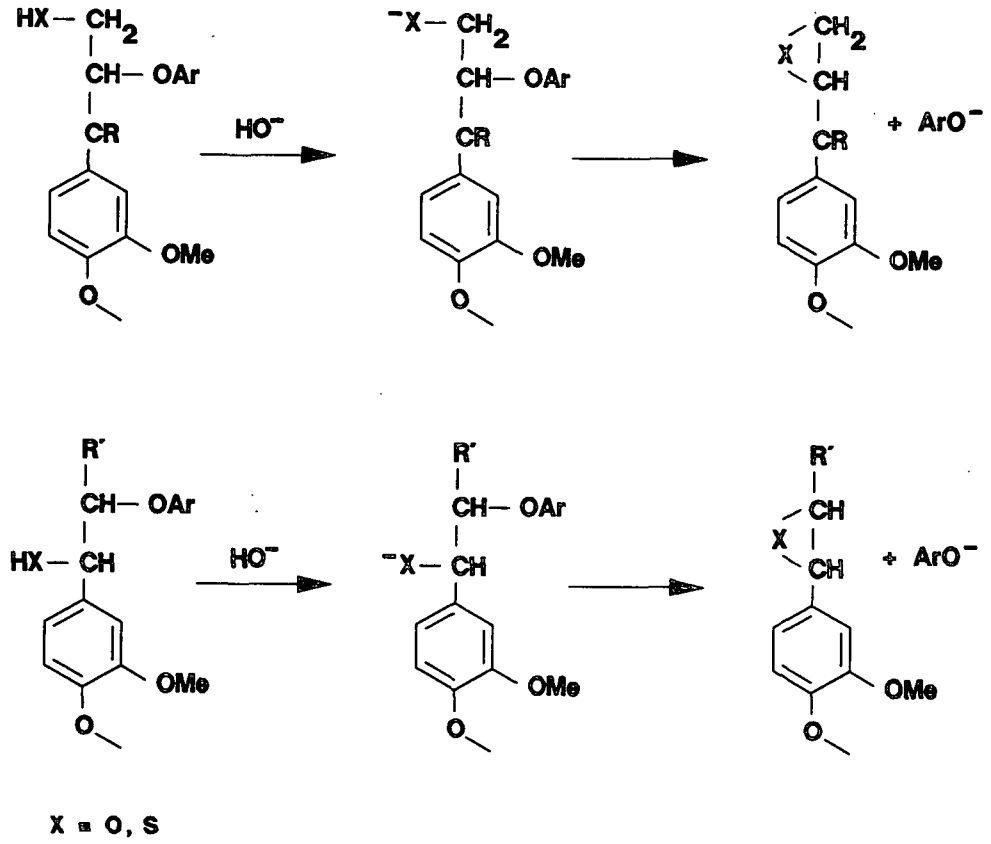

Figure 6. Cleavage of β-aryl ether bonds from non-phenolic end units.[6]

anthraquinone and displace the β-aryl ether. Anthrahydroquinone and anthranol adducts of quinonemethides have been prepared at low temperatures (35-45°C) and shown to be easily degraded.[31]

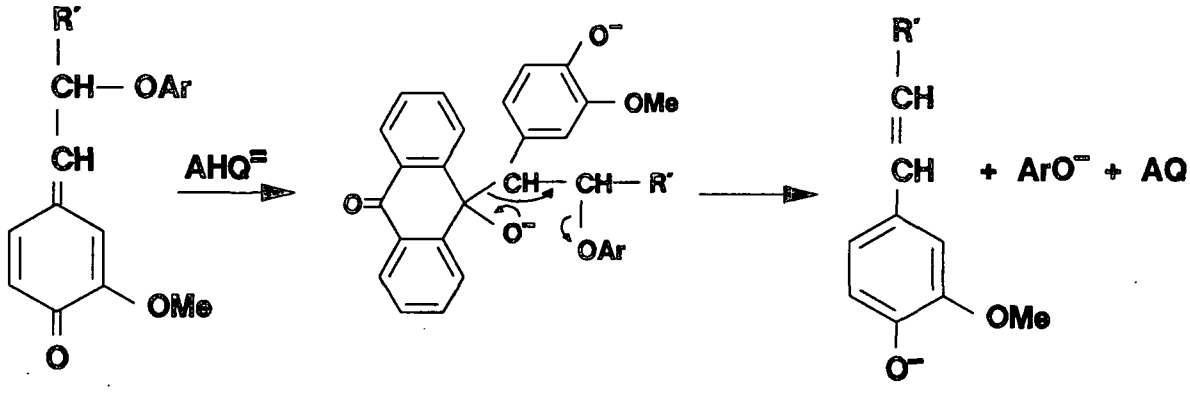

Figure 7. Addition of anthrahydroquinone to quinonemethides and subsequent β-aryl ether cleavage.[6]

The effect of different substituents in lignin model compounds was investigated to better understand the degradation of lignin.[32,33] These compounds were degraded under conditions which simulate soda, kraft, and soda-AQ pulping. The rate-determining step in soda reactions was cleavage of the β-aryl ether bond.[32] In kraft and soda-AQ reactions, however, the slow step was quinonemethide formation.[33] The effectiveness of the additive was found to be $AHQ^{2-} > HS^-$. This order appears to reflect the efficiency of the additive to fragment the model rather than the model undergoing undesirable competing side reactions. Additives affect the product-determining steps rather than the rate-determining steps.

The reactions of lignin were recently investigated from the viewpoint of the HSAB principle.[34] The β-aryl ether bond is described as "soft"; the most promising delignification agent, therefore would be "soft". As the nucleophile becomes increasingly soft, $HO^- < HS^- \approx I^- < AHQ^{2-}$, the degree of lignin degradation increases.

Electron transfer mechanisms are increasingly being suggested for reactions which have been until recently considered ionic in nature.[35] Fleming, *et al.* proposed a redox cycle in which hydrosulfide ion reduces lignin and produces oxidized sulfur species during kraft delignification.[36] Fleming claimed that a kinetic relationship between (1/Kappa number of pulp) and $(\text{charge of additive})^{1/2}$ was indicative of electron transfer. Werthemann, however, found that this relationship was not observed over all hydrosulfide dosages.[37]

Single electron transfer reactions have also been proposed to occur during anthraquinone pulping (Fig. 8).[35] The reduced form of anthraquinone, anthrahydroquinone dianion (AHQ^{2-}) transfers an electron to the quinonemethide

to form an AHQ radical anion (AHQ^-) and a phenoxy radical anion; the latter then fragments to give an aryloxy radical and a β-styrene structure.

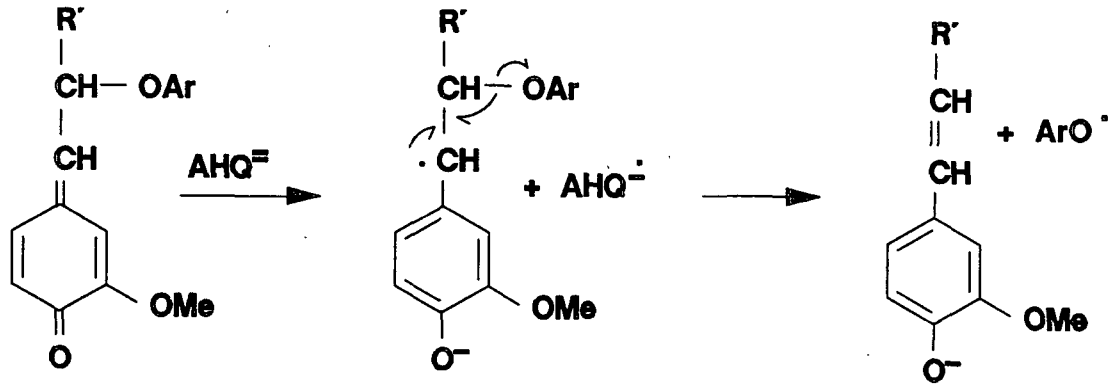

Figure 8. Single electron transfer from anthrahydroquinone to quinonemethides and subsequent β-aryl ether cleavage.[35]

Evidence exists that single electron transfer reactions can occur between lignin model compounds and AHQ^{2-} in organic solvents.[38] A square-root dose relationship for soda-AQ pulping is indicative of a redox catalyst.[36] Addition of anthraquinone to a soda cook caused an increase in free radicals observed by ESR.[39] The radicals observed here are associated with formation of AHQ^-. The maximum concentration of AHQ^- was reached during the initial heating phase and quickly returned to very low levels before the cooking temperature was attained.

Dimmel and co-workers have investigated a number of reactions involving quinonemethides. Anthrahydroquinone ion reacted faster than hydrosulfide and hydroxide ions in capturing quinonemethides during competitive reactions.[40] A lignin model compound which contains a propanol group attached to the β-carbon was reacted in a second study. In this case, the β-aryl ether bond is efficiently cleaved by anthrahydroquinone but not by hydrosulfide or hydroxide ions (Fig. 9).[41] This suggests that anthrahydroquinone ion either

is a very efficient nucleophile, or reacts by a different mechanism, single electron transfer.

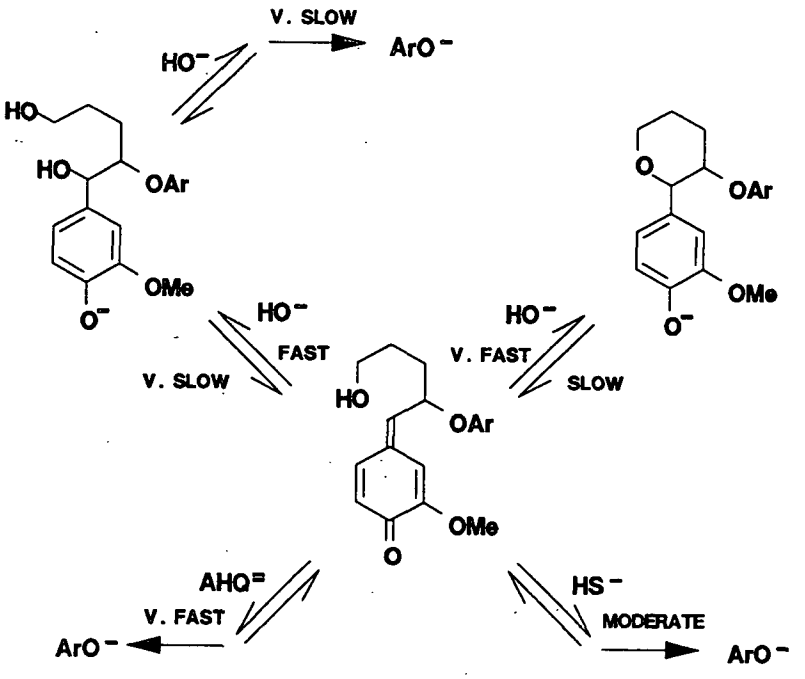

Figure 9. Reactions of β-propanol lignin model compound.[41]

THESIS OBJECTIVES

Alkaline delignification is a multi-step process. Chemical factors responsible for enhanced delignification in kraft pulping include: (1) the greater nucleophilicity of hydrosulfide ion toward quinonemethides, (2) the greater ionizability of the resulting sulfide adduct, (3) the greater nucleophilicity of this sulfur species during neighboring group displacement, and (4) the greater C-S bond length which allows formation of a less strained three-membered ring intermediate. The nucleophilicity of anthrahydroquinone has been cited as a chemical factor responsible for enhanced delignification in pulping systems which use anthraquinone as an additive.

Nucleophilicity has been cited as a chemical factor which may be responsible for the effectiveness of pulping reagents. This property, however, is dependent on the type of substrate under attack as well as the character of the solvent. Previous studies have not adequately explained the role of nucleophilicity in delignification reactions.

The goal of this thesis was to critically examine chemical factors which are responsible for the effectiveness of hydrosulfide and anthrahydroquinone ions in delignification. Emphasis was placed on determining the nucleophilic order of hydroxide, hydrosulfide, and anthrahydroquinone ions. Delignification reactions in which nucleophilicity was cited as a major factor are (1) addition to the unsaturated carbon center of a quinonemethide and (2) neighboring group displacement at a saturated carbon center which breaks a β-aryl ether bond. Two model compounds were chosen to determine the nucleophilicity of hydroxide, hydrosulfide and anthrahydroquinone ions toward unsaturated and saturated carbon centers at high temperatures.

SELECTION OF MODEL COMPOUNDS

Quinonemethides are key intermediates in lignin pulping reactions. They are believed to be attacked by nucleophiles at both their α- and β-carbon atoms (* and **, respectively in Fig. 10). Attack of the β-carbon is predominately from internal nucleophiles located on the α- and γ-carbons. Nucleophilic addition to the α-carbon atom of a quinonemethide is likely to be a reversible reaction; the resulting nucleophile-quinonemethide adduct can either undergo further reaction or revert back to a quinonemethide. In addition to the reversible nature of their reactions, quinonemethides also are very reactive and present a number of problems in interpreting results related to the key reaction steps associated with delignification.

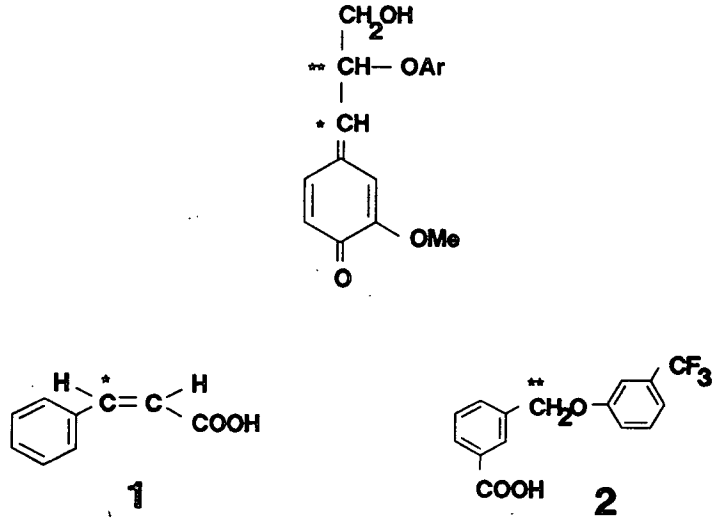

Figure 10. Comparison of reaction sites in a quinonemethide and model compounds 1 and 2 (* indicates unsaturated carbon site, and **, saturated carbon site.).

Two organic compounds unrelated to lignin were chosen to simulate fundamental reactions which occur during alkaline delignification. The first compound chosen was *cis*-cinnamic acid (1) which has an unsaturated conjugated

carbonyl reaction site (*, Fig. 10), similar to the C_α reaction site in quinonemethides. The expected addition-elimination reaction of nucleophiles at this site, outlined in Fig. 11, causes **1** to rearrange to a less sterically crowded configuration, forming *trans*-cinnamic acid (**6**). If elimination is slow relative to protonation of the intermediates, then adducts **3-5** would be observed. The isomerization of **1** has been previously studied in the presence of sulfuric acid. Under acidic conditions, isomerization occurred through an addition-elimination mechanism.[42]

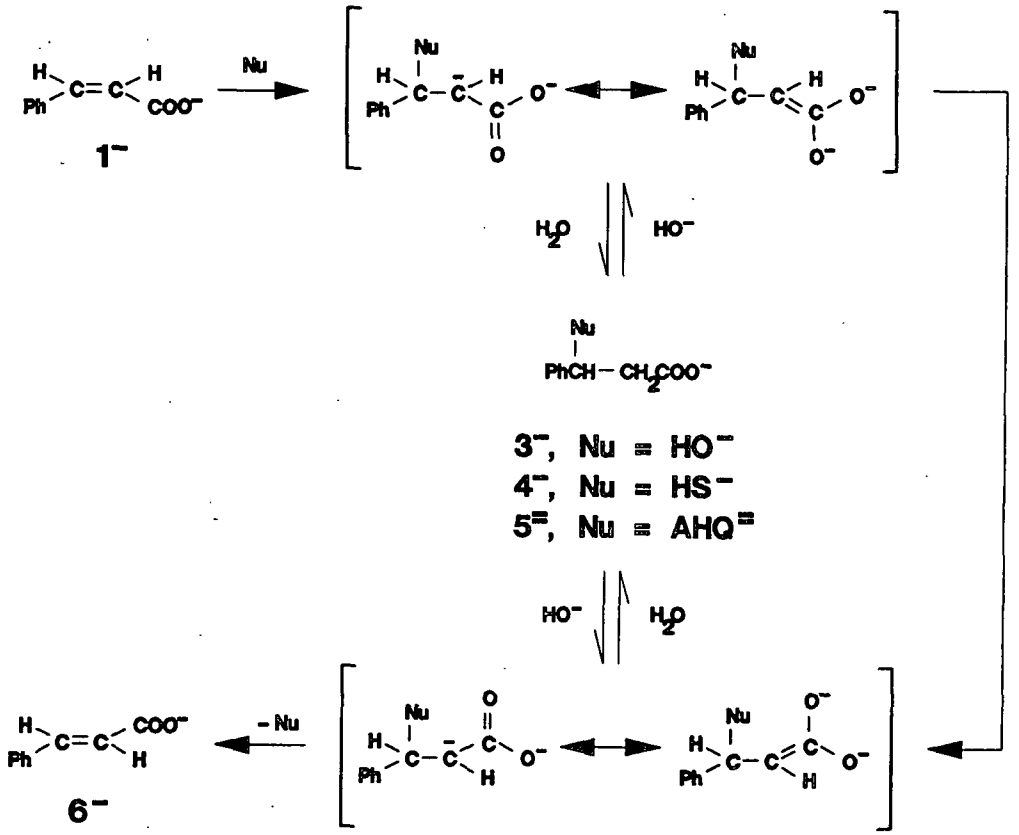

Figure 11. Expected reaction pathway of 1.

The second compound chosen for study was 3-[3′-(α,α,α-trifluoromethyl)phenoxymethyl]benzoic acid (**2**). The reaction site in compound **2** is similar to that in a quinonemethide adduct which undergoes neighboring group

displacement at a saturated carbon center to displace the β-aryl ether (**, Fig. 10). The anticipated reaction pathway of 2, shown in Fig. 12, consists of the nucleophile attacking the reactive benzyl carbon center to form a series of primary products (7-9) and a phenolate ion (10). A benzyl aryl ether was chosen because it is more reactive than methyl or other alkyl aryl ethers toward S_N2 reactions.[8]

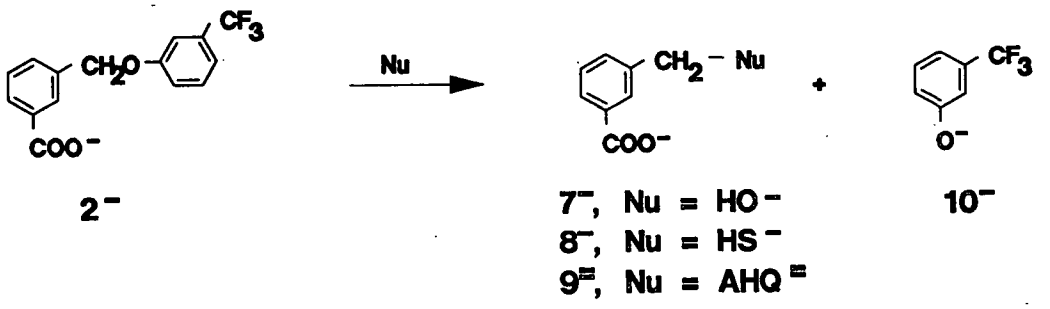

Figure 12. Expected reaction pathway of 2.

The degradation of 2 involves the direct displacement of the phenolate group by the nucleophile. In delignification, however, the phenolate group is displaced by a neighboring group mechanism. Factors other than nucleophilicity, such as ionizability and bond length, may contribute to the observed reactivity of quinonemethide adducts. In addition, the nucleophilic species in the delignification reaction is an alkyl derivative, i.e. a mercaptide, not hydrosulfide ion. The reactivity of alkyl derivatives, however, parallels that of the free ion.[8]

Previous studies with model compounds similar to 2 showed the need for an electron-withdrawing group on the leaving phenolate ion to aid the displacement.[43] Compound 11 was found to be relatively stable under the employed reaction conditions. Compound 12, which contains a nitro group on the phenolate portion of the molecule, was sufficiently reactive in sodium

hydroxide solutions at 170°C. The electron-withdrawing group enhances the reactivity of site under attack and provides additional stabilization of the negative charge on the leaving phenolate ion. The nitro group in compound 12, however, was not stable to hydrosulfide ion. Compound 12, therefore, was not a suitable model compound.

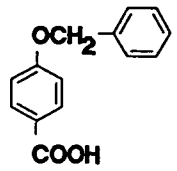

11

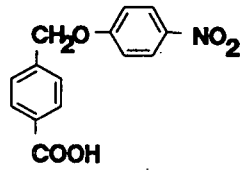

12

Structure-reactivity studies indicate that the trifluoromethyl group is a relatively strong electron-withdrawing group, though not as strong as the nitro group.[8] The trifluoromethyl group was placed at the *meta* position so that its electron-withdrawing ability would be felt only through field effects. Placement of the group at the *ortho* position may cause steric effects, while placement at the *para* position may result in loss of fluoride ion and undesirable quinonemethide formation as shown in Fig. 13.

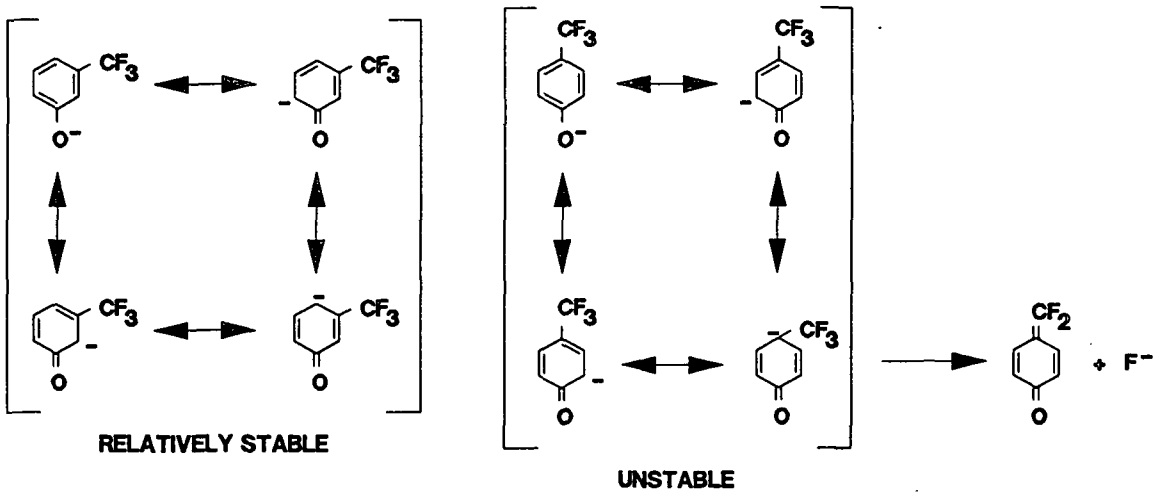

Figure 13. Relationship between placement of electron-withdrawing group and stability at 195°C.

Most wood pulping is conducted in a water medium. The reactions of this investigation were, therefore, studied in water to avoid any ambiguities in nucleophilic order due to solvent effects. A carboxylate group was incorporated into **1** and **2** so that each was soluble in basic solutions.

SYNTHESIS

cis-CINNAMIC ACID AND ASSOCIATED DEGRADATION PRODUCTS

Compound 1 was synthesized by stereoselectively hydrogenating the triple bond in ethyl phenylpropiolate as shown in Fig. 14. The reaction was terminated prior to conversion of the desired product to its fully reduced form, hydrocinnamic acid.

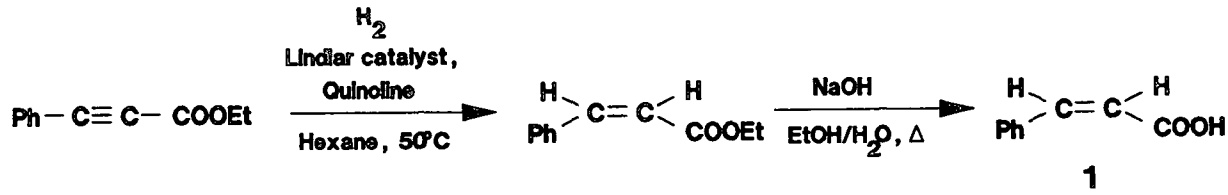

Figure 14. Synthesis of model compound 1.

Several procedures were tried before the above method was found to be successful. Hydrogenation using hydroxylamine-*O*-sulfonic acid,[44] isomerization of *trans*-cinnamic acid using polyphosphoric acid,[45] and hydrogenation of phenylpropiolic acid[46] failed to yield the desired product.

The adducts of 1, compounds **3**-**5**, were also synthesized as shown in Fig. 15. Benzaldehyde and ethyl bromoacetate were reacted under conditions of the Reformatsky reaction to yield 3-hydroxy-3-phenylpropionic acid (**3**).[47] The ethyl ester of **3** was reacted with thiourea to form 3-mercapto-3-phenylpropionic acid (**4**).[48] The AHQ-adduct of cinnamaldehyde[49] (isolated as a hemiacetal) was oxidized in the presence of chromic acid to give 10-hydroxy-10-(1-phenyl-3-carboxypropyl)-9(10*H*)-anthracenone lactone (**5A**). The lactone ring of **5A** will be opened in the presence of aqueous sodium hydroxide to form the carboxylate (**5B**).

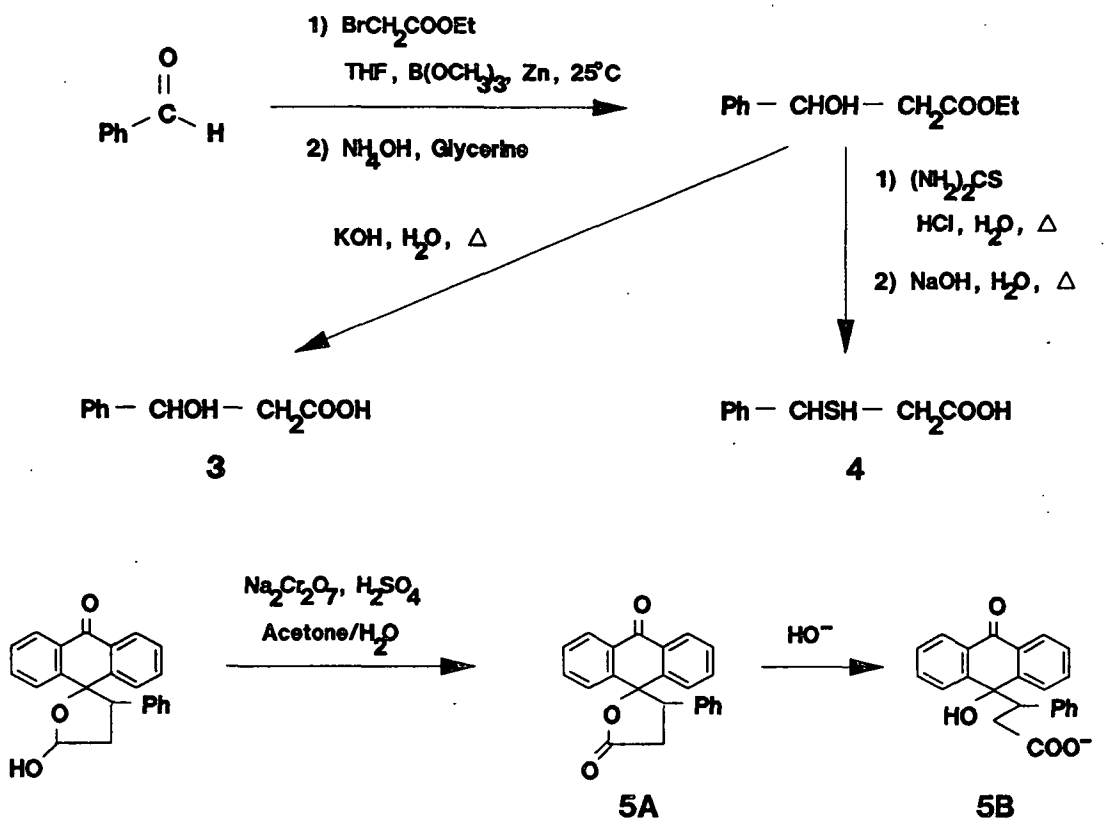

Figure 15. Synthesis of products associated with the degradation of 1.

Deuterated analogs of 1 and 6 were needed to determine the isomerization reaction mechanism of 1. Methods used to synthesize α,β-dideutero-*cis*-cinnamic acid (1-α,β-d_2) and α,β-dideutero-*trans*-cinnamic acid (6-α,β-d_2) are outlined in Fig. 16. Compound 1-α,β-d_2 was formed by subjecting ethyl phenylpropiolate to catalytic deuteration under conditions similar to those used to synthesize 1. A mixture of 6-α,β-d_2 and 6-β-d was obtained, via the Perkin reaction, from deuterated benzaldehyde and deuterated acetic anhydride.[50] The monodeutero product probably resulted from potassium acetate reacting with deuterated acetic anhydride to form partially deuterated acetic anhydride. Deuterated potassium acetate would have been a better choice for the catalyst. Since most of the product was the dideutero species, this mixture was used in subsequent studies.

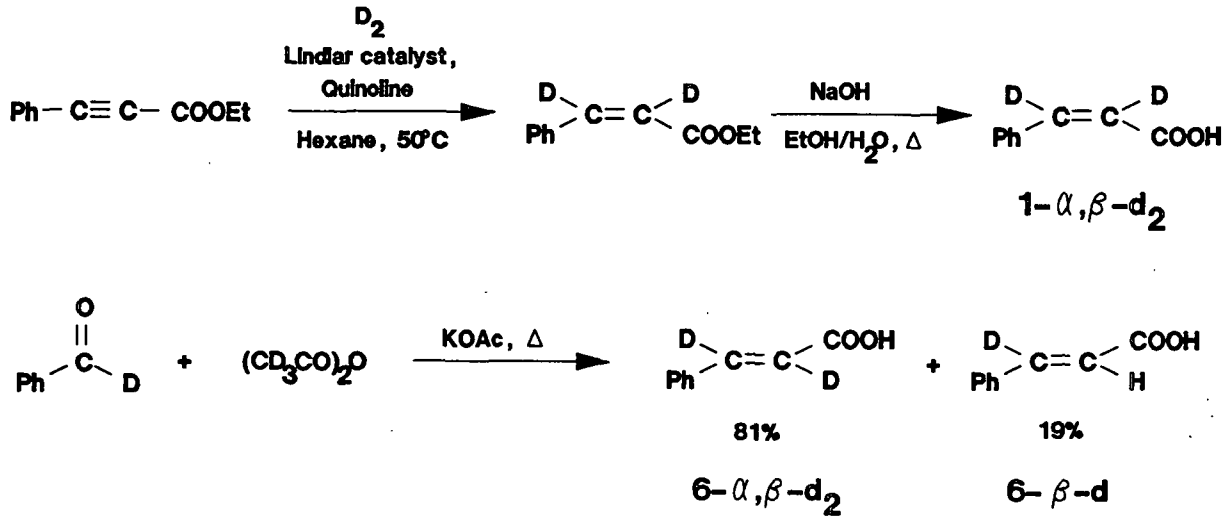

Figure 16. Synthesis of deuterated analogs of *cis*- and *trans*-cinnamic acids.

3-[3′-(α,α,α-TRIFLUOROMETHYL)PHENOXYMETHYL]BENZOIC ACID AND ASSOCIATED DEGRADATION PRODUCTS

Compound 2 was synthesized by coupling methyl α-bromo-3-toluate and 3-(α,α,α-trifluoromethyl)phenol, as shown in Fig. 17.[51] This method was effective in forming a number of compounds having an aryl ether linkage.[43]

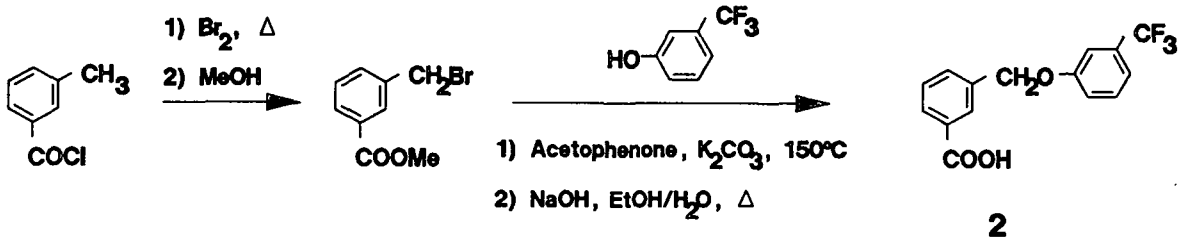

Figure 17. Synthesis of model compound 2.

The primary degradation products of 2, compounds 7-9, were also synthesized as shown in Fig. 18. Two methods for the formation of 3-(α-hydroxymethyl)benzoic acid (7) are outlined. Conversion of 3-bromobenzyl bromide yielded small amounts of the desired compound.[52] Hydrolysis of methyl α-bromo-3-toluate using sulfuric acid also gave compound 7. Treatment of

methyl α-bromo-3-toluate with thiourea formed 3-(α-mercaptomethyl)benzoic acid (8).[53] The reaction of 3-(α-bromomethyl)benzoic acid[54] with anthrahydroquinone yielded 10-hydroxy-10-(3′-carboxybenzyl)-9(10*H*)-anthracenone (9).[49]

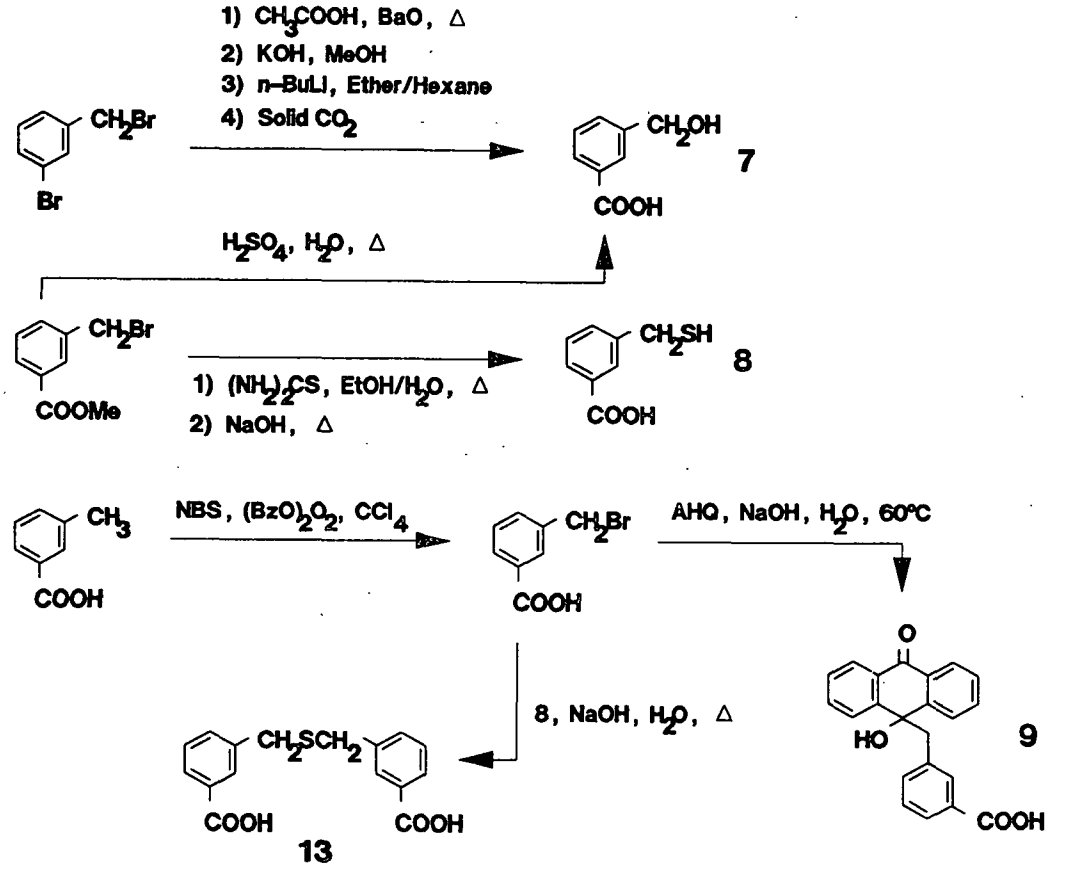

Figure 18. Synthesis of products associated with the degradation of 2.

The synthesis of an observed secondary product, 3-(3′-carboxybenzylthiomethyl)benzoic acid (13), is illustrated by reactions outlined in the bottom portion of Fig. 18. Under basic conditions, 3-(α-bromomethyl)benzoic acid was reacted with 8 to form the desired product.

DEGRADATION OF *cis*-CINNAMIC ACID

MECHANISTIC STUDIES

The degradation of 1 was investigated in oxygen-free water solutions which contained hydroxide, hydrosulfide, and anthrahydroquinone ions. The reactions were followed using gas-liquid chromatographic (GLC) techniques. The identity of each product was confirmed by comparing its GLC and GLC-mass spectrometric (GLC-MS) properties to a synthesized or purchased sample.

The conversion of *cis*-cinnamic acid to *trans*-cinnamic acid is a multi-step reaction. In order for this compound to be a suitable model for investigating nucleophilic addition, the slow step should be the addition step. If either rearrangement or elimination is the slow step, the resulting rate constant will probably not reflect the nucleophilicity of the reagent.

Compound 1 was degraded in aqueous sodium hydroxide at 195°C to simulate soda pulping reactions. The major product was *trans*-cinnamic acid (**6**). The anticipated reaction scheme is outlined in Fig. 19. Hydroxide ion can add to the double bond to produce an adduct (**3**). Either resonance structure of the adduct may then rearrange by a bond rotation around C_α and C_β and then eliminate hydroxide ion to produce *trans*-cinnamic acid (**6**). A mass balance, obtained by adding the observed amounts of *cis*- and *trans*-cinnamic acids and comparing the amount to the starting levels of each, was quite good. The intermediate adduct **3** was not detected. Small amounts of benzaldehyde and benzoic acid, identified by GLC-MS, probably are responsible for the small decrease in the material balance at longer reaction times (Fig. 20). Both by-products were also formed by heating *trans*-cinnamic acid in aqueous sodium hydroxide.

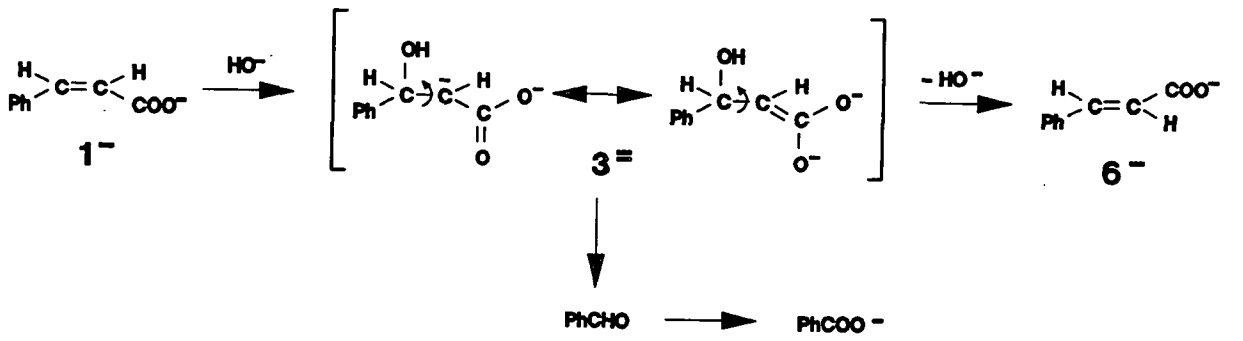

Figure 19. Reaction of 1 in the presence of hydroxide ions at 195°C.

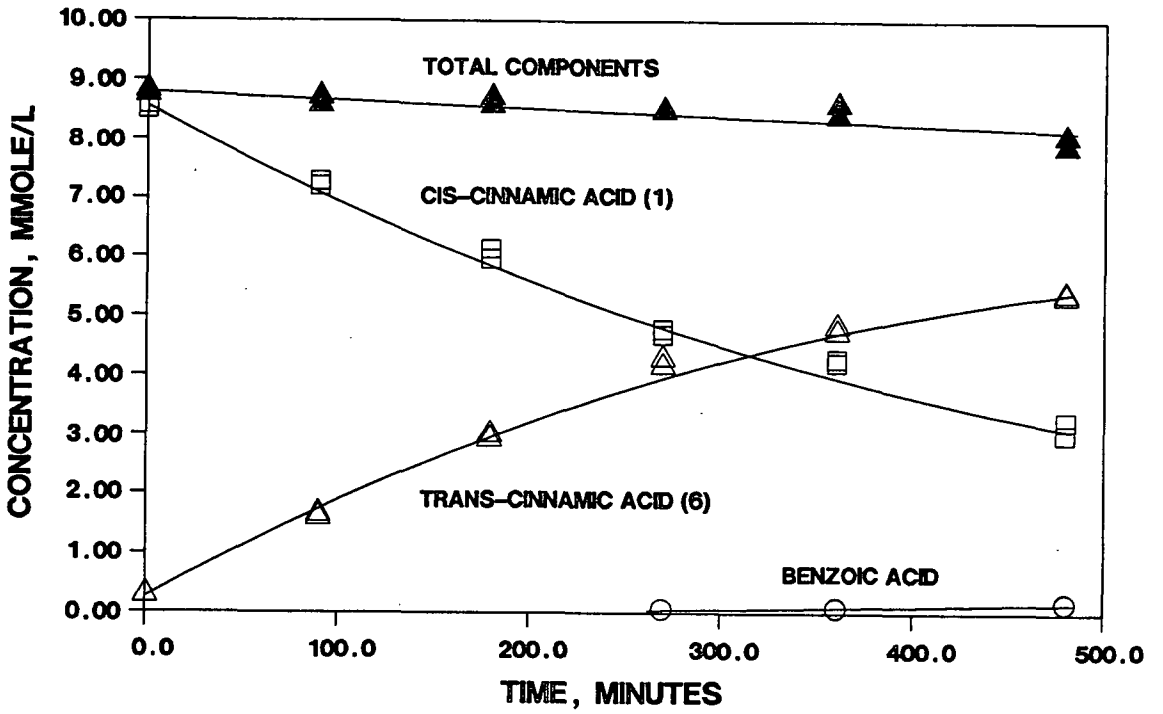

Figure 20. Mass balance for the reaction of 1 in 0.787M NaOH at 195°C.

Compound 3 was degraded in a aqueous sodium hydroxide under conditions similar to the degradation of 1. Analysis of the product mixture showed all of 3 was converted to 6 during the 15 minute warmup period. Based on these results, it was concluded that the slow step was the addition step rather than rearrangement or elimination.

Compound 1 was also degraded in aqueous sodium sulfide at 195°C to simulate kraft pulping reactions. Compound 6 was the major product of the reaction. The expected reaction pathways are a combination of those shown in Fig. 19 and Fig. 21. Hydrosulfide ion can add to the carbon-carbon double bond to produce adduct 4 which can then rearrange and eliminate hydrosulfide ion to form 6. The intermediate adduct 4 was not detected by GC-MS; an authentic sample of 4 was found to rapidly degrade to 6 under the employed reaction conditions. There was near quantitative conversion of *cis* to *trans* (Fig. 22). Benzaldehyde and benzoic acid were again present in small amounts.

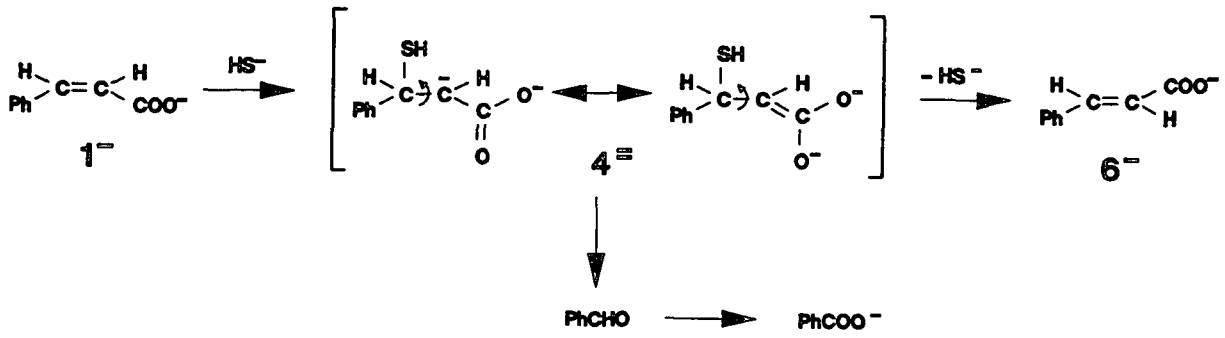

Figure 21. Reaction of 1 in the presence of hydrosulfide ions at 195°C.

When compound 1 was reacted in solutions containing high concentrations (> 1M) of sodium hydroxide or sulfide, hydrocinnamic acid was also observed as a product. The reactions, therefore, were studied at lower base concentrations to minimize by-product formation and maximize conversion to 6. The mechanism by which hydrocinnamic acid is formed was not investigated.

Compound 1 was heated in solutions containing hydroxide and anthrahydroquinone ions to simulate soda-AQ pulping reactions at 195°C. The major product of the reaction was *trans*-cinnamic acid (6). The anticipated reaction scheme is a combination of those outlined in Fig. 19 and Fig. 23. Anthrahydroquinone ion may add to the double bond in 1 to produce intermediate

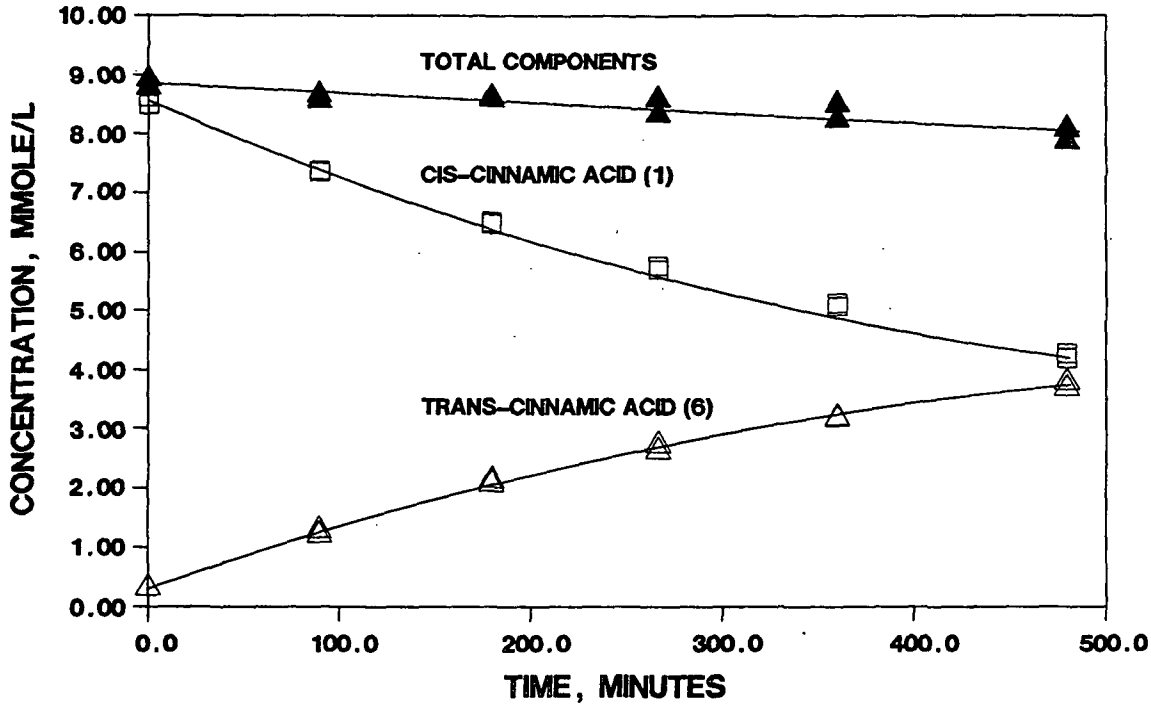

Figure 22. Mass balance for the reaction of 1 in 0.385M NaOH & 0.393M NaSH at 195°C.

adduct 5 which then can rearrange and eliminate anthrahydroquinone ion to form 6. Adduct 5 was not observed in the reaction mixture. An authentic sample of 5 was not stable under the employed reaction conditions and was rapidly converted to 6.

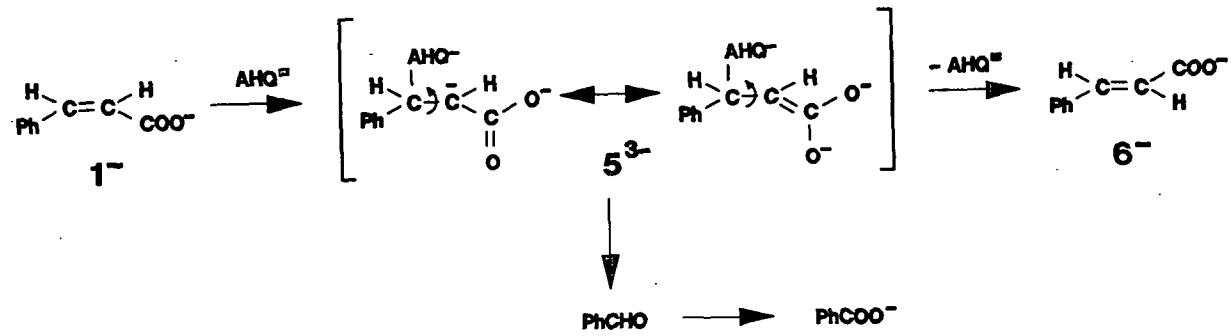

Figure 23. Reaction of 1 in the presence of anthrahydroquinone ions at 195°C.

The material balance was somewhat less complete during reactions of 1 with anthrahydroquinone (Fig. 24); approximately 12% was not accounted as compared to 5-8% in previous reactions (Fig. 20 and 22). Increased amounts of benzaldehyde and benzoic acid were detected with anthrahydroquinone ion as the nucleophile. The level of production of benzaldehyde and benzoic acid was not sufficient, however, to account for the observed incomplete material balance. When adduct 5 was heated in alkali, about 25% was converted to unknown products; unknown side reactions may account for the incomplete material balance.

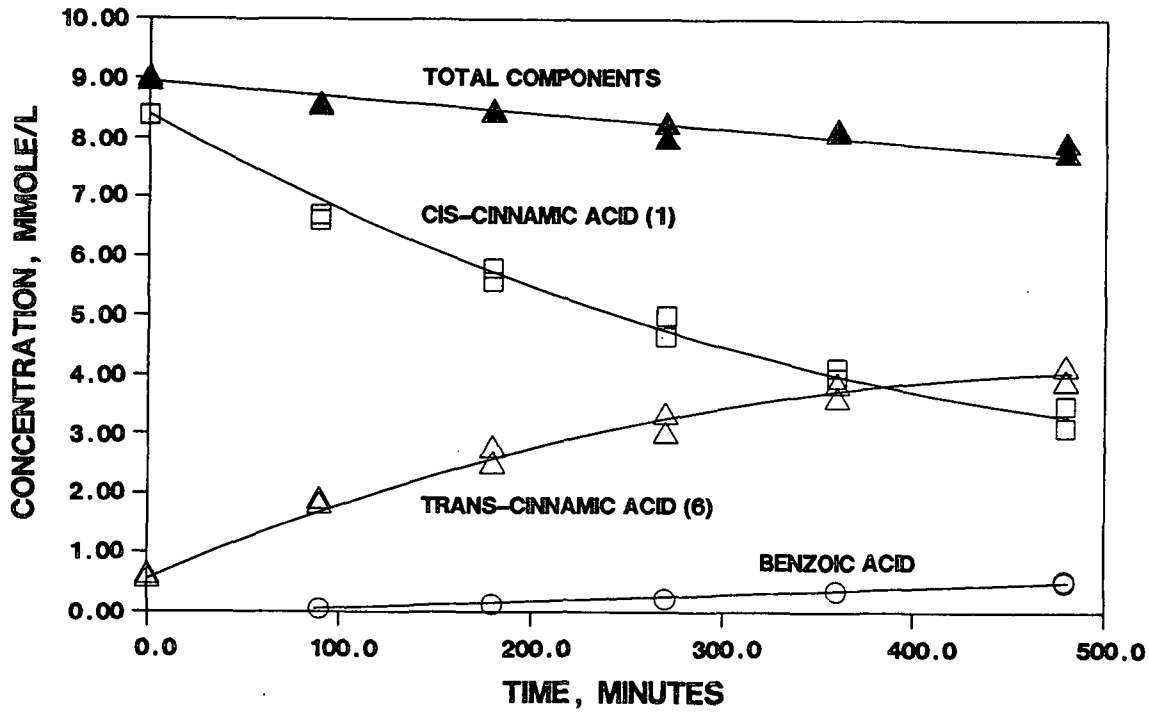

Figure 24. Mass balance for the reaction of 1 in 0.435M NaOH & 0.118M AHQ at 195°C.

An anthrone-coupled product 14 was also detected in all of the reaction mixtures which included anthrahydroquinone ion. Compound 14 was formed in both the presence and absence of 1. The significance of this product is not known; however, its formation suggests a radical mechanism.

This compound has not been reported in pulp mixtures; its production during AQ pulping may be a potential area for future investigation.

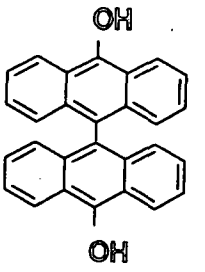

14

The reversibility of the isomerization reaction was also investigated by examining the reactions of *trans*-cinnamic acid (6) at 195°C. Compound **6** was reacted in basic solutions to determine the extent of formation of *cis*-cinnamic acid. Less than 1% was converted to 1 over an eight hour period. It was concluded that there was probably no conversion of **6** to 1 during the reactions of compound 1.

ROLE OF PROTON ABSTRACTION IN ISOMERIZATION MECHANISM

The mechanism of conversion of *cis* to *trans*-cinnamic acid is of great importance in determining nucleophilic orders. The two most plausible mechanisms are shown in Fig. 25. The isomerization of 1 to **6** by abstraction of an olefinic hydrogen atom was considered, primarily because hydroxide ion is a very strong base at 170°.[19] The olefinic hydrogen atoms may be acidic enough that proton abstraction would occur.

Initial studies showed exchange of olefinic hydrogen atoms for deuterium atoms occurred during the reactions of both *cis*- and *trans*-cinnamic acids in sodium deuteroxide/deuterium oxide solutions at 195°C. The role of proton abstraction in promoting isomerization, therefore, was investigated.

If proton abstraction caused isomerization, compound 1 could not be used for determining the nucleophilicity of pulping reagents toward unsaturated carbon centers. The measured reaction rate would indicate the basicity of the reagent rather than its nucleophilicity. The role of proton abstraction in *cis-trans* isomerization was further explored by examining the reactions of α,β-dideutero-*cis*-cinnamic acid (1-α,β-d_2) and α,β-dideutero-*trans*-cinnamic acid (6-α,β-d_2) to determine any isotope effects and follow changes in the deuterium level of the products.

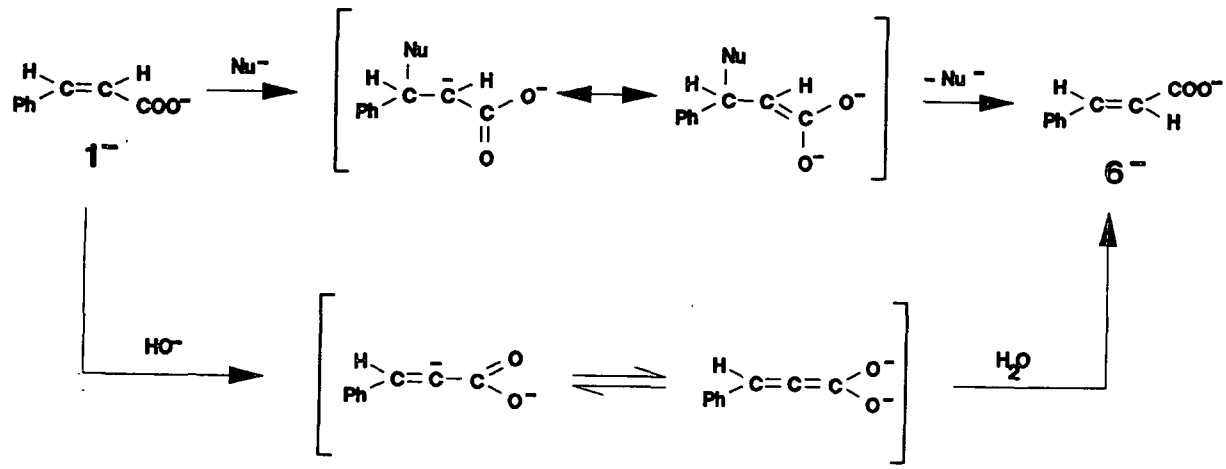

Figure 25. Comparison of isomerization of 1 by a nucleophilic addition-elimination (top) to a proton abstraction mechanism (bottom).

If proton abstraction occurred and was the rate-determining step for the isomerization of *cis* to *trans*, then the observed reaction rate of deuterated *cis*-cinnamic acid would be much less than that of the nondeuterated compound; this is known as a primary isotope effect. Because the carbon-deuterium bond has a lower zero-point energy than that of carbon-hydrogen bond, the dissociation energy of the carbon-deuterium bond is greater. This corresponds to a slower reaction rate. If a primary isotope effect is observed, then the ratio of the nondeuterated compound's reaction rate to that of a vinyl deuterated analog would be approximately 3-8.[8] The reaction rate

for an addition to the carbon center which has an attached deuterium atom will also be affected. The presence of deuterium atoms alters the electronic nature of the carbon atom during nucleophilic addition; its effect on the reaction rate is known as a secondary isotope effect. A small effect on the ratio is observed, in the order of 0.8-1.2.[8] Finally, detection of α,β-dideutero-*trans*-cinnamic acid during the degradation of α,β-dideutero-*cis*-cinnamic acid would indicate that proton abstraction is not the pathway which caused *cis-trans* isomerization.

During the initial reactions of 1-α,β-d_2 with hydroxide ions at 195°C, two important findings were noted. First, a secondary isotope effect, indicative of an addition-elimination mechanism, was observed. The ratio, k_H/k_D, was equal to 1.07. An exchange of one deuterium atom, however, was detected by mass spectroscopy. Proton NMR techniques showed that the α-deuterium atom was exchanged (Fig. 26). These two results seemed contradictory to each other, unless proton abstraction is occurring but is not responsible for *cis* to *trans* isomerization.

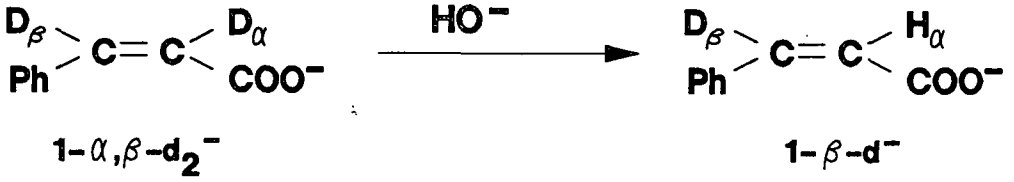

Figure 26. Abstraction of the α-deuterium atom by hydroxide ion at 195°C.

The exchange rates of α,β-dideutero-*cis*-cinnamic acid (1-α,β-d_2) and α,β-dideutero-*trans*-cinnamic acid (6-α,β-d_2) at 195°C were then investigated in more detail (Fig. 27). After 30 minutes, nearly all of 1-α,β-d_2 was converted to 1-β-*d*. The rate of conversion of 6-α,β-d_2 was considerably slower. The site of exchange in 6-α,β-d_2 was the same (α-deuterium) as that

in 1-α,β-d_2. The exchange rate of the *trans* isomer is presumably slower due to steric effects. The α-deuterium atom in 6-α,β-d_2 is protected by the phenyl ring if all of the π-orbitals are in the same plane for maximum conjugation. Since the exchange rate of 6-α,β-d_2 was much slower than that of 1-α,β-d_2, it should be possible to observe production of 6-α,β-d_2 during the reactions of 1-α,β-d_2 if addition-elimination was the mode of isomerization.

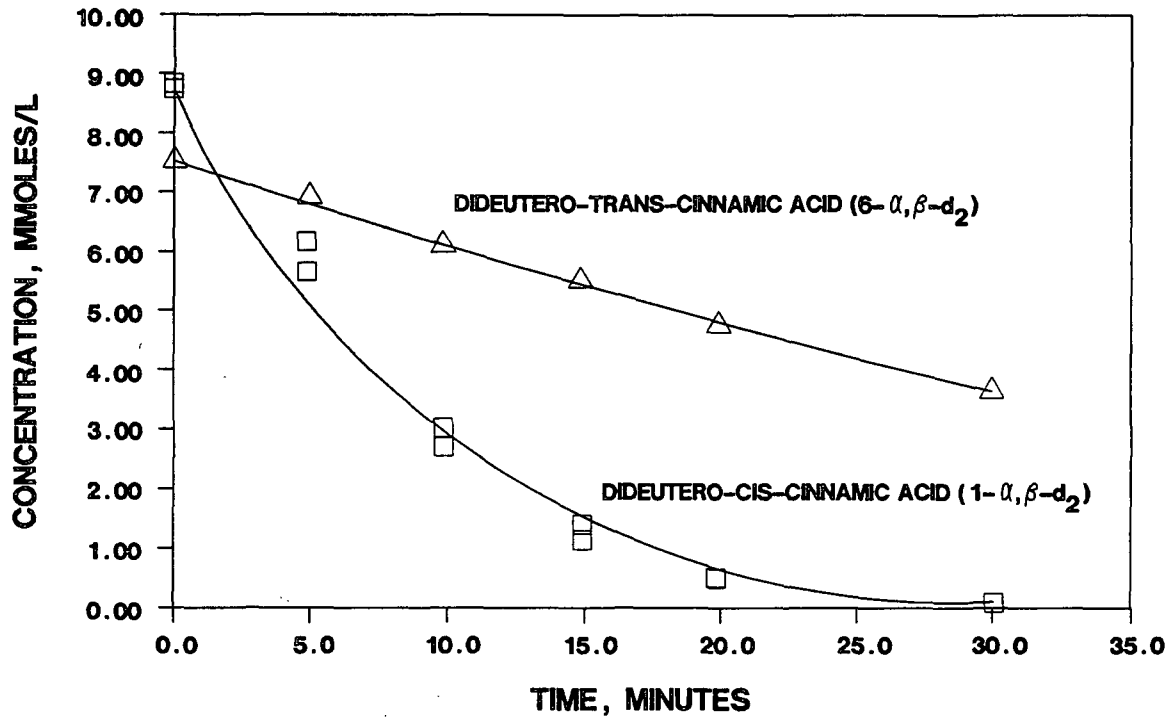

Figure 27. Comparison of the rate of exchange of the α-deuterium atom in 1-α,β-d_2 and 6-α,β-d_2 in 1.19M NaOH at 195°C.

The concentrations of both mono and dideutero species of the *cis* and *trans* isomers were determined during the reaction of 1-α,β-d_2 in basic solutions (Fig. 28 and 29). Examination of the *trans*-cinnamic acid component of the reaction revealed production of small amounts of 6-α,β-d_2 during the initial portion of the reaction (Fig. 29). It should be noted that a small amount of 6-α,β-d_2 impurity was present in the starting material 1-α,β-d_2. Production of 6-α,β-d_2 leveled off and decreased as the isomerization pro-

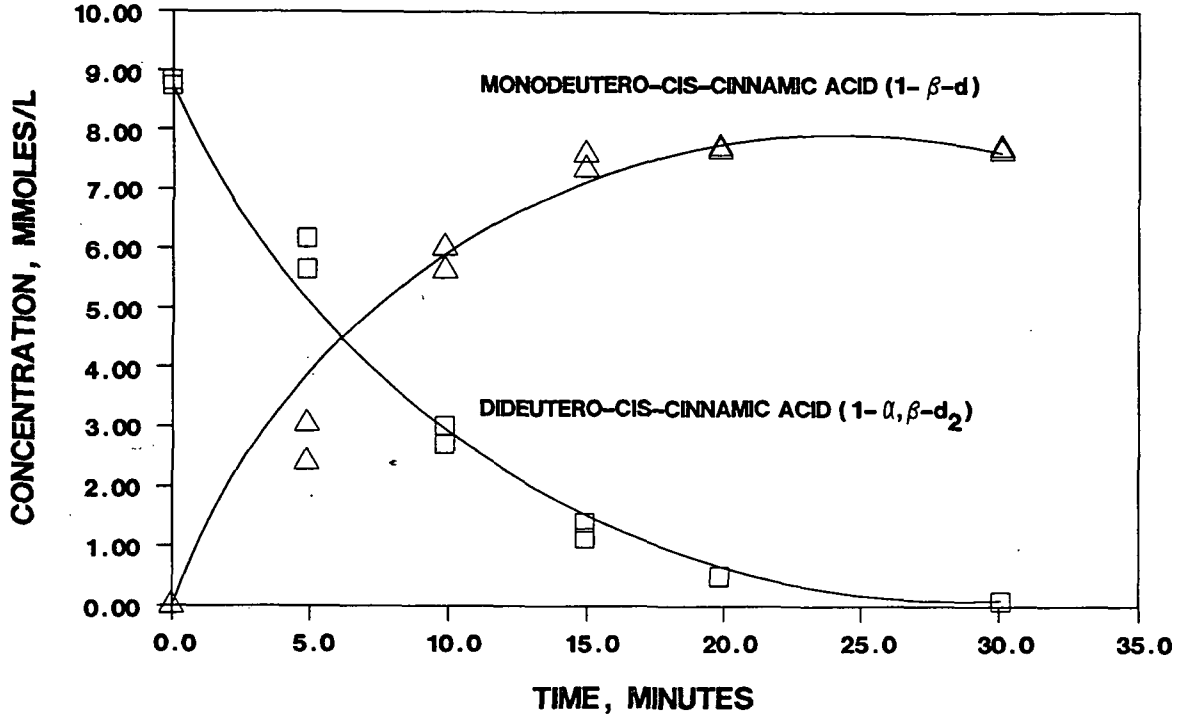

Figure 28. Analysis of *cis* component from the reaction of 1-α,β-d_2 in 1.19M NaOH at 195°C.

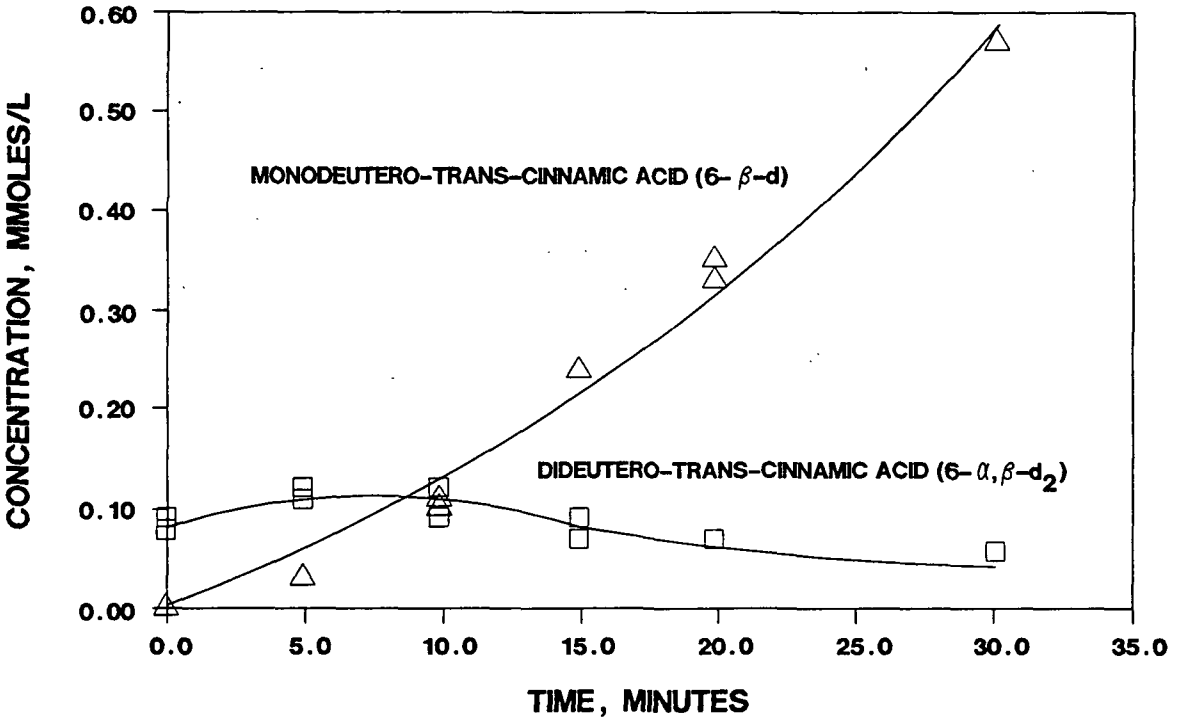

Figure 29. Analysis of *trans* component from the reaction of 1-α,β-d_2 in 1.19M NaOH at 195°C.

ceeded. There are two reasons why 6-α,β-d_2 does not continually increase. First, 6-α,β-d_2 is derived from 1-α,β-d_2 and the concentration of the latter drops rapidly at 195°C in alkali (Fig. 28). Second, 6-α,β-d_2 is slowly converted to 6-β-d (Fig. 27). The observed levels of 6-β-d (Fig. 29) can be explained by an increased level of 1-β-d present which undergoes isomerization to 6-β-d by addition-elimination, and the slow conversion of 6-α,β-d_2 to 6-β-d. If proton abstraction caused *cis-trans* isomerization, there would have been an immediate decrease in concentration of 6-α,β-d_2 instead of a small increase.

The proposed mechanism of deuterium loss with retention of the *cis* configuration is shown in Fig. 30. The α-deuterium atom is readily abstracted by hydroxide ion to form intermediate 1-β-d^{2-}. This species can then be protonated by water to produce β-deutero-*cis*-cinnamic acid.

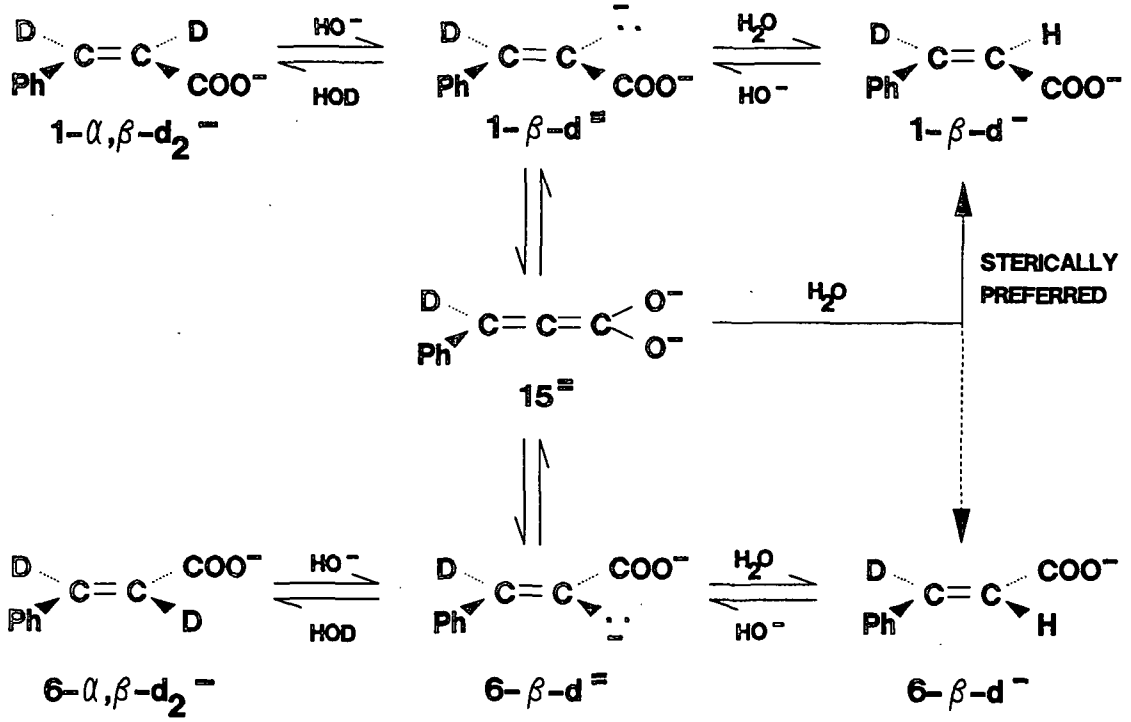

Figure 30. Steric considerations for proton abstraction with isomerization.

The extra electron pair present in 1-β-d^{2-} may be shifted so that the negative charge is placed on an electron-demanding oxygen atom to form an allenic intermediate (15). In the process, the hybridization of the α-carbon atom is changed from sp^2 to sp. The allenic intermediate would appear to be the most stable form of the intermediate because both oxygen atoms, which are more electronegative than carbon atoms, contain the negative charges. The stereochemistry of this species is such that it will probably be protonated by water to form *cis* rather than *trans*. If a water molecule attacks the central carbon atom from the front side to form 6-β-d^-, it must contend with the large phenyl ring. If it attacks from the back side to form 1-β-d^-, it will find a smaller deuterium atom. Protonation on the back side should be favored.

A change in the hybridization of the α-carbon atom from sp to sp^2 which places the negative charge back onto the carbon atom leads to formation of an intermediate having the *trans* orientation (6-β-d^{2-}). This intermediate may then be protonated by water to form 6-β-d^-. The energetics of the system may not favor formation of 6-β-d^{2-} because of the difficulty in shifting electrons from a more electronegative oxygen atom to a less electronegative carbon atom.

According to reactions outlined in Fig. 30, intermediate 15 would be a common intermediate for both 1-α,β-d_2 and 6-α,β-d_2 exchange reactions. If 15 is the most stable form, it would be expected that exchange of the α-deuterium in α,β-dideutero-*trans*-cinnamic acid (6-α,β-d_2) would result in formation of β-deutero-*cis*-cinnamic acid (1-β-d). Since the isomerization rate from *trans*- to *cis*-cinnamic acid was found to be very small, this would suggest that 15 is not an important form.

The behavior of vinyllithium compounds with respect to their geometry has been the subject of several investigations. The isomers, *cis*- and *trans*-propenyllithium have been reported to hold their respective geometries during derivatization.[55] On the other hand, 1-silyl-1-alkenyllithium compounds readily isomerize to the *trans* form, while 1-alkoxy-1-alkenyllithium compounds slowly isomerize.[56] The silicon atom is thought to assist in the ionization of the carbon-lithium bond to provide a linear intermediate which then isomerizes to the more stable form.[57] Corresponding studies of vinylsodium compounds have not been reported.

In summary, the isomerization of *cis*-cinnamic acid was caused by an addition-elimination mechanism. Proton abstraction was not the rate-determining step since a secondary, rather than a primary, isotope effect was observed. Observation of α,β-dideutero-*trans*-cinnamic acid production is evidence that addition-elimination is the mode of isomerization. Proton abstraction clearly occurred but was not responsible for the *cis* to *trans* isomerization. It appears that vinyl carbanions are formed, that these hold their geometry long enough to be protonated, and that a linear allenic intermediate is not formed. This is the first case, to our knowledge, when carbanion geometry is held in a conjugated carbonyl system.

KINETIC STUDIES

The general rate expression for the disappearance of a reactant during an alkaline degradation is given by:[58]

$$\text{Rate} = d[R]/dt = -k\, f\{[R], [HO^-], [Add]\} \qquad (3)$$

where [R] = reactant concentration, mole L^{-1}

t = reaction time, sec

k = rate constant, sec^{-1}

$[HO^-]$ = hydroxide ion concentration, mole L^{-1}

[Add] = additive (hydrosulfide, AHQ ions, etc.) concentration, mole L^{-1}

The rate constant is a function of temperature, pressure, and ionic strength. Reactions of ions are strongly influenced by the ionic strength of the medium; activity coefficients of ions are more sensitive to ionic strength than those of neutral molecules due to the dependence of activity on equilibrium constants.[59] Reactions were conducted at constant temperature, pressure, and ionic strength so that the rate constants could be compared.

Large excesses of hydroxide ion and additive were used so that Eq. (3) was reduced to the following pseudo-first-order rate expression:

$$d[R]/dt = -k_r [R] \tag{4}$$

where [R] = reactant concentration, mol L^{-1}

k_r = pseudo-first-order rate constant for the disappearance of reactant, s^{-1}

Integration and rearrangement resulted in:

$$\ln [R] = -k_r t + \ln [R]_0 \tag{5}$$

where $[R]_0$ = initial reactant concentration, mol L^{-1}

Pseudo-first-order rate constants for the disappearance of reactant were calculated from Eq. (5) using a least squares regression technique. Pseudo-first-order kinetics was verified by showing the reaction followed Eq. (5) over two half lives (Fig. 31).[58] Using the estimate of standard error,

95% confidence intervals were calculated; a measure in the goodness of fit between data and the calculated regression line is given in the R^2 value.

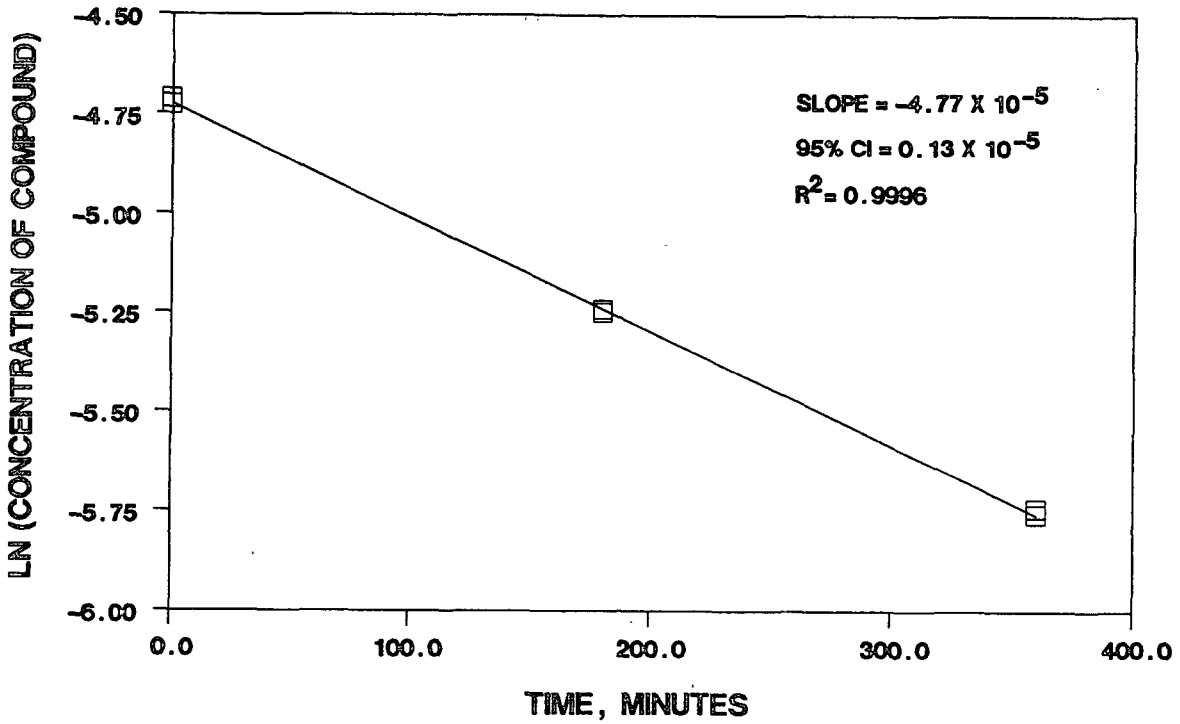

Figure 31. Verification of pseudo-first-order reaction kinetics for 1 at 195°C.

Reactions in the presence of both hydroxide ion and an additive were assumed to be parallel, independent reactions. Therefore, the pseudo-first-order rate constant determined in Eq. (5) is the summation of the rate constants of hydroxide ion and additive (HS^-, AHQ^{2-}) multiplied by their respective concentrations:

$$k_r = k_{HO}\,[HO^-] + k_{Add}\,[Add] \qquad (6)$$

where k_{HO} = rate constant associated with hydroxide ion, s^{-1}

$[HO^-]$ = concentration of hydroxide ion, mol L^{-1}

k_{Add} = rate constant associated with the additive, s^{-1}

[Add] = concentration of additive, mol L^{-1}

The reaction order of hydroxide ion (or additive) can be determined by varying its initial concentration ($[B]_1$ and $[B]_2$).[58] Using the observed rate constants from these reactions and the corresponding concentrations of B (hydroxide, hydrosulfide or anthrahydroquinone ions), the reaction order is solved using Eq. (7):

$$n_B = \frac{\log (d[R]/dt)_1 - \log (d[R]/dt)_2}{\log [B]_1 - \log [B]_2} \qquad (7)$$

Compound 1 was degraded in oxygen-free aqueous solutions which contained hydroxide, hydrosulfide, and anthrahydroquinone ions. Excesses of each reagent were used so that their concentrations remained essentially constant which allowed use of pseudo-first-order rate expressions. Because changes in the ionic strength of the medium could alter the observed reaction rate, the ionic strength was maintained at 0.78 μ except where noted. The reactions of 1 were extensively studied at 195°C. The reaction was briefly investigated at 171°C to determine the effect of temperature on nucleophilic order.

Data from three degradations of 1 in 0.787M sodium hydroxide solution at 194°C were used to determine the rate constant associated with hydroxide ion. The data were analyzed using Eq. (5) to determine the observed rate constant (Fig. 32). The specific rate constant was calculated using Eq. (6) from the observed rate constant; this data is tabulated in Table 4. The average value for k_{HO} is 4.30 ($\pm$ 0.30) x 10^{-5} sec^{-1}.

The hydroxide ion concentration was varied (0.79M versus 0.39M) to verify the reaction order.[58] Sodium chloride was added to maintain a constant ionic strength. Using the observed rate constant from this reaction

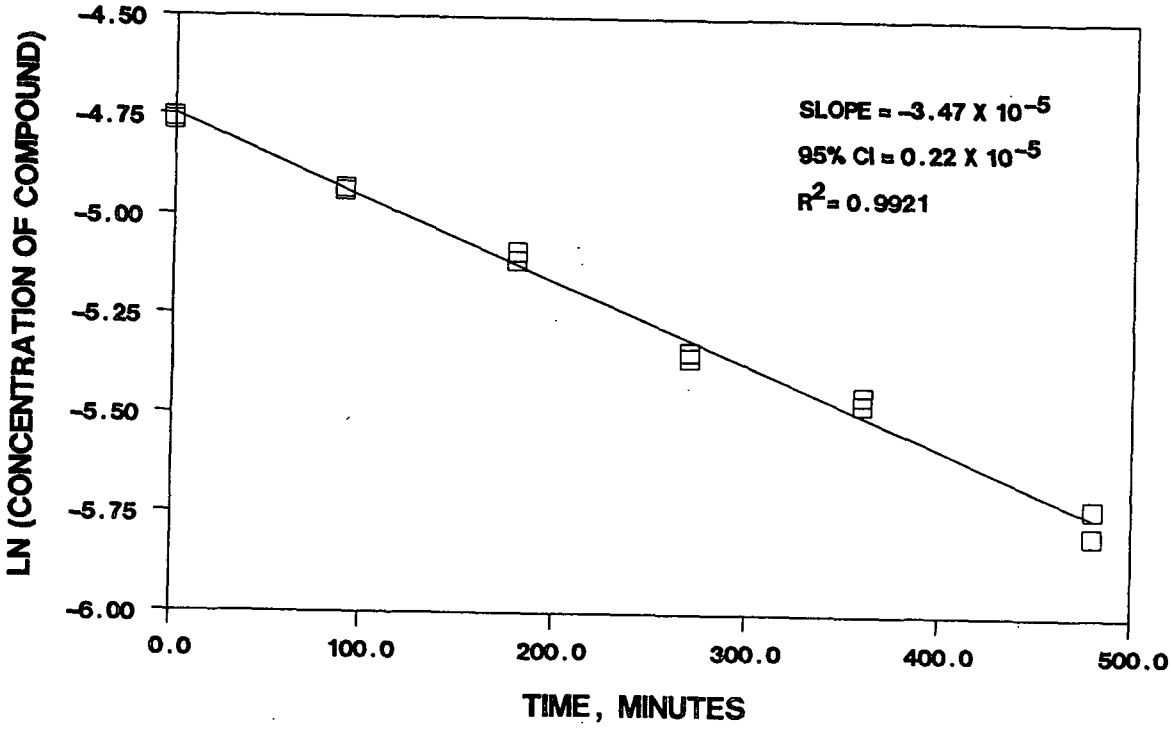

Figure 32. Pseudo-first-order reaction of 1 in 0.787M NaOH at 194°C.

Table 4. Degradation of 1 in a sodium hydroxide solution at 194°C.

Data Set	$10^5 \times k_{HO}$, sec^{-1}
I	4.41 ± 0.23
II	4.41 ± 0.28
III	4.07 ± 0.39

(Fig. 33) and Eq. (7), the reaction order was calculated to be 1.2. The reaction was, therefore, assumed to be first-order.

Data from three degradations of 1 in a solution containing 0.385M sodium hydroxide and 0.393M sodium hydrosulfide at 195°C were used to determine the rate constant associated with hydrosulfide ion. The data were analyzed using Eq. (5) to determine the observed rate constant (Fig. 34). The specific rate constant was calculated from the observed rate constant using

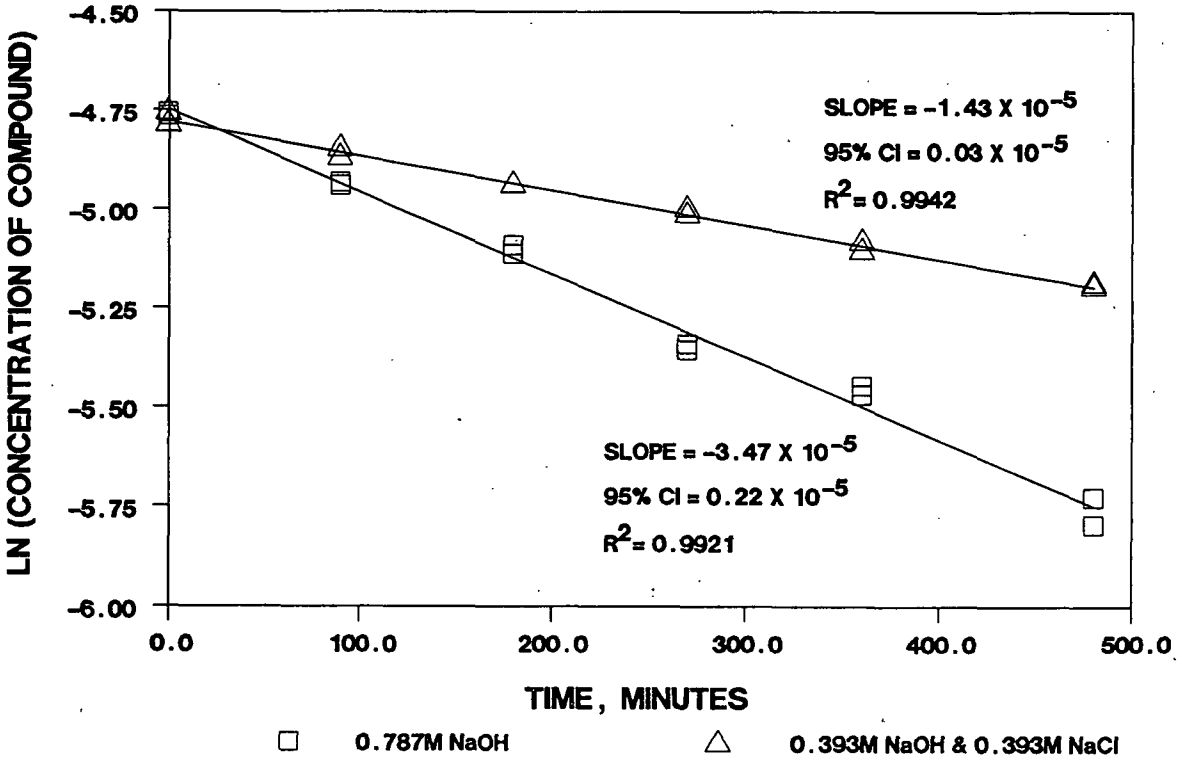

Figure 33. Determination of reaction order for hydroxide ion at 195°C.

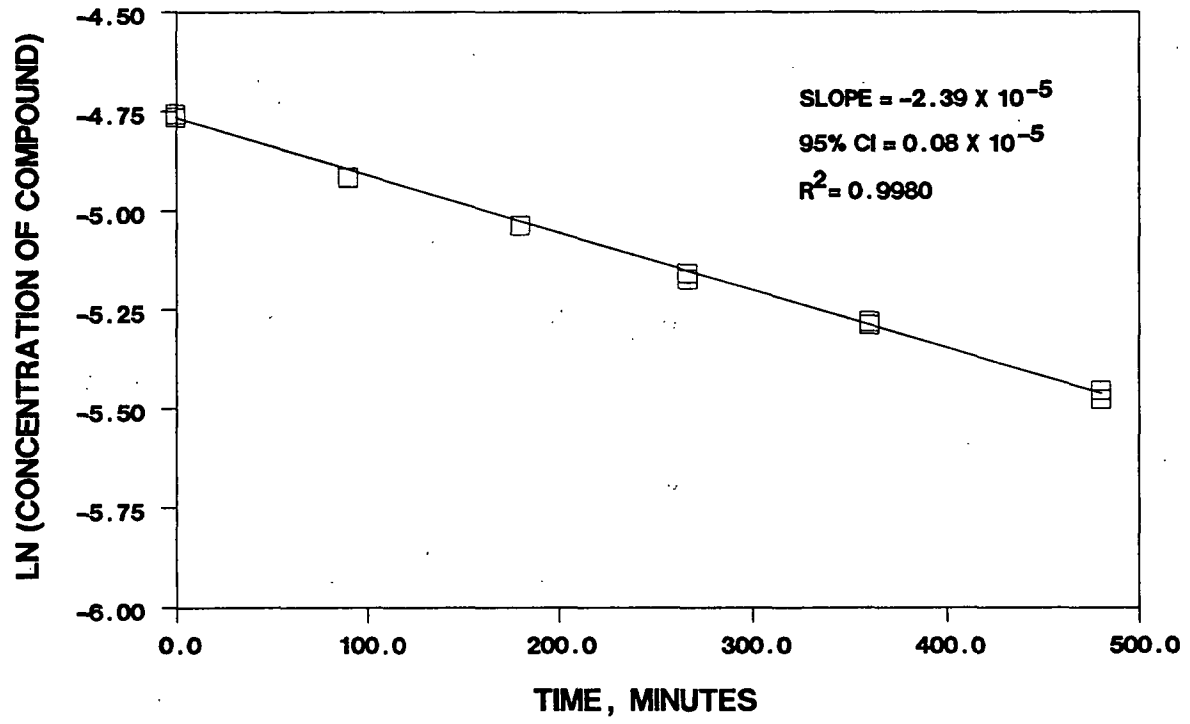

Figure 34. Pseudo-first-order reaction of 1 in 0.385M NaOH & 0.393M NaSH at 195°C.

Eq. (6) (Table 5). The average value for k_{HS} is 1.88 (± 0.46) x 10^{-5} sec^{-1}. The experimental error is propagated through each manipulation giving large confidence intervals in the final result.[60]

Table 5. Degradation of 1 in a sodium sulfide solution at 195°C.

Data Set	10^5 x k_{HS}, sec^{-1}
I	1.88 ± 0.49
II	1.58 ± 0.46
III	2.19 ± 0.44

Analysis of the sulfide solution used in these reactions showed there was a significant amount of sulfoxy species (Table 6). Of prime importance was the level of sulfite and thiosulfate ions. These ions are known to have nucleophilicities similar to that of hydrosulfide ion.[9]

Table 6. Composition of prepared sodium sulfide solutions.

Solution	Na_2S, M	Na_2SO_3, M	Na_2SO_4, M	$Na_2S_2O_3$, M
I - fresh	0.945	0.056	0.0058	0.019
I - 1 wk old	0.932	0.048	0.0059	0.021
II - fresh	1.47	0.086	0.0077	0.022

The reactions of sulfite and thiosulfate ions with 1 at 195°C were then investigated. Compound 1 was degraded in one solution containing 0.870M sodium hydroxide and 0.0881M sodium sulfite and in a second solution containing 0.870M sodium hydroxide and 0.0890M sodium thiosulfate. Analysis of the data showed both sulfite and thiosulfate ions were more reactive than hydrosulfide and hydroxide ion (Table 7). The high reactivity of these species toward unsaturated carbon centers has not been reported. The effect of these species (which would be present in pulping liquors) on the degradation of

quinonemethides may be of some importance. Large confidence intervals are the result of having only one degree of freedom for their calculation.

Table 7. Reaction rate constants of 1 at 195°C.

	Rate constant x 10^5, sec^{-1}
SO_3^{2-}	23.0 ± 4.2
$S_2O_3^{2-}$	10.1 ± 8.7

The reactivity of hydrosulfide and sulfite ions was further investigated to determine the reaction order of these species as well as to test their additive effects. Thiosulfate ion was not tested because of the combination of its lower concentration and lower rate constant in comparison to sulfite ion. The contribution of thiosulfate ion, therefore, was considered minor (less than 5%) when compared to sulfite ion (possibly as high as 50%). Compound 1 was degraded at 195°C under conditions shown in Fig. 35. Rate constants were calculated using the rate constant for hydroxide ion of 4.30 x 10^{-5} sec^{-1} (Table 8).

The data from Table 8 reveal a number of trends. The reaction order for sulfite ion was first-order based on the two observed rate constants. Changes in the concentrations of hydroxide or sulfite do not alter the rate constant. The rate constants from the reactions of hydrosulfide ion, however, are not constant and appear to vary with changes in the hydroxide concentration. There also appears to be a synergism between hydrosulfide and sulfite based on the high rate constant observed when both hydrosulfide and sulfite are together in significant quantities. A synergism between hydrosulfide and sulfite ions has been noted in pulping studies.[61]

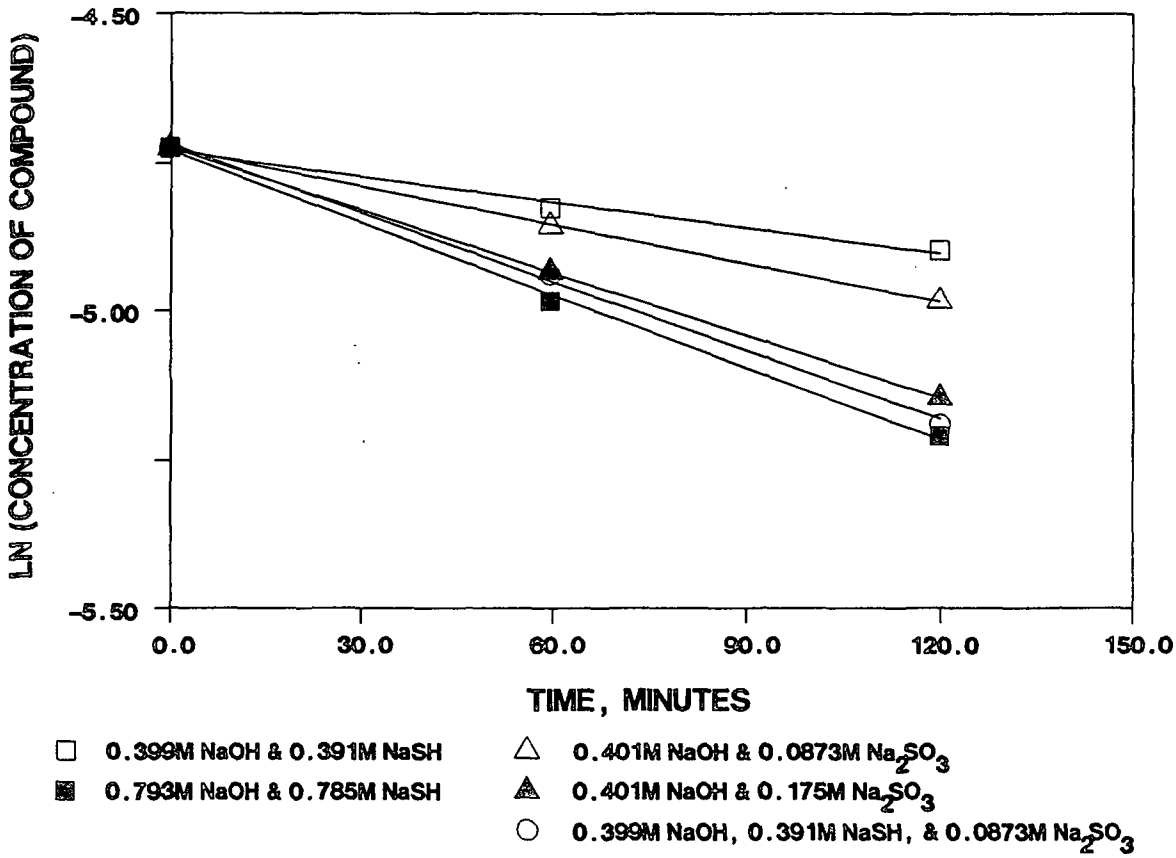

Figure 35. Comparison of reaction rates for 1 under the above conditions at 195°C.

Table 8. Reaction rate constants of 1 at 195°C.

Conditions				
NaOH, M	NaSH, M	Na_2SO_3, M	$10^5 \times k_{HS}$, sec^{-1}	$10^5 \times k_{SO3}$, sec^{-1}
0.399	0.391	-	1.58	-
0.793	0.785	-	4.14	-
0.401	-	0.0873	-	20.4
0.401	-	0.175	-	23.1
0.399	0.391	0.0873	6.92	used avg of 22.2
1.04	0.176	-	5.49	-
0.523	0.523	-	2.60	-

The data shown in Table 8 was examined to determine the source of inconsistency in rate constants. The data was analyzed to determine if

sulfide ion (S^{2-}) influenced the reaction rate. The concentrations of HS^- and S^{2-} were calculated under the above conditions. The equilibrium constant K_2 was varied between 10^{-12} and 10^{-17} for the calculation of $[HS^-]$ and $[S^{2-}]$. There appeared to be no correlation between the concentration of sulfide ion and the increased reaction rate at high hydroxide ion concentrations.

The reaction scheme shown in Fig. 36 was postulated as a possible explanation for the increased reaction rate at higher hydroxide concentrations. Addition to the carbon-carbon double bond is a relatively slow step. The reverse reaction, however, is very fast so that the lifetime for the intermediate adduct is very short. If the adduct is ionized by hydroxide ion, the lifetime of the adduct is substantially increased because the leaving ability of S^{2-} would be much less than that of HS^-.[8] The ionized adduct then will have more time to rearrange and subsequently eliminate hydrosulfide ion (after reprotonation) to form *trans*-cinnamic acid. In effect, the slow step would then appear to be rearrangement rather than addition.

This reaction pathway would include a second hydroxide ion term in the kinetic expression describing the rate of degradation:

$$k_r = k_{HO}\,[HO^-] + k_{HO\text{-}HS}\,[HO^-]\,[HS^-] \qquad (8)$$

The rate constant $k_{HO\text{-}HS}$ was determined using Eq. (8) and the data in Table 8. The values of $k_{HO\text{-}HS}$ (Table 9) appear to be constant over the range of reaction conditions. Variations appear to be dependent on the experimental error rather than true differences.

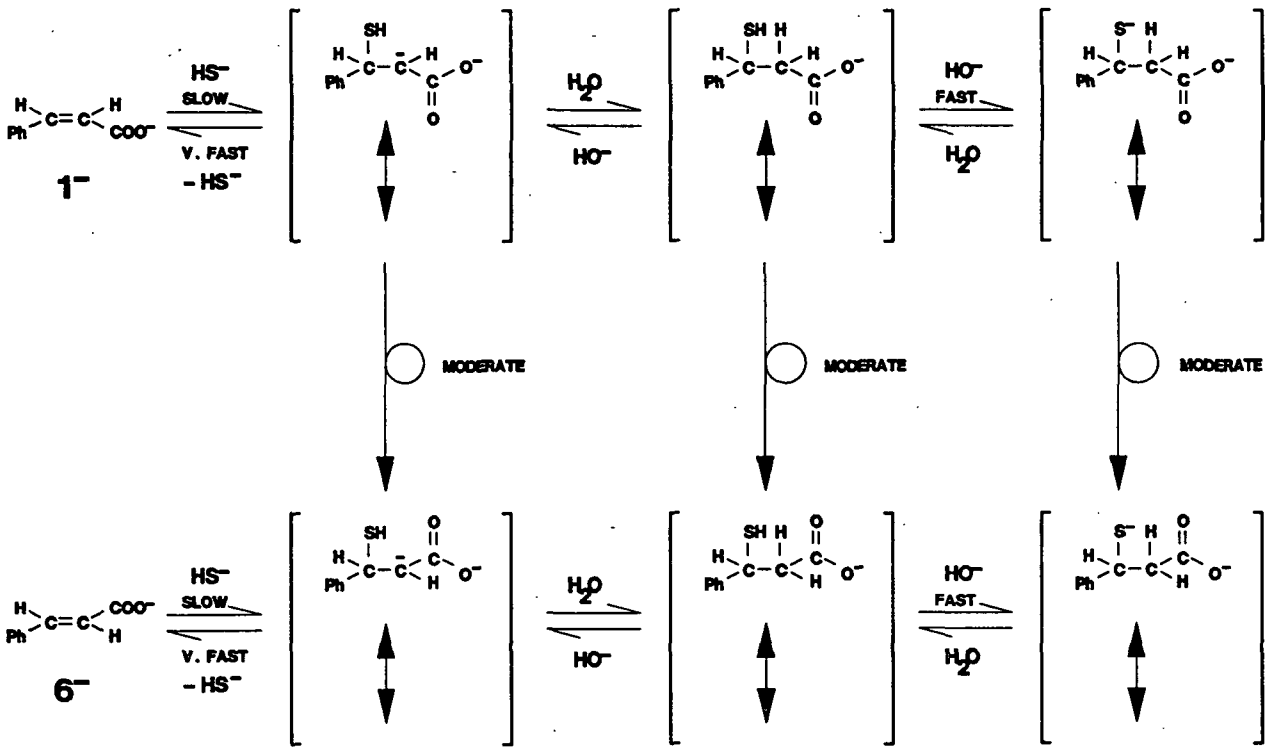

Figure 36. Interaction of hydroxide ion during the degradation of 1 in a solution containing both hydroxide and hydrosulfide ions at 195°C.

Table 9. Determination of k_{HO-HS} over reaction conditions.

$10^5 k_r$, sec^{-1}	NaOH, M	NaSH, M	$10^5 k_{HO-HS}$, $M^{-2} sec^{-1}$
5.57 ± 0.21	1.06	0.175	5.46 ± 2.84
3.69 ± 0.07	0.536	0.523	4.94 ± 0.82
2.39 ± 0.08	0.385	0.393	4.85 ± 1.29
2.28 ± 0.06	0.385	0.393	4.13 ± 1.16
2.52 ± 0.06	0.385	0.393	5.71 ± 1.16
2.35 ± 2.66	0.399	0.391	4.07 ± 17.8
6.70 ± 2.53	0.793	0.785	5.29 ± 4.45

The slow step in the reaction of *cis*-cinnamic acid with hydrosulfide ion appears to involve rearrangement. An increase in hydroxide concentration increases the isomerization rate (Table 9). Hydrosulfide ion apparently is such a good leaving group that it is eliminated before the adduct can rearrange to set the configuration for *trans*-cinnamic acid. At high concentra-

tions of hydroxide ion, the frequency of successful conversion to the *trans* isomer by the addition of hydrosulfide ion appears to be similar to the reaction rate of hydroxide ion. The nucleophilicity of hydrosulfide ion, therefore, appears to be similar to that of hydroxide ion. A definitive value for the nucleophilicity of hydrosulfide ion, however, cannot be given due to the complex nature of the reactions.

Data from four degradations of 1 in solutions containing approximately 0.44M sodium hydroxide and 0.12M anthrahydroquinone were used to determine the rate constant associated with anthrahydroquinone ion. The data were analyzed using Eq. (5) to determine the observed rate constant (Fig. 37). The specific rate constant was calculated from the observed rate constant using Eq. (6); this data is tabulated in Table 10. The average value for k_{AHQ} is 9.03 (± 3.80) x 10^{-5} sec^{-1}.

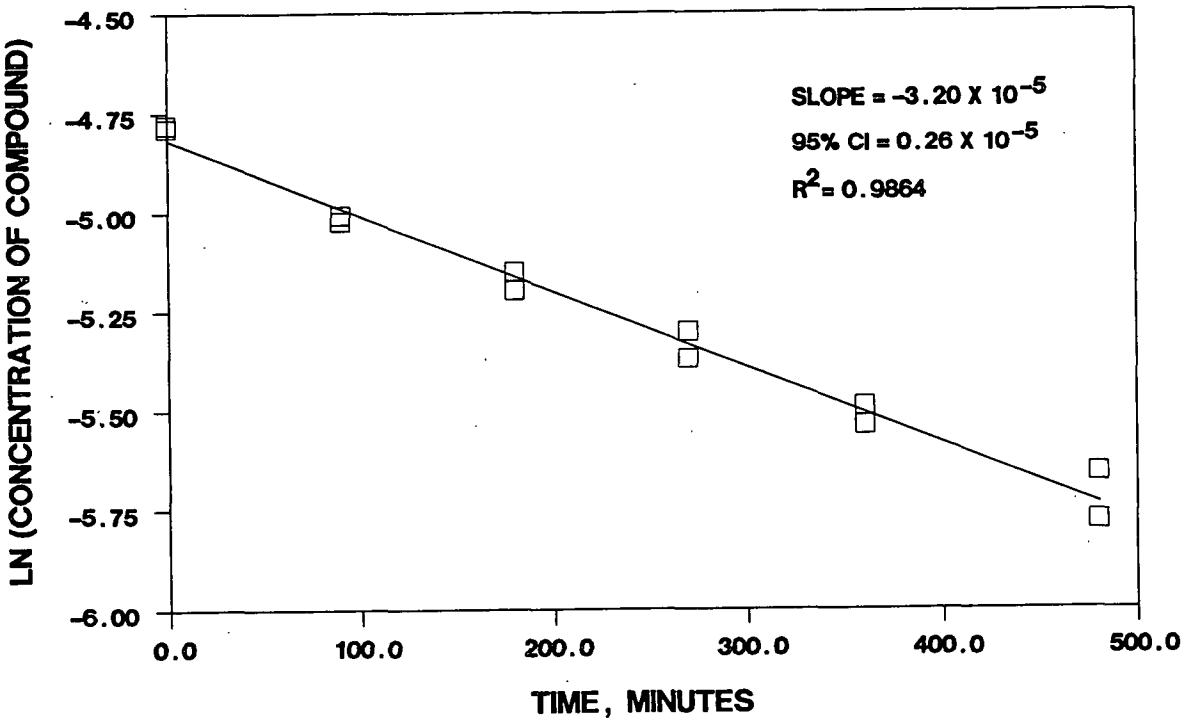

Figure 37. Pseudo-first-order reaction of 1 in 0.435M NaOH & 0.118M AHQ at 195°C.

Table 10. Degradation of 1 in a sodium hydroxide/AHQ solution at 195°C.

Data Set	$10^5 \times k_{AHQ}$, sec^{-1}
I	9.98 ± 4.25
II	7.42 ± 3.23
III	11.23 ± 3.34
IV	7.48 ± 4.39

Because the slow step in the reaction of hydrosulfide ion with 1 was found to be rearrangement and not addition, a similar set of experiments was outlined to determine if different concentrations of hydroxide ion altered the apparent rate constant associated with anthrahydroquinone ion. The concentrations of hydroxide and anthrahydroquinone ions were varied to verify its reaction order and to determine any effect by hydroxide ion. Analysis of the data (Fig. 38) showed that the reaction order of AHQ^{2-} was approximately one. The rate constant associated with anthrahydroquinone ion, however, increased with increased hydroxide ion concentration. Anthrahydroquinone ion is apparently a very good leaving group. The AHQ-adduct may need to be ionized in order for the adduct to have a sufficient lifetime to rearrange into the *trans* configuration.

Rate constants of the reaction of 1 with hydroxide, hydrosulfide, and anthrahydroquinone ions are shown in Table 11. The observed rate constants, calculated using Eqs. (5) and (6), were determined under specific reaction conditions. The true nucleophilic constants associated with hydrosulfide and anthrahydroquinone ions appear to be greater than those reported in Table 11. The rate constants measure the number of reactions which cause the isomerization of 1. Hydrosulfide and anthrahydroquinone ions, however, appeared to add to the double bond at a greater rate than that measured by isomerization. Based on the entire set of data, anthrahydroquinone ion

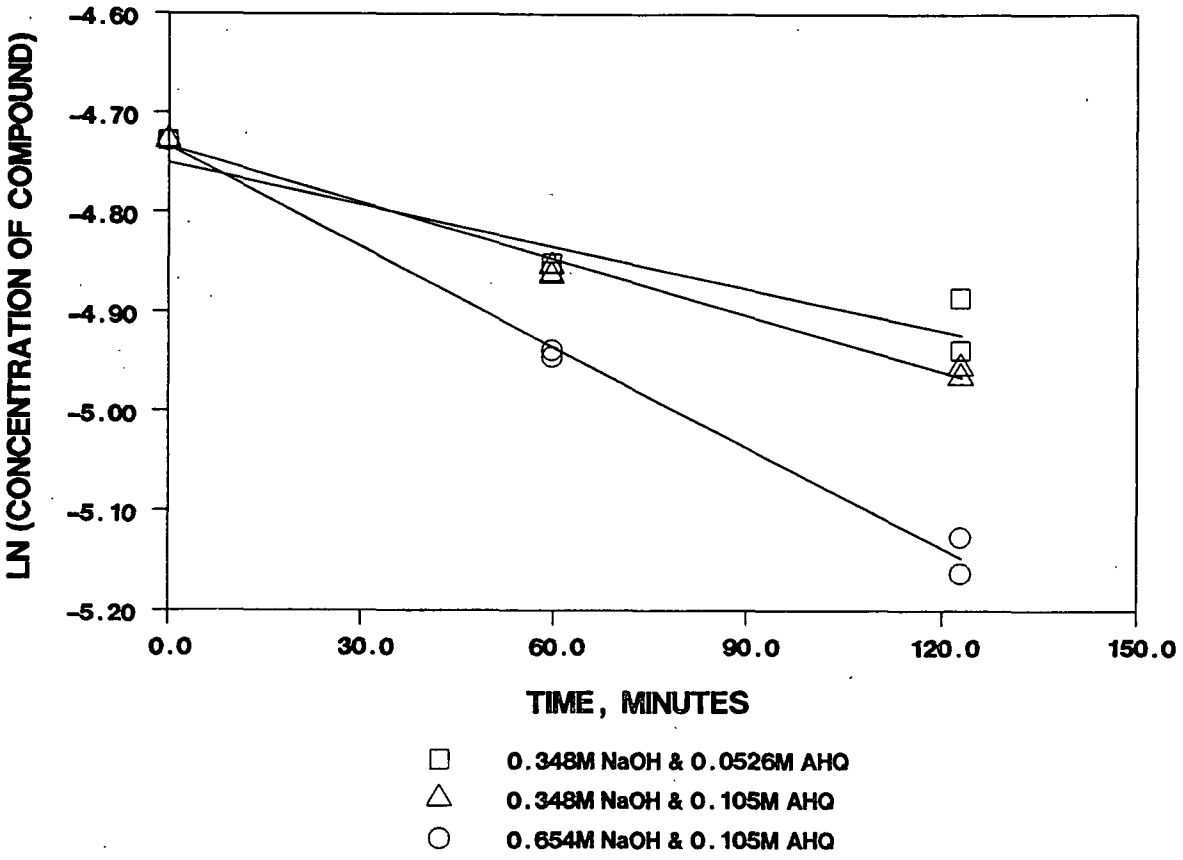

Figure 38. Comparison of observed reaction rates when the concentrations of hydroxide and anthrahydroquinone ions are varied at 195°C.

Table 11. Reaction rate constants of **1** at 195°C.

	10^5 k, sec^{-1}	k_{rel}
NaOH	4.30	1.0
NaSH	1.88	0.44
Na_2AHQ	9.03	2.1

appeared to be the most reactive species toward unsaturated carbon centers, followed by hydroxide and hydrosulfide ions. Hydroxide and hydrosulfide ions appeared to be of similar nucleophilic strength.

Rate constants for reactions investigated at 171°C were also determined (shown in Table 12) under conditions similar to the degradations de-

scribed in Table 11. The relative nucleophilic order ($AHQ^{2-} > HO^- > HS^-$) did not change by lowering the reaction temperature. The relative strength of hydrosulfide and anthrahydroquinone ions increased which may suggest that hydroxide ion was more solvated at 171°C. If the data in Tables 11 and 12 were extrapolated to lower temperatures, a change in nucleophilic order may exist.

Table 12. Reaction rate constants of 1 at 171°C.

	10^6 k, sec^{-1}	k_{rel}
NaOH	7.56	1.0
NaSH	6.77	0.90
Na_2AHQ	22.9	3.0

SUMMARY

The results of this study can be related to our understanding of pulping reactions. Quinonemethides may undergo addition-elimination reactions at an unsaturated carbon center similar to those observed for *cis*-cinnamic acid. The driving force behind the reaction of *cis*-cinnamic acid is formation of a more thermodynamically stable product; the energy difference between *cis* and *trans* is approximately 3-7 kcal mol^{-1}.[62] On the other hand, the driving force behind quinonemethide addition is aromatization of the benzene ring, approximately 36 kcal mol^{-1}.[8] The quinonemethide, therefore, should be much more reactive.

Although quinonemethides and *cis*-cinnamic acid exhibit large differences in their reactivity, the reaction mechanism in both cases is likely addition to a conjugated carbonyl carbon center. Use of *cis*-cinnamic acid gives us information concerning the type of nucleophile which is most attractive to quinonemethides. If the results of the *cis*-cinnamic acid investiga-

tion can be extended to quinonemethides, anthrahydroquinone ion would appear to be a very reactive species with quinonemethides. The reason for this enhanced reactivity may be that AHQ^{2-} is more nucleophilic than hydroxide or hydrosulfide ions. Hydroxide and hydrosulfide ions appear to compete for quinonemethides at near equal levels.

DEGRADATION OF 3-[3′-(α,α,α-TRIFLUOROMETHYL)PHENOXYMETHYL]BENZOIC ACID

MECHANISTIC STUDIES

The degradation of compound **2** was investigated in oxygen-free water solutions which contained hydroxide, hydrosulfide, and anthrahydroquinone ions. The degradation of **2** and formation of products was followed using GLC techniques. The identity of all products were confirmed by synthesizing or purchasing the products and comparing their GLC and GLC-MS properties.

Compound **2** was heated in aqueous sodium hydroxide to simulate soda pulping reactions. The expected products were observed. Hydroxide ion displaced the phenolate ion (**10**) to form the primary product, 3-(α-hydroxymethyl)benzoic acid (**7**) (Fig. 39). Analysis of the reaction products, shown in Fig. 40, indicated roughly a 100% mass balance when adding the concentrations of **2** and **7**; less than a perfect balance existed when adding the concentrations of **2** and **10**.

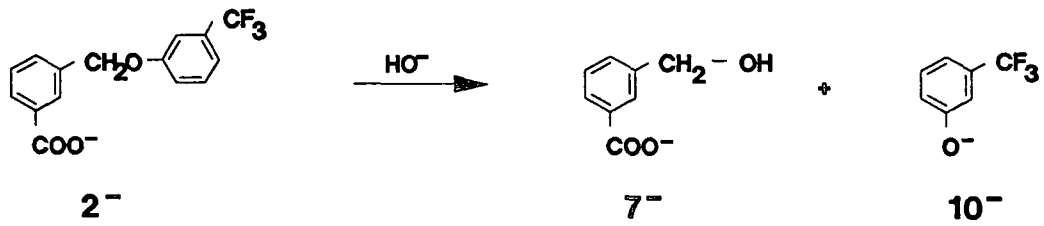

Figure 39. Reaction of **2** in the presence of hydroxide ions at 195°C.

The stability of products **7** and **10** were investigated. Compound **7** did not react with hydroxide ion to form secondary products. Compound **10**, however, degraded after extended reaction times. Its concentration decreased by approximately 40% over a six hour period at 195°C. The presence of hydrosulfide ion had no detectable effect on the degradation rate. Degradation

products of this reaction were not determined by GLC-MS. Resorcinol, a possible product of hydroxide substitution at the site of the trifluoromethyl group on **3**, was not observed. Resorcinol was also found to degrade under similar conditions except at a slower rate.

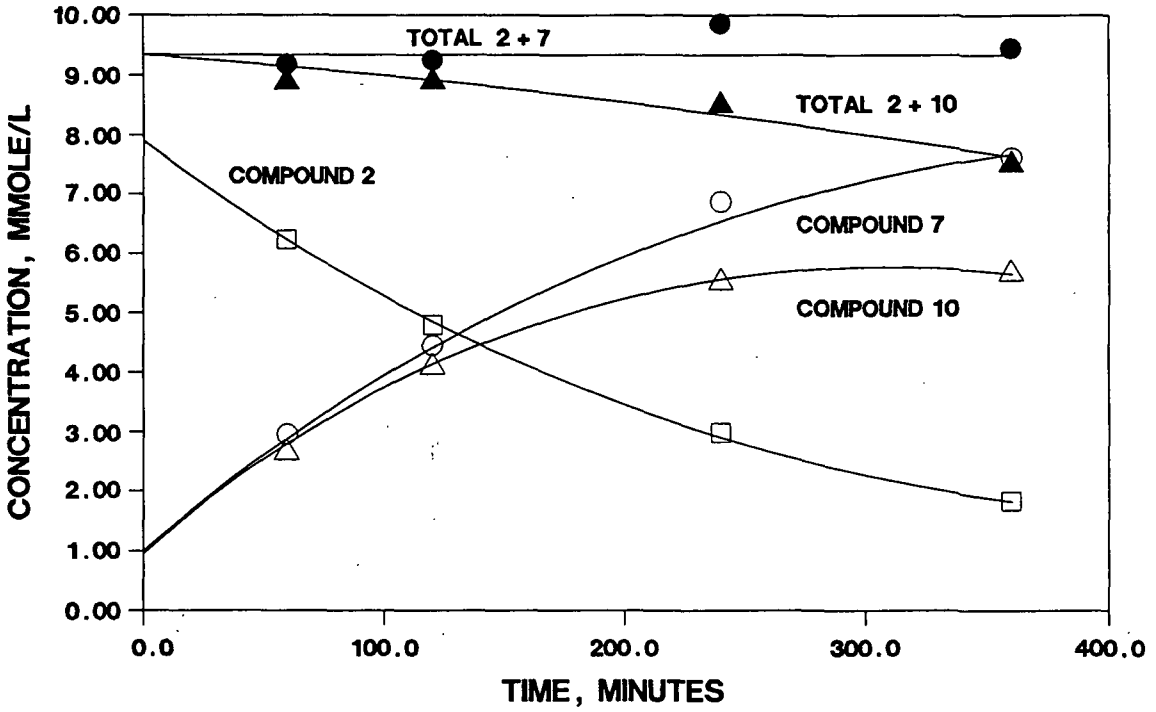

Figure 40. Mass balance for the reaction of **2** in 1.04M NaOH at 195°C.

Reactions similar to those which caused the degradation of **10** did not consume the starting material. The mass balance between **2** and the primary product, **7**, was constant while that between **2** and the product phenol, **10**, was not constant at extended reaction times; indicating only **10** was unstable.

Compound **2** was heated in solutions containing both hydroxide and hydrosulfide ions to simulate kraft pulping reactions. Sodium sulfide was assumed to be completely hydrolyzed in these reactions.[18] The primary products of the reaction were expected to be compound **7**, the phenolate ion (**10**) and 3-(α-mercaptomethyl)benzoic acid (**8**) (Fig. 41). Analysis of the reaction

mixture showed a good mass balance between 2 and 10 (Fig. 42). Compound 7, which was found to be stable to hydrosulfide ion, was observed in trace amounts; this was indicative that hydrosulfide ion is a strong nucleophile. Compound 8, however, was not observed. Instead, three secondary products, 3-toluic acid (16), isophthalic acid (17), and 3-(3'-carboxybenzylthiomethyl)-benzoic acid (13) were detected.

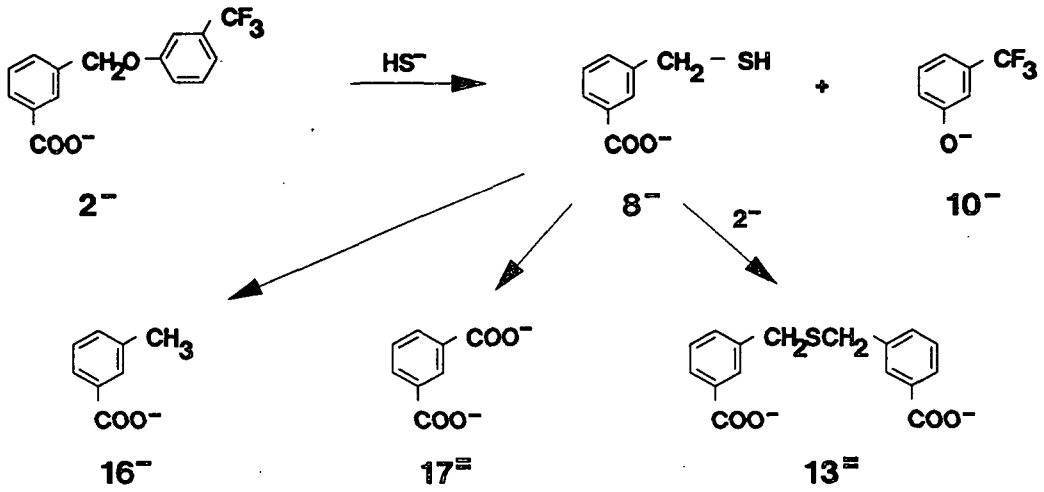

Figure 41. Reaction of 2 in the presence of hydrosulfide ions at 195°C.

An independently synthesized sample of compound 8 was degraded under a variety of conditions to determine mechanisms responsible for formation of 16-17. The following reaction mechanism was postulated (Fig. 43). In the presence of hydroxide ions, compound 8 degraded at a moderate rate to form primarily 16 with small amounts of 17. Mercaptan 8 could lose elemental sulfur and be protonated by water to form 16. Starting material 2 and intermediate 8 were reacted in a sodium deuteroxide/deuterium oxide solution to test for loss of elemental sulfur. Analysis of both product mixtures by GC-MS showed there was incorporation of one deuterium atom into the methyl group. This evidence supports the conclusion that the source of product 16 was the result of carbanion formation. In the presence of hydrosulfide ions or

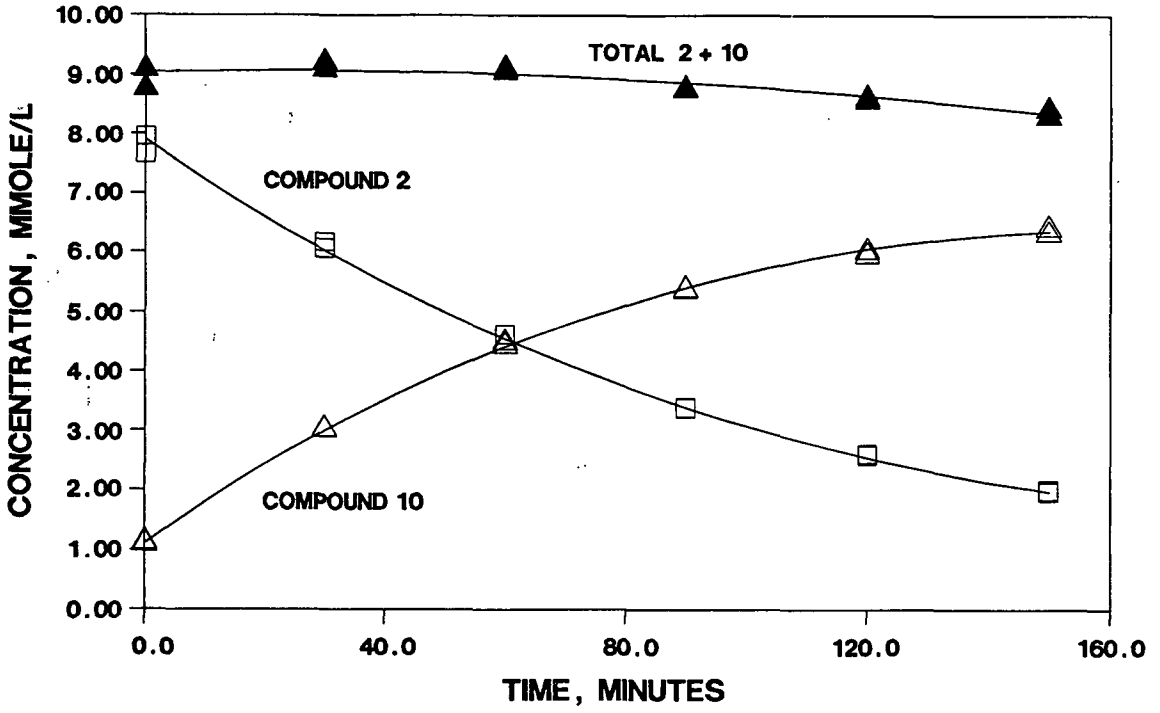

Figure 42. Mass balance for the reaction of 2 in 0.958M NaOH & 0.0874M NaSH at 195°C.

elemental sulfur, however, compound 8 was very rapidly converted to mainly 17 with lesser amounts of 16. Polysulfide, formed from elemental sulfur, may act as an oxidant to form 17.

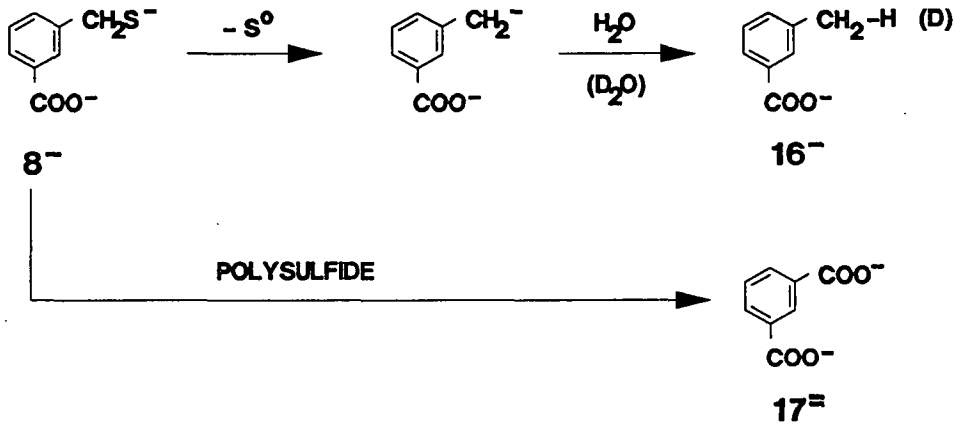

Figure 43. Degradation of 8 at 195°C to form stable products.

Compound **8** was also reacted with **2** to determine the source of 3-(3'-carboxybenzylthiomethyl)benzoic acid (**13**). Analysis of the product mixture showed formation of **16** and **17** as well as **13**. Compound **13** apparently is formed by the nucleophilic attack of **8** on the starting material.

The stability of compound **13** was also investigated. This compound did not appear to react in solutions containing hydroxide and hydrosulfide ions. In addition, the degradation rate of **2** was virtually unaffected by the presence of the dimer (Fig. 44). Compound **13**, therefore, was considered to be a stable end product.

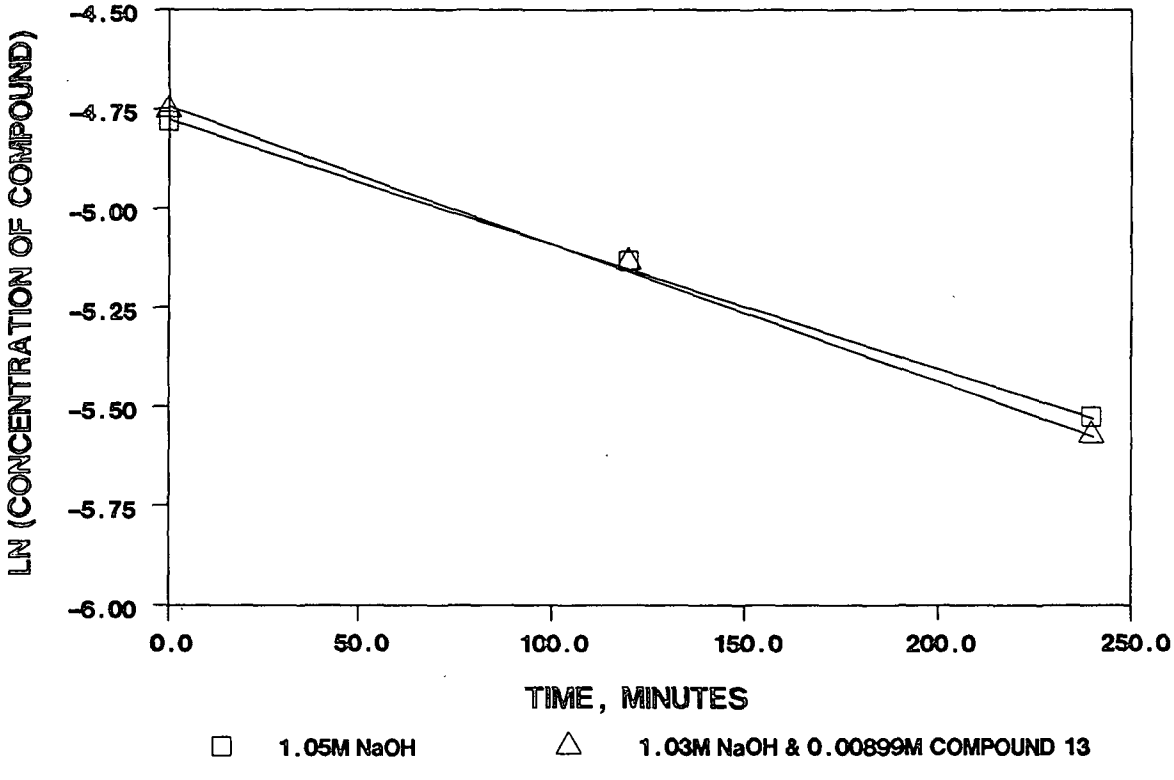

Figure 44. Comparison of reaction rate of **2** at 195°C in the presence of **13**.

Compound **2** was degraded in solutions containing both hydroxide and anthrahydroquinone ions to simulate soda-AQ pulping reactions. The expected primary products were compound **7**, the phenolate ion (**10**) and 10-hydroxy-10-

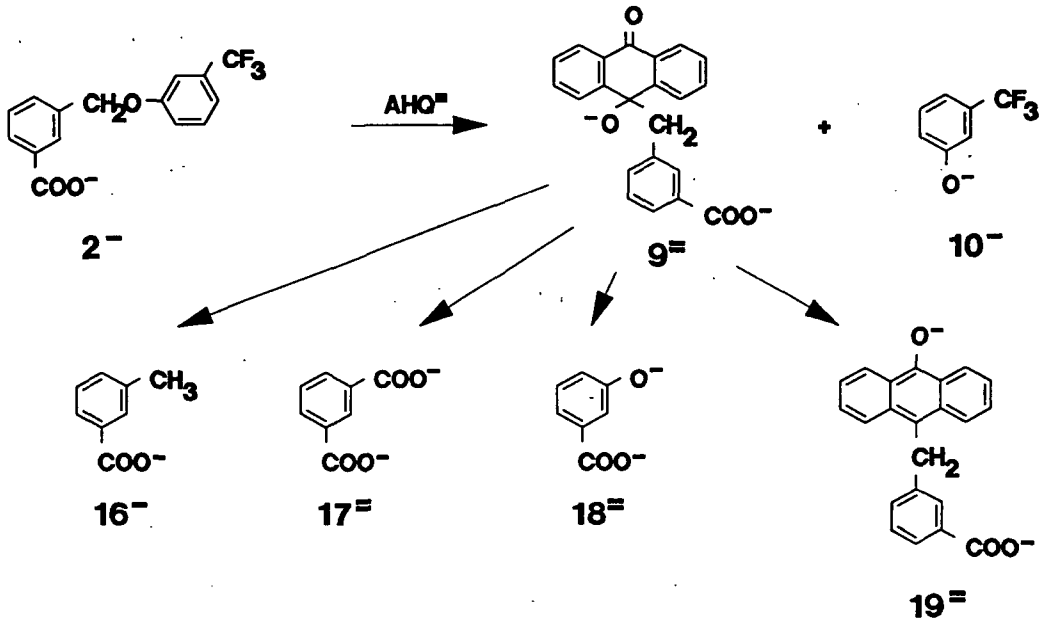

Figure 45. Reaction of 2 in the presence of anthrahydroquinone ions at 195°C.

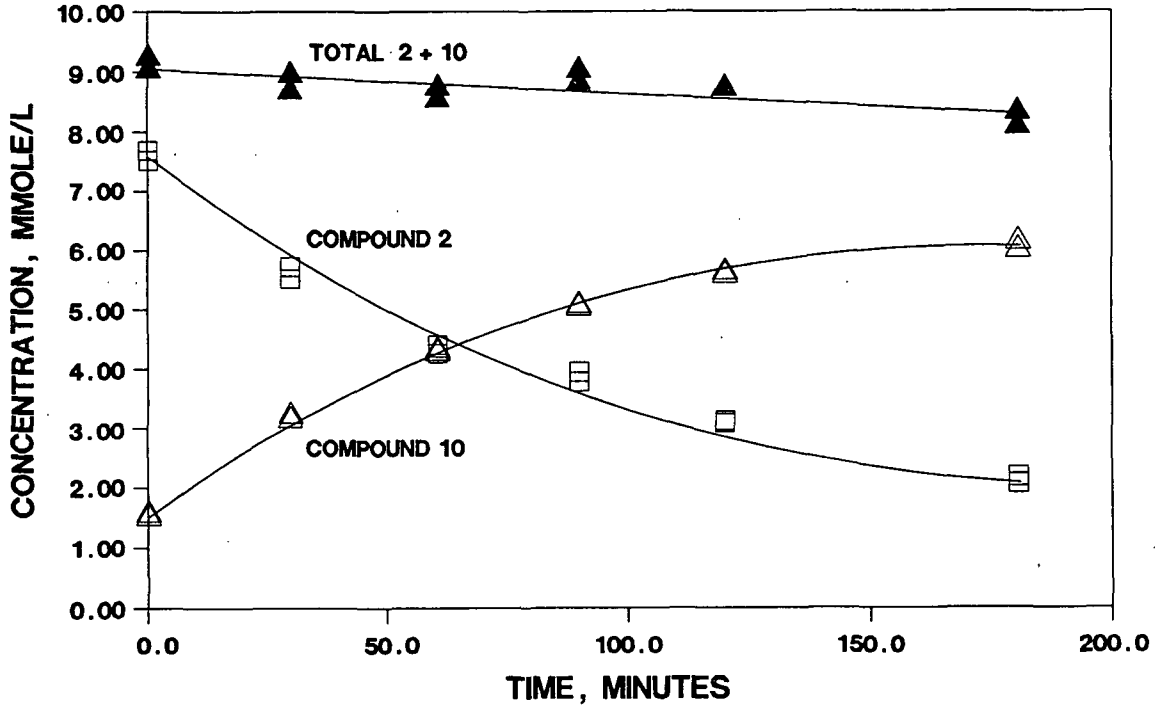

Figure 46. Mass balance for the reaction of 1 in 0.785M NaOH & 0.0872M AHQ at 195°C.

(3′-carboxybenzyl)-9(10*H*)-anthracenone (**9**) (Fig. 45). Analysis of the reaction mixture showed a good mass balance between **2** and **10** (Fig. 46). Again, compound **7** was observed in trace amounts, indicative of the greater nucleophilicity of anthrahydroquinone ion. Compound **9**, however, was observed in only trace amounts. Instead, a number of secondary products, including **16** and **17**, were detected. Moderate amounts of compounds **18** and **19** were also identified by GC-MS. The anthrone-coupled product **14** (p. 41) was also detected.

Compounds **9** and **19** were detected as methylated derivatives after reaction samples were treated with both dimethyl sulfate and diazomethane. Dimethyl sulfate is necessary to methylate the phenolic and aliphatic hydroxyl groups, and diazomethane is used to prepare methyl esters.

The reactions of the compound **9** were investigated to determine its degradation pathways. An independently synthesized sample of **9** was found to degrade to primarily **16** and **17** in soda and soda-AHQ reactions. Minor components of the reaction mixture included compounds **14**, **18**, and **19**. Compound **14** was also formed under reaction conditions in AHQ solutions which did not contain model compounds or their degradation products. Based on these findings, it was concluded that anthrahydroquinone reacted with compound **2** to form primary product **9**, and that product **9** decomposed to form the secondary products **16-19**.

KINETIC STUDIES

Compound **2** was degraded in oxygen-free aqueous solutions which contained hydroxide, hydrosulfide, and anthrahydroquinone ions. Excesses of each reagent were used so that their concentrations remained essentially constant

which allowed use of pseudo-first-order rate expressions. Because changes in the ionic strength of the medium could alter the observed rate constant, the ionic strength was maintained at 1.05 μ except where noted. A temperature of 195°C was also maintained for all reactions.

As in the high temperature reactions of 1, compound 2 was heated over two half-lives to verify that the reaction followed Eq. (5). This data is shown in Fig. 47.

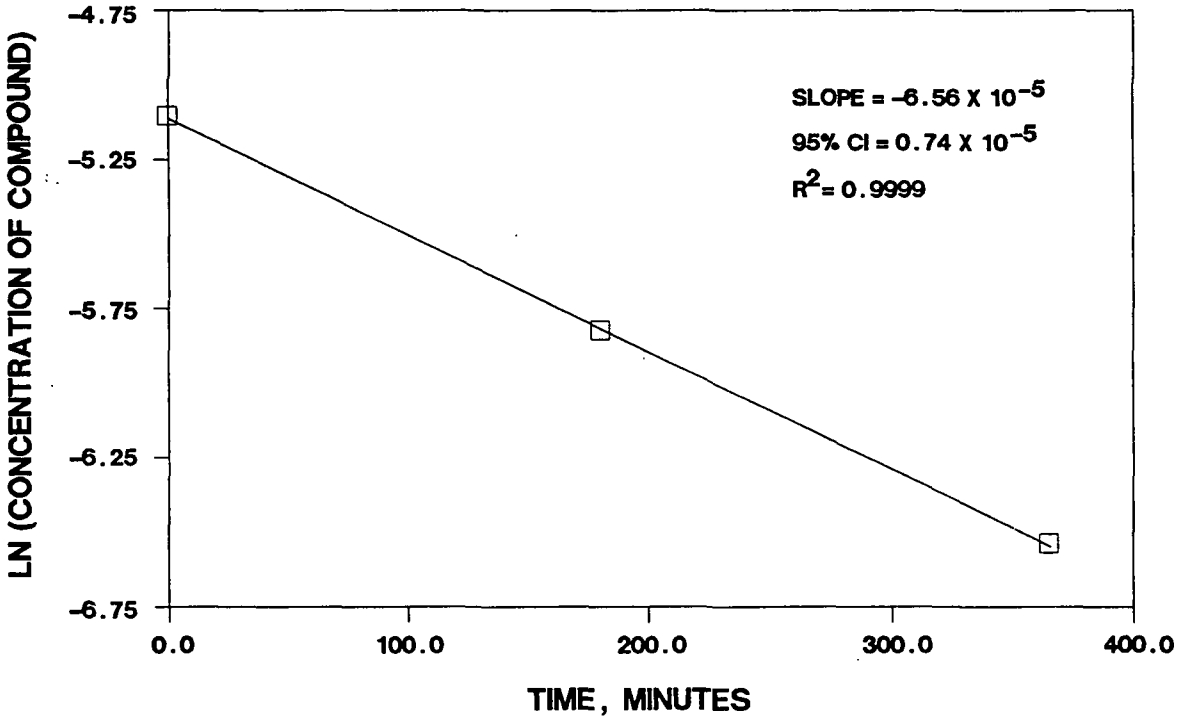

Figure 47. Verification of pseudo-first-order reaction kinetics of 2 at 195°C.

Data from three degradations of 2 in 1.05M sodium hydroxide solution at 195°C were used to determine the rate constant associated with hydroxide ion. The data were analyzed using Eq. (5) to determine the observed rate constant (Fig. 48). The specific rate constant was calculated from the observed rate constant using Eq. (6) (Table 13). The average value for k_{HO} is 5.20 ($\pm$ 0.07) x 10^{-5} sec^{-1}.

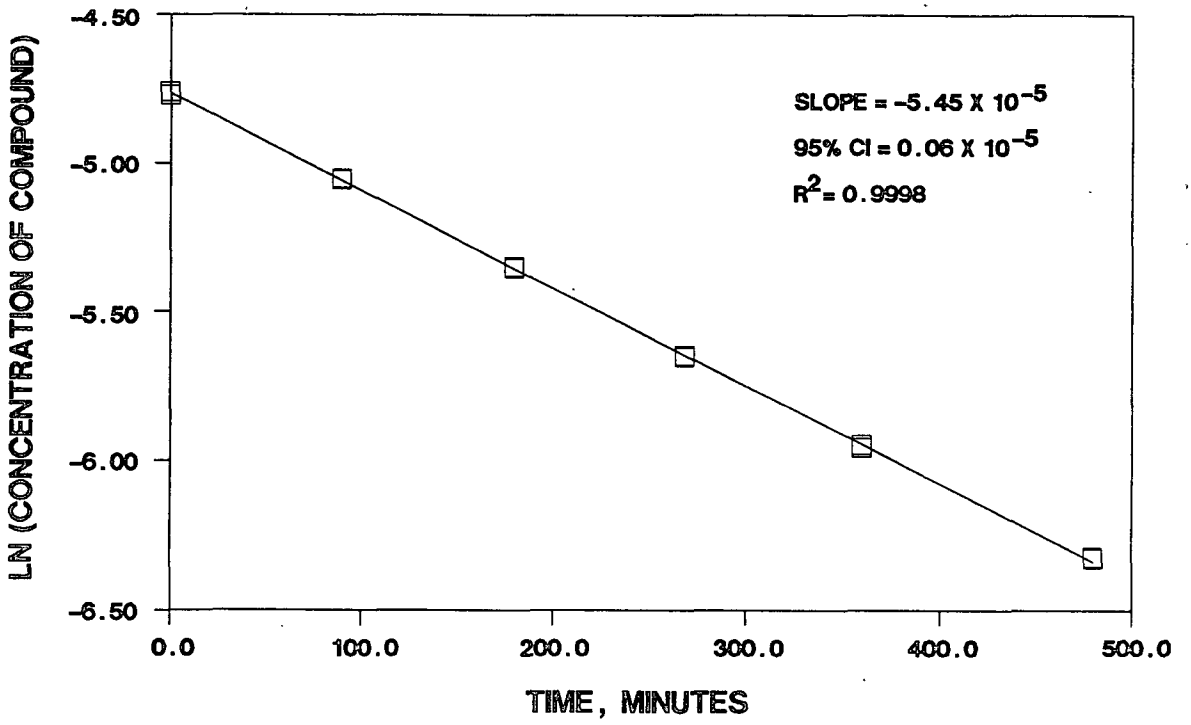

Figure 48. Pseudo-first-order reaction of 2 in 1.05M NaOH at 195°C.

Table 13. Degradation of 2 in a sodium hydroxide solution at 195°C.

Data Set	$10^5 \times k_{HO}$, sec^{-1}
I	5.20 ± 0.05
II	5.24 ± 0.08
III	5.15 ± 0.08

The hydroxide ion concentration was varied (1.05M versus 0.519M) to verify the reaction order.[58] Using the observed rate constants from these reactions (Fig. 49) and Eq. (7), the reaction order was calculated to be 1.1. The reaction was, therefore, assumed to be first-order.

Data from three degradations of 2 in a solution containing 0.958M sodium hydroxide and 0.0873M sodium hydrosulfide at 195°C were used to determine the rate constant associated with hydrosulfide ion. The data were

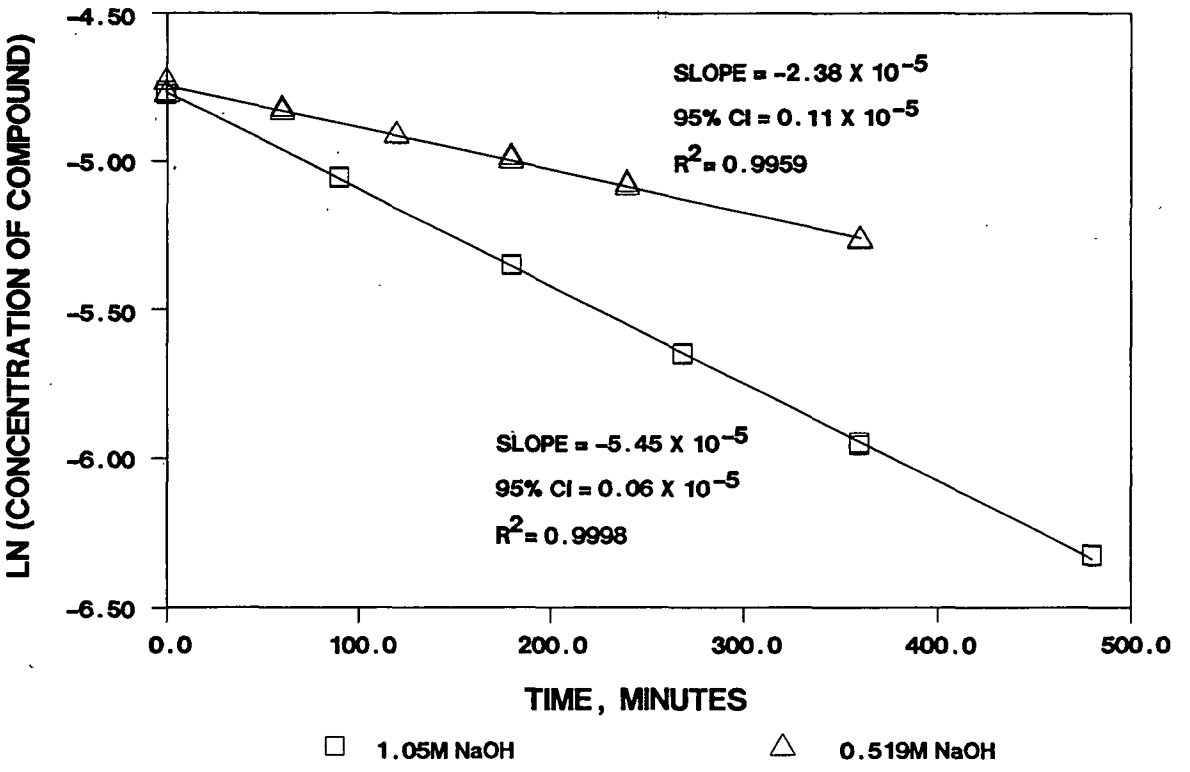

Figure 49. Determination of reaction order for hydroxide ion at 195°C.

analyzed using Eq. (5) to determine the observed rate constant (Fig. 50). The specific rate constant was calculated from the observed rate constant using Eq. (6). This data is tabulated in Table 14. The average value for k_{HS} is 125 (± 5) x 10^{-5} sec^{-1}.

Table 14. Degradation of 2 in a sodium sulfide solution at 195°C.

Data Set	10^5 x k_{HS}, sec^{-1}
I	128 ± 4
II	126 ± 6
III	120 ± 5

Compound 2 appears to react with hydrosulfide ion to form an unstable primary product (8). In a subsequent reaction, compound 8 may react with the starting material to form a dimer 13. This reaction consumes starting material, and thus, would inflate the calculated rate constant of hydro-

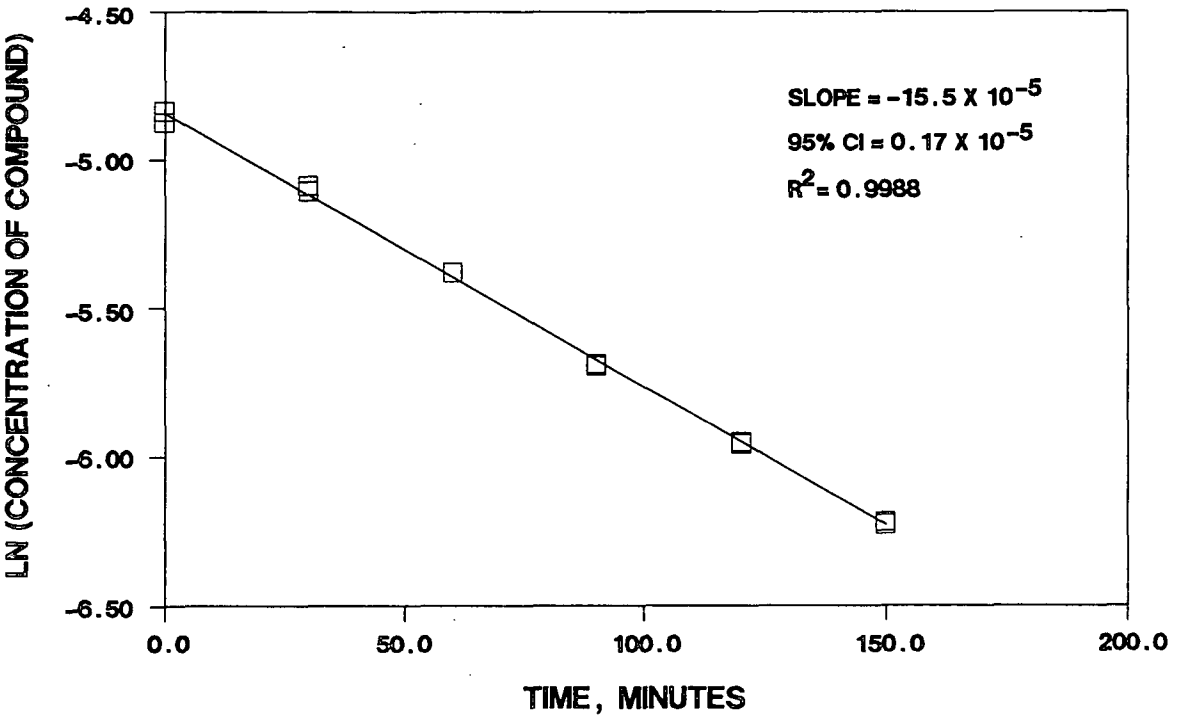

Figure 50. Pseudo-first-order reaction of 2 in 0.958M NaOH & 0.0874M NaSH at 195°C.

sulfide ion. The various reactions occurring were assumed to be those listed in Eq. (9)-(13). Rate expressions, shown in Eqs. (14)-(16), were derived to determine the true rate constant for hydrosulfide ion. In Eq. (15), d[8]/dt is approximately zero using a steady state approximation.[60]

$$2 + HO^- \xrightarrow{k_{HO}} 7 + 10 \quad (9)$$

$$2 + HS^- \xrightarrow{k_{HS}} 8 + 10 \quad (10)$$

$$2 + 8 \xrightarrow{k_{Dimer}} 13 + 10 \quad (11)$$

$$8 \xrightarrow{k_{16}} 16 \quad (12)$$

$$8 \xrightarrow{k_{17}} 17 \quad (13)$$

$$d[2]/dt = -k_{HO}\,[2]\,[HO^-] - k_{HS}\,[2]\,[HS^-] - k_{Dimer}\,[2]\,[8] \quad (14)$$

$$d[8]/dt = \{k_{HS}\,[2]\,[HS^-] - k_{Dimer}\,[2]\,[8] - k_{16}\,[8] - k_{17}\,[8]\} \approx 0 \quad (15)$$

$$d[13]/dt = k_{Dimer}\,[2]\,[8] \quad (16)$$

Compound 13 was quantified in two of the three reactions described in Table 14. These data and the corresponding data from the disappearance of 2 were plotted as concentration-time pairs and fit in a quadratic equation (Fig. 51). The derivatives of these equations were used to determine d[2]/dt and d[13]/dt at various times throughout the degradation. Substitution of Eq. (16) into Eq. (14) resulted in determination of k_{HS}. The results from the two sets of data were averaged to give a value for k_{HS} of 106 x 10^{-5} sec^{-1}. No confidence intervals were assigned since the analysis resulted in large error values due to dependence on time; a 95% confidence interval of ± 5-10 x 10^{-5} would be expected since the rate constant was reduced by only 15%.

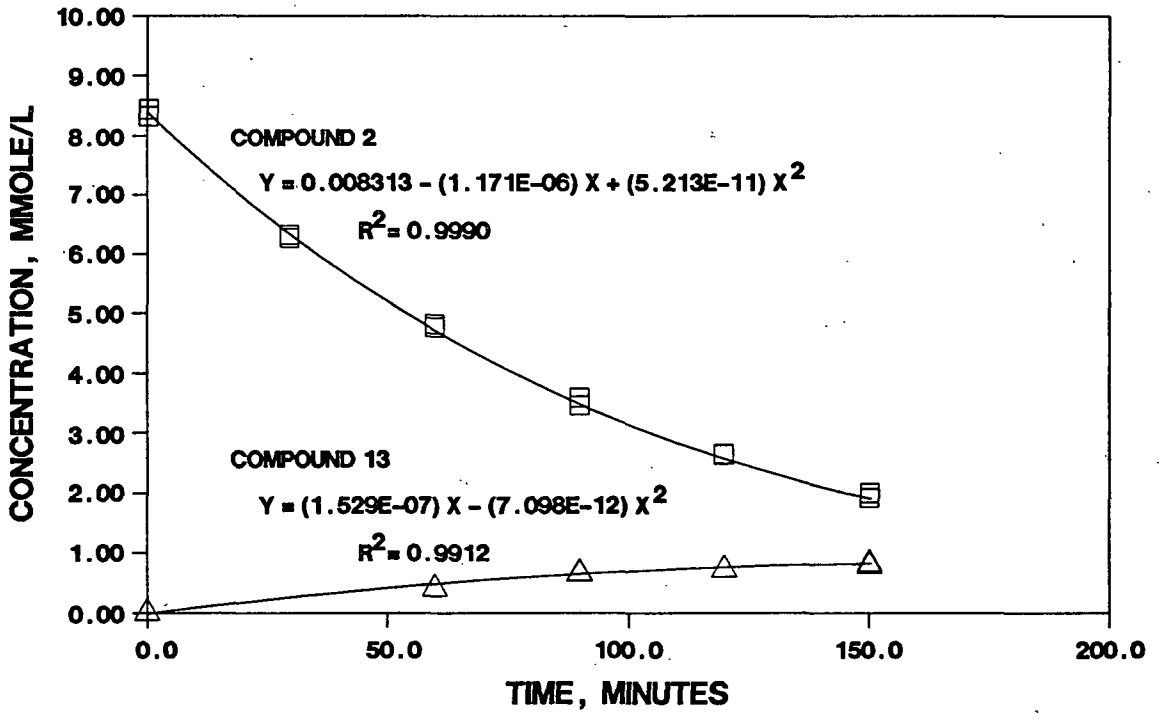

Figure 51. Determination of d[2]/dt and d[13]/dt for calculation of k_{HS} at 195°C.

The effect of sulfoxy species on the degradation of 2 was also investigated. Compound 2 was degraded in one solution containing 0.869M sodium hydroxide and 0.0881M sodium sulfite and in a second solution containing 0.869M sodium hydroxide and 0.0890M sodium thiosulfate. Analysis of the data showed both sulfite and thiosulfate ions were more reactive than hydroxide ion but hydrosulfide ion remained much more reactive (Table 15). The presence of sulfite and thiosulfate ions reduced the average value of the rate constant for hydrosulfide ion to from 106 x 10^{-5} sec^{-1} to 103 x 10^{-5} sec^{-1}.

Table 15. Reaction rate constants of 2 at 195°C.

	Rate constant x 10^5, sec^{-1}
SO_3^{2-}	43.1 ± 12.3
$S_2O_3^{2-}$	47.3 ± 23.2

Data from four degradations of 2 in solutions containing approximately 0.79M sodium hydroxide and 0.087M anthrahydroquinone were used to determine the rate constant associated with anthrahydroquinone ion. The data were analyzed using Eq. (5) to determine the observed rate constant (Fig. 52). The specific rate constant was calculated from the observed rate constant using Eq. (6). This data is tabulated in Table 16. The average value for k_{AHQ} is 89.9 (± 8.5) x 10^{-5} sec^{-1}.

Table 16. Degradation of 2 in a sodium hydroxide/AHQ solution at 195°C.

Data Set	10^5 x k_{AHQ}, sec^{-1}
I	84.8 ± 6.1
II	101.0 ± 7.6
III	83.9 ± 11.9

Rate constants of the reaction of 2 with hydroxide, hydrosulfide, and anthrahydroquinone ions are shown in Table 17. The values were calculated

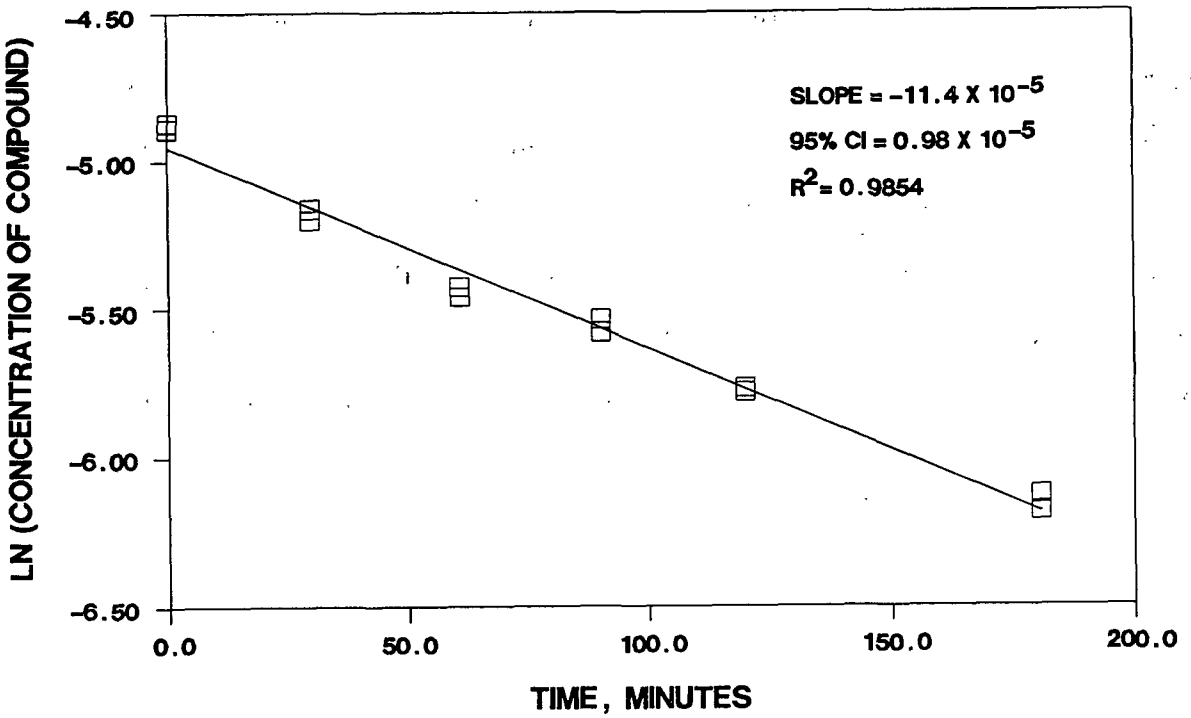

Figure 52. Pseudo-first-order reaction of 1 in 0.785M NaOH & 0.0872M AHQ at 195°C.

using Eqs. (5) and (6). Hydrosulfide and anthrahydroquinone ions were much more nucleophilic toward saturated carbon centers than hydroxide ion.

Table 17. Reaction rate constants of 2 at 195°C.

	10^5 k, sec^{-1}	k_{rel}
NaOH	5.20	1.0
NaSH	103.	19.8
Na_2AHQ	89.9	17.3

SUMMARY

Knowledge of the nucleophilicity of these species toward saturated carbon centers has implication towards understanding the important steps during pulping. The β-aryl ether can be cleaved by a neighboring group mechanism in which the nucleophile is an attached substituent, ie. an alcohol,

not hydroxide ion. The nucleophilicities of alcohols and mercaptans toward saturated carbon centers are known to parallel those of hydroxide and hydrosulfide ions at room temperature.[8] Presumably, the nucleophilicity of substituted anthrahydroquinone ions would be similar to that of anthrahydroquinone. The reactivity of quinonemethide adducts having internal nucleophiles at either the α- or γ-carbon which upon ionization can displace the β-aryl ether during a neighboring group mechanism, therefore, may parallel the nucleophilic order reported in this study.

CONCLUSIONS

The type of substrate under attack has a significant effect on nucleophilic order as demonstrated by hard-soft-acid-base theory. Hydrosulfide and anthrahydroquinone ions were much more reactive than hydroxide ion toward the saturated carbon center in 3-[3′-(α,α,α-trifluoromethyl)phenoxymethyl]benzoic acid. Toward the unsaturated carbon center in *cis*-cinnamic acid, anthrahydroquinone ion was more reactive than hydroxide and hydrosulfide ions. Hydroxide and hydrosulfide ions appear to be similar in nucleophilic strength.

Solvation may also affect the nucleophilicity of these pulping reagents. The enhanced reactivity of hydrosulfide ion with the saturated carbon center compared to hydroxide ion suggests that solvation is still present at pulping temperatures. In addition, the reactivity of hydroxide ion toward *cis*-cinnamic acid relative to anthrahydroquinone and hydrosulfide ions decreased at a lower reaction temperature. This may suggest that hydroxide ion was becoming increasingly solvated at lower temperatures.

The efficiency of the kraft process appears to be due to the reactivity of the ionized sulfide adduct which displaces the β-aryl ether by a neighboring group mechanism. Sulfur species were found to be more nucleophilic toward saturated carbon centers than oxygen species. The neighboring group displacement mechanism involves nucleophilic attack at a saturated carbon center. The resulting sulfur adduct will, thus, react much faster to displace the β-aryl ether because of its greater nucleophilicity.

Hydroxide and hydrosulfide would appear to have a similar reactivity toward quinonemethides. Anthrahydroquinone ion, on the other hand, would be

the most effective reagent in adding to quinonemethides. Its greater nucleophilicity toward a conjugated carbonyl carbon center may explain its effectiveness as a pulping additive in catalytic amounts.

The effectiveness of hydrosulfide and anthrahydroquinone ions appears to be influenced by the concentration of hydroxide ion. At low base concentrations, hydrosulfide and anthrahydroquinone ion may be readily eliminated from the adduct, liberating the nucleophile and a quinonemethide. At high base concentrations, the C_α-substituent (AHQ or HS) will be ionized to a greater extent; the ionized C_α-substituents will be more potent nucleophiles (compared to the unionized forms) and effectively promote neighboring group displacement reactions at the β-carbon. High levels of hydroxide ion, however, could also decrease the efficiency of the additive pulping process since hydroxide ion will compete with the hydrosulfide ion during addition reactions to quinonemethides. The resulting C_α-OH adduct is less able to react via the neighboring group mechanism to displace the β-aryl ether.

EXPERIMENTAL METHODS

GENERAL ANALYTICAL PROCEDURES

Melting points were determined on a Thomas Hoover capillary melting point apparatus which was calibrated against a certified thermometer. Infrared (IR) spectra were obtained using sodium chloride discs on a Perkin-Elmer 700 spectrophotometer. The spectra were referenced to polystyrene film. Nuclear magnetic resonance (NMR) spectra were obtained on a Jeol FX100 Fourier transform spectrometer at 40°C. Deuterated dimethyl sulfoxide was used as the solvent except when noted. All chemical shifts were referenced to internal tetramethylsilane.

Thin layer chromatography (TLC) analyses were performed on microscope slides coated with silica gel (Merck GF-254). Solvent systems used for development are described in the appropriate sections. Components were detected by either exposing the developed chromatograms to iodine, or by spraying the developed chromatograms with methanol:sulfuric acid (4:1, vol.) and then charring on a hot plate (>150°C).

Gas-liquid chromatography (GLC) analyses were performed on a Hewlett-Packard 5890A instrument equipped with a flame-ionization detector and interfaced to a Hewlett-Packard 3392A integrator. Helium was used as the carrier gas (20 mL min^{-1}). The following columns and conditions were used:

(A) OV-17 (3%) on Chromosorb W HP (100-120 mesh) in glass tubing (6 ft x 2 mm) rigged for on-column injection. The operating conditions were: injector, 300°C; detector, 310°C; and column, 100°C for 1 minute, 10° min^{-1} to 200°C, 30° min^{-1} to 300°C, and held at 300°C.

(B) Same as (A) except the temperature program was 130°C for 1 minute, 10° min^{-1} to 250°C, 30° min^{-1} to 300°C, and held at 300°C.

(C) Same as (B) except the initial column temperature was 160°C.

Quantitative GLC utilized internal standards. Molar response factors were calculated using Eq. (15):

$$F_X = A_r M_r \tag{15}$$

where F_X = response factor of compound x relative to the internal standard

A_r = ratio of the internal standard peak area to that of compound x

M_r = mole ratio of compound x to internal standard

Values for response factors were determined by subjecting solutions of known ratios to the appropriate workup and analytical procedure. The response factors were calculated as the average of the values obtained. Retention times and response factors for these analyses are given in Table 18.

Mass spectroscopy (MS) was performed on a Hewlett-Packard 5985 instrument. Spectra for individual components were obtained by either GLC-MS or direct insertion probe-MS (DIP-MS). Separation by GLC was typically performed on OV-17 (3%) on Chromosorb W HP (100-120 mesh) in glass tubing (6 ft x 2 mm) rigged for on-column injection. Conditions were similar to those described above. The GLC-MS interface was maintained at 250°C. Electron impact (EI) MS utilized helium as the carrier gas (30 mL min^{-1}), a source temperature of 200°C, and an ionizing voltage of 70 eV. Negative chemical ionization (NCI) MS utilized methane as the carrier gas (30 mL min^{-1}), a source temperature of 100°C, and an ionizing voltage of 230 eV. Programming conditions of the probe for DIP-MS were 30°C to 350°C at 30° min^{-1}.

Table 18. Gas Chromatographic Retention Times (T_r) and Response Factors (F_x).

Conditions	Compound	T_r, min	F_x
A	Benzaldehyde	1.9	1.77[a]
A	Benzoic acid	3.2	1.04[b]
A	Phenylacetic acid	4.4	1.00[b]
A	Hydrocinnamic acid	5.7	0.872[b]
A	*cis*-Cinnamic acid	6.3	0.912[b]
A	*trans*-Cinnamic acid	7.4	0.924[b]
B	3-Toluic acid	2.2	1.17[c]
B	3-Hydroxybenzoic acid	4.9	1.52[c]
B	3-(α-Hydroxymethyl)benzoic acid	6.3	1.96[c]
B	Isophthalic acid	6.3	1.45[c]
B	3-(α-Mercaptomethyl)benzoic acid	6.7	2.44[c]
B	3-[3′-(α,α,α-Trifluoromethyl)phenoxymethyl]-benzoic acid	10.9	0.894[c]
B	4-Benzyloxybenzoic acid	12.4	1.00[c]
B	3-(3′-Carboxybenzylthiomethyl)benzoic acid	16.8	1.15[c]
B	10-Hydroxy-10-(3′-carboxybenzyl)-9(10*H*)-anthracenone	22.2	1.35[c]
C	3-Trifluoromethylphenol	3.6	1.15[d]
C	4-Isopropylphenol	7.3	1.00[d]

[a]Calculated relative to phenylacetic acid.
[b]As the methyl ester, calculated relative to phenylacetic acid.
[c]As the methyl ester, calculated relative to 4-benzyloxybenzoic acid.
[d]As the benzoate derivative, calculated relative to 4-isopropylphenol.

The amount of dissolved oxygen present in oxygen-free distilled water was determined by treating a water sample (300 mL) with manganese sulfate solution (1 mL) and alkali-iodide-azide reagent (1 mL), followed by concentrated sulfuric acid (1 mL). An aliquot (201 mL) was then titrated against standard sodium thiosulfate solution to the starch endpoint.

Sodium hydroxide concentrations were determined by titration against potassium hydrogen phthalate to the phenolphthalein endpoint.

Sodium sulfide concentrations were determined by titration with 0.100M mercuric chloride followed with an Orion silver/sulfide specific ion

electrode and a Orion 901 ionalyzer.[63] Each sample was titrated until a reading of -450 to -400 mV was reached. This method was found to be as accurate as the fixed increment method of addition where the endpoint was identified by plotting the second derivatives of mV and mL.

Anthrahydroquinone concentrations were determined by quantitative GLC techniques. An solution of anthrahydroquinone in 0.5M sodium hydroxide was filtered in a nitrogen atmosphere through a medium glass-sintered filter to remove any precipitate. A standard aliquot was diluted with oxygen-free distilled water, and aliquots of this solution were used for workup and analysis. Each sample was oxidized by 0.01M potassium permanganate. The internal standard, anthracene (in chloroform), was added to the mixture which was then extracted into chloroform, dried over anhydrous sodium sulfate and partially evaporated. Samples were analyzed using GC under the following conditions: OV-17 (3%) on Chromosorb W HP (100-120 mesh) in glass tubing (6 ft x 2 mm) rigged for on-column injection; injector, 285°C; detector, 300°C; and column, 200°C for 1 minute, 10° min^{-1} to 250°C, 30° min^{-1} to 285°C and held at 285°C. Retention times (min) were: anthracene, 3.1; and anthraquinone, 5.1. The response factor for anthraquinone was determined to be 1.24. There was a solubility limit of 0.20M anthrahydroquinone in 0.5M sodium hydroxide.

SOLUTIONS, REAGENTS AND CATALYSTS

Potassium Hydrogen Phthalate

Reagent grade potassium acid phthalate was dried at 125°C overnight and stored in a desiccator.

Phenolphthalein Indicator

Phenolphthalein (52.8 mg) was dissolved in water-ethanol (50 mL each) solution.

Standard Sodium Hydroxide Solution

A sufficient amount of sodium hydroxide was dissolved in CO_2-free water to prepare a 0.1M solution. The solution was titrated against potassium hydrogen phthalate to the phenolphthalein endpoint.

Standard Hydrochloric Acid Solution

Concentrated hydrochloric acid was diluted to approximately 0.2M and standardized with a standard 0.1M sodium hydroxide solution to the phenolphthalein endpoint.

Oxygen-free Water

Approximately 2 liters of distilled water was placed in a 4 L flask and was boiled until the volume of water had been reduced by approximately one-half. The hot water was then transferred to a 1 L bottle and was degassed with nitrogen until cool, approximately two hours. The bottle was sealed and stored under a nitrogen atmosphere for later use.

Manganese Sulfate Solution

Reagent grade manganese sulfate monohydrate (18.24 g) was dissolved in water with stirring and diluted to 50 mL. The solution was filtered and stored in a glass-stoppered bottle.

Alkali-iodide-azide Reagent

Sodium hydroxide (50.0 g) was dissolved in distilled water. Potassium iodide (15.0 g) was then dissolved in the solution with the aid of heat. The solution was then diluted to 100 mL. A solution of sodium azide (1.0 g) in water (4 mL) was combined with the above solution, and the final solution was stored in a paraffin-lined bottle.

Starch Indicator

Soluble starch (2.0 g) was slurried in water (10 mL) and then slowly added to a solution of salicylic acid (0.20 g) in hot distilled water. The solution was then diluted to 100 mL and stored in a glass-stoppered bottle.

Stock Potassium Biiodate Solution

Potassium biiodate was dried in an oven at 105°C for four hours and cooled in a desiccator. Dried potassium biiodate (8.1233 g) was dissolved in water, diluted to 500 mL (0.5000N) and stored in a glass-stoppered bottle.

Standard Potassium Biiodate Solution

Stock potassium biiodate solution (50.00 mL) was diluted to 1000 mL and stored in a glass-stoppered bottle.

Standard Sodium Thiosulfate Solution

Distilled water was boiled and then allowed to cool. Sodium thiosulfate (3.9542 g) was dissolved in the water and diluted to 1000 mL (0.025N). The solution was stored in an aluminum foil covered glass bottle and chloroform (5 mL) was added as a preservative.

The solution was standardized prior to each use with standard potassium biiodate solution. Potassium iodide (2.0 g) was dissolved in water (100-150 mL). Concentrated sulfuric acid (several drops) and standard potassium biiodate solution (25.00 mL) was added to the solution which was then diluted to approximately 200 mL. The solution was titrated against standard sodium thiosulfate solution to the starch endpoint.

Sodium Chloride

Reagent grade sodium chloride was recrystallized from ethanol:water (2:3, vol.) mixture. Further recrystallizations were accomplished by addition of absolute ethanol.

Sodium 4-Toluenesulfonate

Sodium 4-toluenesulfonate was recrystallized from ethanol:water (5:2, vol.) mixture.[64] Further recrystallizations were accomplished by addition of absolute ethanol.

Sodium Iodide

Reagent grade sodium iodide was dried at 50°C in a vacuum oven for two hours.

Stock Sodium Sulfide Solution

Crystals of reagent grade sodium sulfide nonahydrate were washed in a Buchner funnel under a nitrogen atmosphere. The wet crystals (120 g) were transferred to a beaker containing 200 mL of oxygen-free distilled water. The mixture was stirred until crystals were completely dissolved. This solution was diluted to 500 mL and placed in a parafilm-sealed Nalgene bottle. This

solution was stored under a nitrogen atmosphere. The concentration of sulfide solutions was determined by pipetting known amounts into a solution containing 40 mL of 4M sodium hydroxide, 60 mL of oxygen-free distilled water, and 2.0 g anhydrous sodium sulfite. Each solution was titrated against 0.100M mercuric chloride.[63]

Stock Anthrahydroquinone Solution

Anthrahydroquinone was prepared using a modified method of Dean Smith.[65] All necessary equipment was placed in a glovebag which was then deflated and inflated with nitrogen three times. A solution of sodium hydroxide with known concentration (0.600M) was prepared using oxygen-free distilled water and 30% ultrapure sodium hydroxide. Previously weighed quantities of anthraquinone (5.2 g, 0.025 mol) and sodium dithionite (4.8 g, 0.027 mol) were placed in a beaker with stirbar. To the beaker was added 100 mL of the prepared sodium hydroxide solution; the mixture was stirred for at least two hours, at which time the solution was dark red. The resulting mixture was acidified dropwise with concentrated sulfuric acid to precipitate anthrahydroquinone as a yellow solid. The solid was filtered using a gas dispersion rod and house vacuum to remove the aqueous phase. The solid was washed with distilled water and filtered three additional times. The resulting solid was dissolved in the prepared sodium hydroxide solution and diluted to 100 mL. The solution was then transferred to a flask with stopper, sealed with parafilm and stored under nitrogen until use. The concentration of the solution was determined by quantitative GLC.

Diazomethane

In a 250 mL round bottom flask with clear glass joints was combined 5 g of potassium hydroxide, 8 mL of water, and 25 mL of absolute ethanol in that order. The flask was fitted with a condenser and a 250 mL receiving flask which was placed in an ice water bath. A second receiving flask (50 mL) containing 20-25 mL of diethyl ether was connected in series to the first receiving flask and was placed in the ice water bath also. The reaction flask was then lowered into a water bath heated to 65-70°C. After equilibrium, a 125 mL dropping funnel containing a portion of the solution, 21.5 g Diazald (Aldrich Chem. Co.) in 150 mL of ether, was attached to the top of the reaction flask and added dropwise. All of the solution was added after a period of 50 minutes. An additional 40 mL ether was then added to rinse the system. The collected diazomethane in ether was then labelled and refrigerated for later use.

Benzaldehyde

Reagent grade benzaldehyde was fractionally distilled (b.p. 52-53°C, 3 mm). The initial fraction was discarded, and the remainder was stored in an amber bottle over 4 Å molecular sieves.

Ethyl Bromoacetate

Reagent grade ethyl bromoacetate was fractionally distilled (b.p. 43-44°C, water aspirator). The initial fraction was discarded, and the remainder was stored in an amber bottle over 4 Å molecular sieves.

Activated Zinc

Reagent grade zinc was rinsed with reagents in the following order: 10% sodium hydroxide, 10% acetic acid, water, absolute ethanol, acetone, and diethyl ether. The zinc was then dried in a vacuum oven at 100°C for two hours.

Tetrahydrofuran

Reagent grade tetrahydrofuran was fractionally distilled over lithium aluminum hydride. The initial fraction was discarded, and the remainder was stored in an amber bottle over 4 Å molecular sieves.

Benzil

Reagent grade benzil was recrystallized from carbon tetrachloride.

1,4-Dioxane

Reagent grade 1,4-dioxane was fractionally distilled over lithium aluminum hydride. The initial fraction was discarded, and the remainder was stored in an amber bottle over 4 Å molecular sieves.

Potassium Cyanide

Reagent grade potassium cyanide was dried at 140°C for 48 hours.

SYNTHESIS OF COMPOUNDS

cis-Cinnamic Acid (1)

Ethyl phenylpropiolate (10.0 g, 57.4 mmol) was dissolved in hexane (100 mL). Lindlar catalyst (Aldrich Chemical Co.) (1.0 g) and quinoline (1.0

g) were added to the solution. The mixture was warmed to 50°C ± 5° and flushed with nitrogen. The vessel was then flushed with hydrogen three times and pressurized with hydrogen from a balloon. Hydrogen was added to the balloon as needed. The reaction was monitored by TLC and GC. The reaction was terminated after seven and one-half hours. The mixture was filtered, and the resulting yellow filtrate was extracted with 5% hydrochloric acid solution to remove the quinoline. The hexane layer was dried over anhydrous sodium sulfate, and the solvent was evaporated off using a rotary evaporator. The resulting liquid was vacuum distilled to give 6.8 g (67%) of the desired ester (123-126°C, 3 mm Hg).

The ester (13.6 g) was refluxed in a mixture of 30 mL of 95% ethanol and 120 mL of 10% sodium hydroxide solution for 2 hours. The product mixture was acidified, extracted into diethyl ether, dried and evaporated to yield a solid which was recrystallized three times from hexane to give 8.2 g (44%) of the desired compound as a white crystalline solid: m.p. 58-60.5°C (54-56°C,[46] 67.5-68.0°C[42]); IR (mull) cm^{-1} 3750 (O-H), 1950, 1880, 1810 (Ar-H overtones), 1690 (C=O), and 1630 (C=C); ^{1}H-NMR δ 5.96 (d, J = 12.8 Hz, 1, Ph-C<u>H</u>=CH-COOH), 6.89 (d, J = 12.8 Hz, 1, Ph-CH=C<u>H</u>-COOH), 7.26-7.64 (m, 5, aryl-<u>H</u>), and 12.41 (br s, 0.7, COO<u>H</u>); ^{13}C-NMR δ 120.9 (d, Ph-CH=<u>C</u>H-COOH), 127.8, 128.5, 129.3 (aryl-<u>C</u>), 134.7 (s, C_1), 140.1 (d, Ph-<u>C</u>H=CH-COOH), and 167.1 (s, <u>C</u>OOH); MS m/e 148 (65, M^+), 147 (100), 131 (16), 103 (40), 102 (19), 91 (20), 77 (31), and 51 (15).

<u>Ethyl 3-Hydroxy-3-phenylpropionate</u>

The procedure of Rathke and Lindert[47] yielded 31.0 g (80%) of the desired compound as a yellow-green liquid: 142-145°C, 3 mm Hg.

3-Hydroxy-3-phenylpropionic Acid (3)

Ethyl 3-hydroxy-3-phenylpropionate (5.0 g, 26 mmol) was refluxed in 5% potassium hydroxide solution for 4.5 hours. The product mixture was acidified with 6M hydrochloric acid, extracted into diethyl ether, dried and evaporated. The resulting solid was recrystallized from water to yield 3.3 g (77%) of the desired product as a white solid: m.p. 89.5-91.0°C (92-93°C,[66] 93-94°C[67]); IR (mull) cm^{-1} 3300 (O-H) and 1700 (C=O); ^{1}H-NMR δ 2.55 (d, J = 7.0 Hz, 2, CH_2), 4.96 (t, J = 6.8 Hz, 1, CH), 5.30 (br s, 0.6, OH), 7.1-7.4 (m, 5, aryl-H), and 11.95 (s, 0.7, COOH); ^{13}C-NMR δ 44.5 (t, CH_2), 69.5 (d, CH), 125.6, 126.7, 127.9 (aryl-C), 144.7 (s, C_1), and 171.9 (s, COOH); MS m/e 166 (43, M^+), 107 (100), 79 (70), 77 (53), and 51 (14).

3-Mercapto-3-phenylpropionic Acid (4)

The procedure of Apfeld and Dimmel[48] was modified to produce the desired compound. Ethyl 3-hydroxy-3-phenylpropionate (4.0 g, 21 mmol), thiourea (1.7 g, 23 mmol), and concentrated hydrochloric acid (10 mL) in water (100 mL) were refluxed with stirring for 49 hours. The mixture was then refluxed for an additional six hours following the addition of 50% sodium hydroxide solution (10 mL). The mixture was acidified after cooling, extracted into diethyl ether, dried and evaporated to yield an odorous white solid was recrystallized from water in 1.81 g (45%) yield: m.p. 90-100°C (109°C[68]); IR (mull) cm^{-1} 1710 (C=O); ^{1}H-NMR and ^{13}C-NMR showed presence of impurities; MS m/e 182 (27, M^+), 183 (3, M+1), 184 (1, M+2), 149 (31), 107 (100), 79 (24), 77 (30), 51 (12), 45 (11). GLC-MS showed presence of desired dimethylated product. No attempt was made to further purify the solid.

10-Hydroxy-10-(1-phenyl-3-carboxypropyl)-9(10*H*)-anthracenone Lactone (5A)

10-Hydroxy-10-(1-phenyl-3-oxopropyl)-9(10*H*)-anthracenone hemiacetal[69] (252 mg, 0.737 mmol) was dissolved in acetone (10 mL). A chromic acid solution was prepared by dissolving sodium dichromate dihydrate (242 mg, 0.814 mmol) in water (5 mL) containing concentrated sulfuric acid (0.15 mL, 2.7 mmol). This solution was added to the acetone solution over a period of 15 minutes and then stirred for an additional 21 hours. The resulting mixture was diluted with water, extracted into diethyl ether, dried and evaporated to yield the desired product as a tan solid: m.p. 206-209°C; IR (mull) cm^{-1} 1780 (lactone carbonyl), 1660 (carbonyl), 1600 (aromatic); ^{1}H-NMR (DMSO-d_6) δ 3.06 (d of d, J = 8 and 17 Hz, 1, CH-$CH_{cis}\underline{H}_{trans}$), 3.56 (d of d, J = 13, 17 Hz, 1, CH-$C\underline{H}_{cis}H_{trans}$), 4.03 (d of d, J = 8, 13 Hz, 1, $C\underline{H}$-$CH_{cis}H_{trans}$), 6.22 (d, J = 7 Hz, 2, $C_{2'}$ and $C_{6'}$-$\underline{H}$), 6.89 (t, J = 7 Hz, 2, $C_{3'}$ and $C_{5'}$-$\underline{H}$), 7.05 (t, J = 7 Hz, 1, $C_{4'}$-$\underline{H}$), 7.4-8.2 (m, 8, aryl-$\underline{H}$);[70] ^{13}C-NMR δ 32.1 ($\underline{C}H_2$), 57.4 ($\underline{C}H$), 85.4 ($\underline{C}_{10}$), 124.7, 125.8, 126.4, 126.7, 127.5, 127.7, 128.8, 128.9, 130.2, 130.7, 132.7, 132.9, 133.1, 134.3, 134.4, 139.3, 143.0 (aryl-$\underline{C}$), 175.4 (lactone $\underline{C}$), 181.0 (anthracenone $\underline{C}$);[70] MS m/e 340 (10, M^+), 341 (2, M+1), and 104 (100).

α,β-Dideutero-*cis*-cinnamic Acid (1-α,β-d_2)

The deuterium analog of *cis*-cinnamic acid was synthesized in a similar manner to that described *cis*-cinnamic acid. The reaction vessel was pressurized with deuterium gas and repressurized as deuterium was consumed. Recrystallization yielded 2.2 g (50%) of the desired product as a white crystalline solid: m.p. 64-65°C; IR (mull) cm^{-1} 3750 (H-O), 1950, 1890 and 1820 (aryl-H overtones), 1690 (C=O), and 1610 (C=C); ^{1}H-NMR δ 7.23-7.71 (m, 5, aryl-$\underline{H}$), and 12.41 (s, 0.7, COO$\underline{H}$); ^{13}C-NMR δ 127.6, 128.3, 129.1 (aryl-$\underline{C}$),

134.5 (s, C_1), and 166.9 (s, COOH); MS m/e 150 (74, M^+), 149 (100), 133 (10), and 105 (26).

Benzaldehyde-formyl-*d*

The procedure used was previously described by Burgstahler and co-workers.[71] The reaction mixture was extracted into diethyl ether, washed with 5% sodium carbonate solution, water, and saturated sodium chloride solution, dried over anhydrous sodium sulfate and evaporated. This yielded a yellow liquid which was distilled (65-67°C, 3-5 mm) to give 2.11 g (39%) of the desired product as a liquid: ^{1}H-NMR δ 7.47-8.00 (m, aryl-H) (No peak was observed at $\approx$ 10 ppm which would correspond to ArCHO.).

α,β-Dideutero-*trans*-cinnamic Acid (6-α,β-d_2)

The procedure of Johnson[50] was modified as follows. Benzaldehyde-formyl-*d* (1.01 g, 9.4 mmol), acetic anhydride-d_6 (1.54 g, 14 mmol), and potassium acetate (0.55 g, 5.6 mmol) were refluxed under nitrogen for four hours at which time only a solid remained. The solid was dissolved in diethyl ether and extracted into 1M sodium hydroxide. The basic solution was acidified with 6M hydrochloric acid and extracted into diethyl ether. The resulting product was recrystallized from a 20% ethanol-water solution to yield 0.53 g (37%) of the desired product as white-yellow platelets: m.p. 132.5-133°C; ^{1}H-NMR (DMSO-d_6) δ 6.52 (s, 0.19, Ar-CD=CH-COOH), 7.33-7.76 (m, 5, aryl-H) and 12.30 (br s, 0.8, COOH). Based on the NMR data, approximately 19% of the product was monodeuterated and the remainder, dideuterated. The product was sufficiently deuterated for further experiments. In order to produce fully dideuterated product, deuterated potassium acetate or a catalyst other than potassium acetate should be used.

Methyl α-Bromo-3-toluate

The method described by Fuson and Cooke[72] was used to obtain the desired compound in a yield of 27.2 g (36%): m.p. 40-42.5°C (46-47°C[72]); IR (mull) cm^{-1} 1720 (C=O); ^{1}H-NMR ($CDCl_3$) δ 3.92 (s, 3, O-C$\underline{H}_3$), 4.50 (s, 2, ArC$\underline{H}_2$-Br), and 7.32-8.06 (m, 4, aryl-$\underline{H}$).

3-[3'-(α,α,α-Trifluoromethyl)phenoxymethyl]benzoic Acid (2)

The following procedure was modified from Haslam and co-workers who synthesized similar compounds.[51] Methyl α-bromo-3-toluate (10.0 g, 43.6 mmol) and potassium carbonate (6.7 g, 48.3 mmol) were dissolved in acetophenone (50 mL). The solution was heated to 150°C with stirring. A solution of 3-(α,α,α-trifluoromethyl)phenol (7.8 g, 48.4 mmol) in acetophenone (25 mL) was added dropwise to the heated solution over a period of one-half hour. The mixture was then allowed to react at 150°C for an additional eight hours with stirring. The acetophenone was then removed by steam distillation. The remaining residue was extracted into toluene; the toluene extracts were combined and evaporated.

The resulting liquid was added to a solution containing 10% sodium hydroxide (100 mL) and 95% ethanol (20 mL). The mixture was refluxed for two hours. The product was acidified, extracted into diethyl ether, dried over anhydrous sodium sulfate and evaporated. The resulting solid was recrystallized from 40% methanol in water to yield 9.2 g (71%) of the desired product as a yellow-white solid: m.p. 116-118°C; ^{1}H-NMR δ 5.29 (s, 2, ArC$\underline{H}_2$-O-), 7.26-8.09 (m, 8, aryl-H), and 13.06 (s, 1, COO$\underline{H}$); ^{13}C-NMR δ 69.1 (t, Ar$\underline{C}H_2$-O-), 111.2 (d, $C_{2'}$), 117.1 (d, $C_{6'}$), 118.8 (d, $C_{4'}$), 128.2, 128.5,

128.6, 130.4, 130.9, 131.7 (aryl-C), 136.8 (s, C_3), 158.2 (s, $C_{1'}$), and 166.8 (s, COOH); MS m/e 296 (12, M^+), 135 (100), 89 (7), and 77 (8).

3-(α-Hydroxymethyl)benzoic Acid (7)

The method of Gilman[52] yielded 0.53 g (8%) of the desired product as a yellow-white solid: m.p. 108-110°C (111°C,[73] 114.5-115°C[52]); IR (mull) cm^{-1} 3750 (OH), 1680 (C=O), and 1590 (aryl); ^{1}H-NMR δ 4.59 (s, 2, $ArCH_2$-OH), 5.33 (br s, 1, OH), 7.36-7.96 (m, 4, aryl-H), and 12.89 (br s, 1, COOH); ^{13}C-NMR δ 62.9 (t, $ArCH_2$-OH), 126.9, 127.3, 127.9, 130.3, 130.4 (aryl-C), 142.6 (s, C_3), and 167.0 (s, COOH); MS m/e 152 (72, M^+), 135 (12), 123 (60), 107 (67), 105 (51), 89 (18), 79 (100), and 77 (100).

This compound was also prepared by refluxing a mixture containing methyl α-bromo-3-toluate (4.0 g), concentrated sulfuric acid (6 mL) and water (100 mL) for four hours. The solution was made basic with 10% sodium hydroxide and extracted with diethyl ether to remove any starting material. The aqueous layer was acidified, extracted into diethyl ether, dried, and evaporated to yield a solid. The solid was recrystallized from water to yield 1.79 g of product identified as the above compound: m.p. 110.5-112°C; ^{1}H-NMR δ 4.58 (s, 2, $ArCH_2$-OH), 5.29 (br s, 1, OH), 7.36-7.96 (m, 4, aryl-H), and 12.76 (br s, 1, COOH).

3-(α-Mercaptomethyl)benzoic Acid (8)

The method of Folli and Iarossi[53] yielded 3.7 g (85%) of the desired product as a white solid: m.p. 94-97°C (105-106°C[53]); IR (mull) cm^{-1} 1690 (C=O), and 1580 (aryl); ^{1}H-NMR δ 3.81 (s, 2, $ArCH_2$-SH), and 7.34-7.96 (m, 4, aryl-H); ^{13}C-NMR δ 27.3 (t, ArCH2-SH), 127.3, 128.2, 128.7, 130.9, 132.1

(aryl-C), 141.7 (s, C_3), and 166.9 (s, COOH); MS m/e 168 (45, M^+), 169 (4, M+1), 170 (2, M+2), 135 (100), 89 (11), and 77 (18).

3-(α-Bromomethyl)benzoic Acid

The procedure of Tcheou and co-workers[54] was modified to yield 9.6 g (24%) of the desired product as a white solid: m.p. 151-153°C; ^{1}H-NMR δ 4.78 (s, 2, CH_2), 7.41-8.04 (m, 4, aryl-H), and 12.78 (br s, 0.7, COOH).

3-(3'-Carboxybenzylthiomethyl)benzoic Acid (13)

3-(α-Bromomethyl)benzoic acid (2.0 g, 9.30 mmol) and 3-(α-mercaptomethyl)benzoic acid (1.6 g, 9.45 mmol) were dissolved in 1M sodium hydroxide (40 mL). The solution was refluxed with stirring for 8 hours. The mixture was cooled and acidified with 6M hydrochloric acid, extracted into diethyl ether, dried, and evaporated to yield a solid. The product was recrystallized from 95% ethanol to yield 1.8 g (49%) of the desired product as a yellow-white solid: m.p. 197-198°C (197°C[74]); IR (mull) cm^{-1} 1685 (C=O), and 1610 (C=C); ^{1}H-NMR δ 3.77 (s, 4, CH_2), 7.35-7.90 (m, 8, aryl-H), and 12.94 (br s, 1.3, COOH); ^{13}C-NMR δ 34.8 (t, CH_2), 127.5, 128.2, 129.3, 130.6, 132.8 (aryl-C), 138.4 (s, C_3), and 166.7 (s, COOH); MS m/e 302 (11, M^+), 167 (23), 135 (100), 121 (9), 89 (15), 77 (25), and 45 (12).

10-Hydroxy-10-(3'-carboxybenzyl)-9(10*H*)-anthracenone (9)

The method of Dimmel and Shepard[49] to synthesize AHQ-adducts was used to prepare anthrahydroquinone and the desired adduct. A sufficient quantity of anthrahydroquinone (≈ 10-12 mmol) was prepared under a nitrogen atmosphere. The solid was then dissolved in a mixture containing 30 mL of water and 7.5 mL of 30% sodium hydroxide solution. 3-(α-Bromomethyl)benzoic

acid (2.0 g, 9.3 mmol) was quickly added in solid form to the stirring solution. The solution immediately turned from a red to a tan color. Additional sodium hydroxide was added, and the mixture was heated to 55-60°C for 1 hour and then allowed to cool. The mixture was filtered to remove precipitated anthraquinone. The filtrate was acidified, extracted into diethyl ether, dried over anhydrous sodium sulfate, and evaporated to a yellow solid. Recrystallization from 95% ethanol yielded 1.05 g (33%) of the desired product as a white solid: m.p. 212-215°C; IR (mull) cm^{-1} 3480 (H-O), 1680 (C=O), and 1590 (C=C); ^{1}H-NMR δ 3.22 (s, 2, C$\underline{H}_2$), 6.22 (d of t, J = 1.5 Hz and 7.7 Hz, 1, $C_{4'}$-$\underline{H}$), 6.48 (br s, 0.7, O$\underline{H}$), 6.71 (t, J = 1.5 Hz, 1, $C_{2'}$-$\underline{H}$), 6.93 (t, J = 7.7 Hz, 1, $C_{5'}$-$\underline{H}$), 7.38-8.03 (m, 9, other aryl-$\underline{H}$), and 12.47 (br s, 0.7, COO$\underline{H}$); ^{13}C-NMR δ 54.9 (t, $\underline{C}H_2$), 72.4 (s, C_{10}), 125.1, 126.4, 126.8, 127.0, 127.4, 129.4, 130.3, 130.8, 133.0, 133.9 (aryl-$\underline{C}$), 135.1 (s, $C_{3'}$), 147.1 (s, C_{4a}, C_{5a}), 166.5 (s, $\underline{C}$OOH), and 181.6 (s, C_9); MS m/e 344 (0.2, M^+), 209 (100), 152 (14). Assignment of NMR chemical shifts were aided by assignments given in Ref. 49.

4-Benzyloxybenzoic Acid (12)

The procedure for synthesis of this compound was described by Haslam and co-workers.[51] The resulting product was recrystallized from ethanol to yield 23.6 g (86%) of the desired product as a white crystalline solid: m.p. 191-193°C (188-190°C,[75] 193°C[76]); IR (mull) cm^{-1} 3300-2500 (O-H), 1670 (C=O); ^{1}H-NMR δ 5.18 (s, 2, C$\underline{H}_2$-O), 7.09 (d, J = 9 Hz, 2, C_3 and C_5-$\underline{H}$), 7.40 (m, 5, benzyl ring protons), 7.90 (d, J = 9 Hz, 2, C_2 and C_6-$\underline{H}$), and 12.62 (s, 1, COO$\underline{H}$).

PROCEDURES FOR KINETIC ANALYSIS

Reaction System

The degradation experiments were carried out in a series of 4-mL capacity pressure vessels (bombs) which were made of a 316 stainless steel. A pressure seal was obtained by compressing a Teflon sealing ring (replaced every other degradation run) between the bomb lip and cover with a retaining bolt. Up to 14 bombs were placed on a metal plate which was rotated by a motor and chain-drive system. Rotation was stopped at various times to remove representative bombs.

The bombs and rotation assembly were placed in an oil bath containing UCON Heat Transfer Fluid 500 (Union Carbide). The bath was heated by two 500 watt knife heaters and one 250 watt knife heater. Two heaters were constantly employed while the third was switched by an RTD digital controller with probe (Omega Engineering 4201-PF2 and PR-11-2-100-¼-12½-E). This unit also provided a readout of the bath temperature. The temperature was also monitored using a thermometer which was calibrated against a certified thermometer.

Preparation of Bombs for Reaction

Appropriate amounts of the reactants were weighed in air. The reactants, equipment needed for preparing and dispensing the reaction solutions, and the bombs were placed in the glovebag which was then sealed. The air was replaced with nitrogen using a deflation-inflation cycle repeated three times. Sodium hydroxide solutions used in degradation studies were prepared from ultrapure sodium hydroxide (30% solution) (Alfa Products). All solutions were prepared with oxygen-free water and dispensed by automatic

pipet into bombs. The bombs were then filled, sealed and removed from the glovebag.

Model Compound Degradation

The oil bath was preheated overnight to the desired temperature. The bombs were sealed and removed from the glove bag. The bomb caps were further tightened to minimize chances of leakage. The bombs were placed in a rotating plate, and the assembly was placed in the oil bath. An additional knife heater was used to counteract the subsequent temperature drop until the temperature had risen back to within 0.3°C of the desired temperature. This heatup normally required about 5-8 minutes; a total of 15-30 minutes was allowed for the oil bath to stabilize. After the stabilization period, bombs representing the "0" time were removed from the oil bath and immediately cooled in an ice-water bath. The other bombs were removed and cooled at the desired reaction times. Each bomb was cooled in the ice-water bath for five minutes and then opened. The bomb contents were placed in a 15 mL vial; the bomb was then rinsed with a sodium hydroxide solution which contained internal standard, followed by a second sodium hydroxide solution rinse. These rinsings were added to the vial. The contents of the vial were then worked up depending on analytical procedures needed for the sample.

Methylation of Reaction Mixture Using Diazomethane

Each sample was transferred from its vial to a separatory funnel (125 mL) containing water (10 mL). The solution was then acidified with 6M hydrochloric acid (25 mL) and extracted with diethyl ether (3 x 25 mL). The combined ether extract was dried over anhydrous sodium sulfate (3.0 g). Each ether solution was treated with methanol (1 mL) and diazomethane in ether

solution (2 mL, ≈ 12-50 eq.) for 30-90 minutes. The excess diazomethane and ether was evaporated off using a rotary evaporator to reduce the volume to 1-2 mL. The solution was transferred to an amber vial and diluted to 4-5 mL with rinsings. The samples were then refrigerated until GC analysis.

Benzoylation of Reaction Mixture[32]

Each sample was transferred from its vial to an Erlenmeyer flask (25 mL). Toluene (3 mL), benzoyl chloride (100 μL, 11 eq.) and benzyltributylammonium bromide catalyst (≈ 8 mg) were added to each flask which was then stoppered and stirred for 30 minutes. The aqueous layer was pipetted off, and the toluene layer was rinsed with 1M sodium hydroxide (2 x 3 mL) and water (2 x 3 mL); the contents were stirred for 2 minutes with each wash, and the aqueous layer was then removed. The toluene layer was dried over 2.0 g of anhydrous sodium sulfate for 30 minutes and transferred to an amber vial. All samples were refrigerated until GC analysis.

Methylation of Reaction Mixture Using Dimethyl Sulfate

Each sample (containing ≈ 0.5M sodium hydroxide) was transferred to an Erlenmeyer flask (25 mL). Dimethyl sulfate (1.0 mL, 130 eq.) was added to the sample which was then stirred for 15 minutes. The excess dimethyl sulfate was neutralized by adding concentrated ammonium hydroxide (4.5 mL) and stirring the solution for an additional 15 minutes. The solution was extracted into chloroform (2 x 2 mL). The combined chloroform extract was dried over 2.0 g of anhydrous sodium sulfate and transferred to an amber vial. All samples were refrigerated until GC analysis. This method was less consistent than benzoylation for the analysis of phenolic components and was not routinely used for their determination.

ACKNOWLEDGEMENTS

I would like to thank the Institute of Paper Chemistry, its member companies, faculty, staff and students, for the opportunity to pursue my graduate education here. Special thanks go to LeRoy Borchardt, Glen Yates, Art Webb, and Connie Weber whose analytical services were invaluable to my thesis.

I would also like to thank the members of my thesis advisory committee, Dr. Don Dimmel, Dr. Earl Malcolm, and Dr. Leo Schroeder, for their thought-provoking discussions and guidance. Special thanks go to Don Dimmel, who served as my advisor, for his friendship, patience, and encouragement.

Finally, I would like to thank my wife, Julie, for her never-ending love, understanding, and support, and my son, Christopher, who through his struggles and recovery has helped me put my life back into perspective.

REFERENCES

1. American Paper Institute. 1987 Statistics of Paper, Paperboard, and Wood Pulp. New York, American Paper Institute, 1987:33.

2. Bryce, J. R. G. In Pulp and Paper: Chemistry and Chemical Technology. Casey, J. P. (Ed.). 3rd ed. New York, John Wiley and Sons, Inc., 1980:I,377-492.

3. McGinnis, G. D.; Shafizadeh, F. In Pulp and Paper: Chemistry and Chemical Technology. Casey, J. P. (Ed.). 3rd ed. New York, John Wiley and Sons, Inc., 1980:I,1-38.

4. Sjöström, E., Tappi 60(9):151-4(1977).

5. Glasser, W. G. In Pulp and Paper: Chemistry and Chemical Technology. J. P. Casey (Ed.). 3rd ed. New York, John Wiley and Sons, Inc., 1980:I,39-111.

6. Gierer, J., Holzforschung 36:43-51(1982).

7. Holton, H., Pulp Paper Can. 78:T218-23(1977).

8. March, J. Advanced Organic Chemistry: Reactions, Mechanisms and Structure. 2nd ed. New York, McGraw-Hill Book Co., 1977.

9. Swain, C. G.; Scott, C. B., J. Am. Chem. Soc. 75:141-7(1953).

10. Wells, P. R., Chem. Rev. 63:171-219(1963).

11. Edwards, J. O.; Pearson, R. G., J. Am. Chem. Soc. 84:16-24(1962).

12. Pearson, R. G., J. Am. Chem. Soc. 85:3533-9(1963).

13. Klopman, G., J. Am. Chem. Soc. 90:223-34(1968).

14. Ritchie, C. D., J. Am. Chem. Soc. 105:7313-8(1983).

15. Pearson, R. G., J. Org. Chem. 52:2131-6(1987).

16. Parker, A. J., Chem. Rev. 69:1-32(1969).

17. Gilbert, F. A., Jr. Mechanisms of High Temperature Alkaline Degradation of Methyl α-*D*-Glucopyranoside and 1,6-Anhydro-β-*D*-glucopyranose. Doctoral Dissertation. Appleton, WI, The Institute of Paper Chemistry, 1975. 97 p.

18. Blythe, D. A. An Investigation of the Role of Sodium Sulfide in Cellulosic Chain Cleavage During Kraft Pulping. Doctoral Dissertation. Appleton, WI, The Institute of Paper Chemistry, 1984. 151 p.

19. Smith, D. A.; Dimmel, D. R., J. Wood Chem. Technol. 4:75-90(1984).

20. Brauman, J. I.; Olmstead, W. N.; Lieder, C. A., J. Am. Chem. Soc. 96:4030-1(1974).

21. Bohme, D. K.; Mackay, G. I.; Payzant, J. D., J. Am. Chem. Soc. 96:4027-8(1974).

22. Olmstead, W. N.; Brauman, J. I., J. Am. Chem. Soc. 99:4219-28(1977).

23. Asubiojo, O. I.; Brauman, J. I., J. Am. Chem. Soc. 101:3715-24(1979).

24. Bohme, D. K.; Mackay, G. I., J. Am. Chem. Soc. 103:978-9(1981).

25. Adler, E., Wood Sci. Technol. 11:169-218 (1977).

26. Miksche, G. E., Acta Chem. Scand. 26:4137-42(1972).

27. Gierer, J.; Ljunggren, S., Sv. Papperstidn. 82:503-12(1979).

28. Gierer, J.; Ljunggren, S., Sv. Papperstidn. 86:R100-6(1983).

29. Gierer, J., Wood Sci. Technol. 14:241-66(1980).

30. Axegård, P.; Wikén, J.-E., Sv. Papperstidn. 86:R178-84(1983).

31. Landucci, L. L.; Ralph, J., J. Org. Chem. 47:3486-95(1982).

32. Dimmel, D. R.; Schuller, L. F., J. Wood Chem. Technol. 6:535-64(1986).

33. Dimmel, D. R.; Schuller, L. F., J. Wood Chem. Technol. 6:565-90(1986).

34. Savov, K.; Kiryushina, M. F.; Zarubin, M. Y., Nov. Tselul.-Khartienata. Promst. 16(5):4-5(1986).

35. Dimmel, D. R., J. Wood Chem. Technol. 5:1-14(1985).

36. Fleming, B. I.; Bolker, H. I.; Kubes, G. J.; MacLeod, J. M.; Werthemann, D. P., Tappi 63(11):73-7(1980).

37. Werthemann, D. P., Tappi 65(7):98-101(1982).

38. Dimmel, D. R.; Perry, L. F.; Palasz, P. D.; Chum, H. L., J. Wood Chem. Technol. 5:15-36(1985).

39. Doyle, J. E.; Looney, F. D., Appita 36:219-25(1982).

40. Dimmel, D. R.; Shepard, D., J. Wood Chem. Technol. 2:73-95(1982).

41. Dimmel, D. R.; Schuller, L. F.; Apfeld, P. B., J. Wood Chem. Technol. 7:97-113(1987).

42. Noyce, D. S.; King, P. A.; Kirby, F. B.; Reed, W. L., J. Am. Chem. Soc. 84:1632-5(1962).

43. Reed, G. A., The Nucleophilicity of Hydrosulfide Under Pulping Conditions. Master's Thesis. Appleton, WI, The Institute of Paper Chemistry, 1984. 36 p.

44. Appel, R.; Büchner, W., Justus Liebigs Ann. Chem. 654:1-8(1962).

45. Rao, Y. S.; Filler, R., J. Chem. Soc., Chem. Commun. (12):471-2(1976).

46. Chaloner, P. A., J. Chem. Soc., Perkin Trans. 2 (7):1028-32(1980).

47. Rathke, M. W.; Lindert, A., J. Org. Chem. 35:3966-7(1970).

48. Apfeld, P. B.; Dimmel, D. R., J. Wood Chem. Technol. 2:269-78(1982).

49. Dimmel, D. R.; Shepard, D., J. Org. Chem. 47:22-9(1982).

50. Johnson, J. R. In Organic Reactions. Adams, R.; Bachmann, W. E.; Fieser, L. F.; Johnson, J. R.; Snyder, H. R. (Eds.). New York, John Wiley and Sons, Inc., 1942:I,210-65.

51. Haslam, E.; Haworth, R. D.; Mills, S. D.; Rogers, H. J.; Armitage, R.; Searle, T., J. Chem. Soc.:1836-42(1961).

52. Gilman, H.; Melstrom, D. S., J. Am. Chem. Soc. 70:4177-9(1948).

53. Folli, U.; Iarossi, D., Gazz. Chim. Ital. 99:1306-12(1969); Chem. Abs. 72:110969s(1970).

54. Tcheou, F.-K.; Shih, Y.-T.; Lee, K.-L., J. Chin. Chem. Soc. 17:150-3(1950); Chem. Abs. 47:3254g(1953).

55. Seyferth, D.; Vaughan, L. G., J. Am. Chem. Soc. 86:883-90(1964).

56. Knorr, R.; von Roman, T., Angew. Chem. Int. Ed. Engl. 23:366-8(1984).

57. Zweifel, G.; Murray, R. E.; On, H. P., J. Org. Chem. 46:1292-5(1981).

58. Moore, J. W.; Pearson, R. G. Kinetics and Mechanism. New York, John Wiley and Sons, Inc., 1981:37-82.

59. Laidler, K. J. Reaction Kinetics: Volume II - Reactions in Solution. London, Pergamon Press, 1963:1-83.

60. Meyer, S. L. Data Analysis for Scientists and Engineers. New York, John Wiley and Sons, Inc., 1977:39-48.

61. Olm, L.; Teder, A., Sv. Papperstidn. 89(16):20-2, 25-6 (1986).

62. Crombie, L., Q. Rev., Chem. Soc. 6:101-40(1952).

63. TAPPI Test Method T 694 pm-82.

64. Brandon, R. E. Alkaline Degradation of 1,5-Anhydrocellobiitol. Doctoral Dissertation. Appleton, WI, The Institute of Paper Chemistry, 1973. 164 p.

65. Smith, D. A. The Demonstration of Electron-transfer Reactions and Their Effect on Model Lignin Condensation Reactions Under Alkaline Pulping Conditions. Doctoral Dissertation. Appleton, WI, The Institute of Paper Chemistry, 1986. 115 p.

66. Cohen, S. G.; Weinstein, S. Y., J. Am. Chem. Soc. 86:725-8(1964).

67. Noyce, D. S.; Lane, C. A., J. Am. Chem. Soc. 84:1635-8(1962).

68. Tanaka, H.; Yokoyama, A., Chem. Pharm. Bull. 9:66-70(1961).

69. This compound was graciously donated by D. R. Dimmel (see Ref. 49).

70. Analysis performed by Spectral Data Services, Inc., Champaign, IL.

71. Burgstahler, A. W.; Walker, D. E., Jr.; Kuebrich, J. P.; Schowen, R. L., J. Org. Chem. 37:1272-3(1972).

72. Fuson, R. C.; Cooke, H. G., Jr., J. Am. Chem. Soc. 62:1180-3(1940).

73. Langguth, St., Chem. Ber. 38:2062-4(1905).

74. Ehrlich, F., Chem. Ber. 34:3366-77(1901).

75. Cohen, J. B.; Dudley, H. W., J. Chem. Soc. 97:1732-51(1910).

76. Schroeder, D. C.; Schroeder, J. P., J. Org. Chem. 41:2566-71(1976).

APPENDIX I

EXPERIMENTAL DATA*

DEGRADATIONS OF *cis*-CINNAMIC ACID AND RELATED COMPOUNDS

Table 19. Degradation of *cis*-cinnamic acid (1) in 1.06M sodium hydroxide and 0.176M sodium 4-toluenesulfonate at 195.7°C.

Time, minutes	*cis*-Cinnamic acid (1), M	*trans*-Cinnamic acid (6), M	Hydrocinnamic acid, M	Benzaldehyde, M	Benzoic acid, M
0.0	0.00880	0.00080	0.00000	0.00000	0.00000
0.0	0.00900	0.00085	0.00000	0.00000	0.00000
180.0	0.00528	0.00369	0.00000	0.00007	0.00005
180.0	0.00525	0.00386	0.00000	0.00009	0.00005
360.0	0.00319	0.00558	0.00000	0.00020	0.00027
360.0	0.00316	0.00559	0.00000	0.00016	0.00027

$k_r = 4.77 \pm 0.13^{**} \times 10^{-5}$ sec^{-1}

Table 20. Degradation of 1 in 1.06M sodium hydroxide and 0.175M sodium hydrosulfide at 195.7°C.

Time, minutes	*cis*-Cinnamic acid (1), M	*trans*-Cinnamic acid (6), M	Hydrocinnamic acid, M	Benzaldehyde, M	Benzoic acid, M
0.0	0.00901	0.00106	0.00000	0.00000	0.00000
0.0	0.00876	0.00102	0.00000	0.00000	0.00000
180.0	0.00500	0.00399	0.00040	0.00016	0.00007
180.0	0.00495	0.00390	0.00036	0.00013	0.00007
360.0	0.00268	0.00478	0.00124	0.00021	0.00029
360.0	0.00266	0.00445	0.00118	0.00022	0.00031

$k_r = 5.57 \pm 0.21 \times 10^{-5}$ sec^{-1}

---

*All concentrations are reported at reaction temperature. The thermal expansivity of water was taken into account in determining concentrations. The thermal expansivity of the salt solutions were assumed to be similar to that of water.

**Calculated as the 95% confidence interval.

Table 21. Degradation of 1 in 0.552M sodium hydroxide and 0.531M sodium 4-toluenesulfonate at 195.7°C.

Time, minutes	*cis*-Cinnamic acid (1), M	*trans*-Cinnamic acid (6), M	Hydrocinnamic acid, M	Benzaldehyde, M	Benzoic acid, M
0.5	0.00808	0.00044	0.00000	0.00000	0.00000
0.5	0.00791	0.00044	0.00000	0.00000	0.00000
270.0	0.00558	0.00263	0.00000	0.00006	0.00000
270.0	0.00558	0.00255	0.00000	0.00007	0.00000
540.0	0.00379	0.00382	0.00000	0.00022	0.00008
540.0	0.00389	0.00409	0.00000	0.00021	0.00008

$k_r = 2.27 \pm 0.10 \times 10^{-5}$ sec^{-1}

Table 22. Degradation of 1 in 0.536M sodium hydroxide and 0.523M sodium hydrosulfide at 195.7°C.

Time, minutes	*cis*-Cinnamic acid (1), M	*trans*-Cinnamic acid (6), M	Hydrocinnamic acid, M	Benzaldehyde, M	Benzoic acid, M
0.5	0.00816	0.00071	0.00000	0.00000	0.00000
0.5	0.00825	0.00075	0.00000	0.00000	0.00000
270.0	0.00452	0.00356	0.00021	0.00016	0.00002
270.0	0.00458	0.00371	0.00015	0.00016	0.00002
540.0	0.00250	0.00462	0.00074	0.00017	0.00006
540.0	0.00247	0.00453	0.00084	0.00015	0.00005

$k_r = 3.69 \pm 0.07 \times 10^{-5}$ sec^{-1}

Table 23. Degradation of 1 in 0.71M sodium hydroxide at 195.4°C.

Time, minutes	*cis*-Cinnamic acid (1), M	*trans*-Cinnamic acid (6), M	Hydrocinnamic acid, M	Benzaldehyde, M	Benzoic acid, M
0.0	0.00903	0.00053	0.00000	0.00000	0.00000
60.2	0.00812	0.00154	0.00000	0.00000	0.00000
120.4	0.00721	0.00232	0.00000	0.00000	0.00000
179.9	0.00625	0.00307	0.00000	0.00006	0.00001
239.9	0.00562	0.00380	0.00000	0.00009	0.00003
300.1	0.00508	0.00443	0.00000	0.00011	0.00005

$k_r = 3.27 \pm 0.23 \times 10^{-5}$ sec^{-1}

Table 24. Degradation of 1 in 0.91M sodium deuteroxide at 195.4°C.

Time, minutes	*cis*-Cinnamic acid (1), M	*trans*-Cinnamic acid (6), M	Hydrocinnamic acid, M	Benzaldehyde, M	Benzoic acid, M
0.0	0.00852	0.00075	0.00000	0.00000	0.00000
60.2	0.00669	0.00200	0.00000	0.00000	0.00000
120.4	0.00596	0.00321	0.00000	0.00005	0.00000
179.9	0.00499	0.00437	0.00000	0.00010	0.00004
239.9	0.00410	0.00486	0.00000	0.00019	0.00006
300.1	0.00340	0.00539	0.00000	0.00025	0.00014

$k_r = 4.96 \pm 0.50 \times 10^{-5}$ sec^{-1}

Table 25. Degradation of 1 in 1.03M sodium hydroxide at 195.9°C.

Time, minutes	*cis*-Cinnamic acid (1), M	*trans*-Cinnamic acid (6), M	Hydrocinnamic acid, M	Benzaldehyde, M	Benzoic acid, M
0.4	0.00868	0.00068	0.00000	0.00000	0.00000
119.6	0.00607	0.00284	0.00000	0.00005	0.00000
240.6	0.00333	0.00456	0.00047	0.00006	0.00015
360.4	0.00250	0.00552	0.00039	0.00010	0.00030
479.9	0.00204	0.00571	0.00010	0.00025	0.00048

$k_r = 5.25 \pm 1.73 \times 10^{-5}$ sec^{-1}

Table 26. Degradation of α,β-dideutero-*cis*-cinnamic acid (1-α,β-d_2) in 1.03M sodium hydroxide at 195.9°C.

Time, minutes	*cis*-Cinnamic acid, M	*trans*-Cinnamic acid, M	Hydrocinnamic acid, M	Benzaldehyde, M	Benzoic acid, M
0.4	0.00891	0.00064	0.00000	0.00000	0.00000
119.6	0.00639	0.00298	0.00000	0.00007	0.00000
240.6	0.00439	0.00448	0.00000	0.00016	0.00012
360.4	0.00312	0.00580	0.00000	0.00027	0.00028
479.9	0.00219	0.00627	0.00000	0.00032	0.00049

$k_r = 4.90 \pm 0.14 \times 10^{-5}$ sec^{-1}

Table 27. Degradation of 1-α,β-d_2 in 1.19M sodium hydroxide at 193.2°C.

Time, minutes	*cis*-Cinnamic acid, M 1-α,β-d_2	1-β-d	1	*trans*-Cinnamic acid, M 6-α,β-d_2	6-β-d
0.2	0.00874	0.00000	0.00000	0.00008	0.00000
0.2	0.00883	0.00000	0.00000	0.00009	0.00000
4.9	0.00617	0.00240	0.00000	0.00012	0.00003
4.9	0.00565	0.00304	0.00000	0.00011	0.00003
9.9	0.00270	0.00601	0.00000	0.00012	0.00010
9.9	0.00302	0.00563	0.00000	0.00009	0.00011
15.0	0.00140	0.00734	0.00000	0.00009	0.00024
15.0	0.00113	0.00758	0.00000	0.00007	0.00024
19.9	0.00049	0.00766	0.00008	0.00007	0.00033
19.9	0.00050	0.00770	0.00008	0.00007	0.00035
30.1	0.00008	0.00764	0.00032	0.00006	0.00057
30.1	0.00008	0.00769	0.00032	0.00006	0.00057

$k_D = 2.66 \pm 0.21 \times 10^{-3}$ sec^{-1}

Table 28. Degradation of 6-α,β-d_2 in 1.19M sodium hydroxide at 193.4°C.

Time, minutes	*trans*-Cinnamic acid, M 6-α,β-d_2	6-β-d
0.0	0.00752	0.00143
5.0	0.00693	0.00173
9.9	0.00611	0.00250
14.9	0.00551	0.00323
20.0	0.00475	0.00388
30.0	0.00364	0.00482

$k_D = 4.10 \pm 0.43 \times 10^{-4}$ sec^{-1}

Table 29. Degradation of 1-α,β-d_2 in 1.04M sodium hydroxide at 191.8°C.

Time, minutes	*cis*-Cinnamic acid, M 1-α,β-d_2	1-β-d	1	*trans*-Cinnamic acid, M 6-α,β-d_2	6-β-d
0.0	0.00839	0.00000	0.00000	0.00017	0.00000
0.0	0.00841	0.00000	0.00000	0.00015	0.00000
5.3	0.00576	0.00224	0.00000	0.00018	0.00004
9.9	0.00344	0.00438	0.00000	0.00016	0.00012
15.1	0.00208	0.00561	0.00000	0.00013	0.00021
15.1	0.00201	0.00570	0.00000	0.00014	0.00023
20.3	0.00116	0.00654	0.00000	0.00014	0.00037
20.3	0.00115	0.00652	0.00000	0.00013	0.00033
30.1	0.00039	0.00723	0.00016	0.00011	0.00056

Table 30. Degradation of 1-α,β-d_2 in 1.04M sodium hydroxide at 193.4°C.

Time, minutes	*cis*-Cinnamic acid, M 1-α,β-d_2	1-β-d	1	*trans*-Cinnamic acid, M 6-α,β-d_2	6-β-d
0.0	0.00856	0.00000	0.00000	0.00017	0.00000
5.1	0.00579	0.00288	0.00000	0.00021	0.00006
5.1	0.00571	0.00288	0.00000	0.00018	0.00006
10.0	0.00303	0.00557	0.00000	0.00016	0.00017
10.0	0.00295	0.00556	0.00000	0.00016	0.00018
15.3	0.00146	0.00687	0.00000	0.00012	0.00029
15.3	0.00142	0.00693	0.00000	0.00013	0.00030
20.3	0.00073	0.00745	0.00006	0.00010	0.00036
20.3	0.00071	0.00742	0.00007	0.00010	0.00039
30.2	0.00020	0.00752	0.00019	0.00008	0.00059

Table 31. Degradation of 1 in 0.787M sodium hydroxide at 194.2°C.

Time, minutes	*cis*-Cinnamic acid (1), M	*trans*-Cinnamic acid (6), M	Benzoic acid, M
0.3	0.00852	0.00026	0.00000
0.3	0.00850	0.00024	0.00000
89.8	0.00724	0.00133	0.00000
89.8	0.00733	0.00140	0.00000
179.9	0.00602	0.00244	0.00000
179.9	0.00606	0.00244	0.00000
269.9	0.00494	0.00334	0.00000
269.9	0.00468	0.00354	0.00000
359.8	0.00416	0.00403	0.00006
359.8	0.00413	0.00405	0.00006
479.9	0.00328	0.00457	0.00013
479.9	0.00306	0.00450	0.00014

$k_r = 3.47 \pm 0.18 \times 10^{-5}$ sec^{-1}

Table 32. Degradation of 1 in 0.787M sodium hydroxide at 194.8°C.

Time, minutes	*cis*-Cinnamic acid (1), M	*trans*-Cinnamic acid (6), M	Benzoic acid, M
0.2	0.00849	0.00024	0.00000
0.2	0.00856	0.00024	0.00000
90.0	0.00719	0.00139	0.00000
90.0	0.00726	0.00143	0.00000
179.8	0.00613	0.00256	0.00000
179.8	0.00595	0.00262	0.00000
270.0	0.00478	0.00362	0.00006
270.0	0.00469	0.00373	0.00006
360.1	0.00420	0.00413	0.00007
360.1	0.00427	0.00420	0.00009
480.1	0.00324	0.00466	0.00015
480.1	0.00302	0.00469	0.00016

$k_r = 3.47 \pm 0.22 \times 10^{-5}$ sec^{-1}

Table 33. Degradation of 1 in 0.787M sodium hydroxide at 194.8°C.

Time, minutes	*cis*-Cinnamic acid (1), M	*trans*-Cinnamic acid (6), M	Benzoic acid, M
0.1	0.00853	0.00031	0.00000
90.0	0.00715	0.00145	0.00000
90.0	0.00724	0.00152	0.00000
180.1	0.00608	0.00246	0.00000
180.1	0.00596	0.00258	0.00000
269.9	0.00481	0.00354	0.00005
269.9	0.00469	0.00359	0.00005
360.5	0.00431	0.00407	0.00008
360.5	0.00433	0.00417	0.00008
480.2	0.00359	0.00457	0.00014
480.2	0.00320	0.00476	0.00017

$$k_r = 3.20 \pm 0.31 \times 10^{-5}\ sec^{-1}$$

Table 34. Degradation of 1 in 0.385M sodium hydroxide and 0.393M sodium hydrosulfide at 194.7°C.

Time, minutes	*cis*-Cinnamic acid (1), M	*trans*-Cinnamic acid (6), M	Benzoic acid, M
0.2	0.00860	0.00030	0.00000
0.2	0.00846	0.00030	0.00000
90.0	0.00735	0.00127	0.00000
90.0	0.00733	0.00120	0.00000
180.0	0.00647	0.00213	0.00000
180.0	0.00649	0.00207	0.00000
266.9	0.00569	0.00262	0.00000
266.9	0.00576	0.00272	0.00000
359.9	0.00506	0.00316	0.00000
359.9	0.00511	0.00318	0.00000
480.0	0.00419	0.00367	0.00000
480.0	0.00427	0.00378	0.00000

$k_r = 2.39 \pm 0.08 \times 10^{-5}$ sec^{-1}

Table 35. Degradation of 1 in 0.385M sodium hydroxide and 0.393M sodium hydrosulfide at 194.7°C.

Time, minutes	*cis*-Cinnamic acid (1), M	*trans*-Cinnamic acid (6), M	Benzoic acid, M
0.1	0.00820	0.00037	0.00000
0.1	0.00810	0.00036	0.00000
120.0	0.00696	0.00152	0.00000
120.0	0.00688	0.00157	0.00000
239.9	0.00579	0.00255	0.00000
239.9	0.00580	0.00256	0.00000
360.3	0.00495	0.00341	0.00000
360.3	0.00482	0.00340	0.00000
480.0	0.00426	0.00380	0.00000
480.0	0.00426	0.00400	0.00000
600.2	0.00358	0.00407	0.00000
600.2	0.00359	0.00429	0.00000

$k_r = 2.28 \pm 0.06 \times 10^{-5}$ sec^{-1}

Table 36. Degradation of 1 in 0.385M sodium hydroxide and 0.393M sodium hydrosulfide at 194.9°C.

Time, minutes	*cis*-Cinnamic acid (1), M	*trans*-Cinnamic acid (6), M	Benzoic acid, M
0.1	0.00844	0.00032	0.00000
0.1	0.00837	0.00035	0.00000
119.9	0.00698	0.00169	0.00000
119.9	0.00710	0.00160	0.00000
241.1	0.00576	0.00279	0.00000
241.1	0.00575	0.00270	0.00000
359.9	0.00492	0.00351	0.00000
359.9	0.00495	0.00350	0.00000
480.0	0.00403	0.00387	0.00000
480.0	0.00412	0.00398	0.00000
599.7	0.00340	0.00429	0.00000
599.7	0.00338	0.00440	0.00000

$k_r = 2.52 \pm 0.06 \times 10^{-5}$ sec^{-1}

Table 37. Degradation of 1 in 0.393M sodium hydroxide and 0.393M sodium chloride at 194.6°C.

Time, minutes	*cis*-Cinnamic acid (1), M	*trans*-Cinnamic acid (6), M	Benzoic acid, M
0.2	0.00829	0.00020	0.00000
0.2	0.00855	0.00022	0.00000
89.9	0.00777	0.00081	0.00000
89.9	0.00766	0.00080	0.00000
179.8	0.00712	0.00138	0.00000
179.8	0.00715	0.00140	0.00000
270.0	0.00660	0.00194	0.00000
270.0	0.00670	0.00196	0.00000
359.9	0.00609	0.00241	0.00000
359.9	0.00625	0.00248	0.00000
480.0	0.00558	0.00302	0.00000
480.0	0.00551	0.00298	0.00000

$k_r = 1.43 \pm 0.08 \times 10^{-5}$ sec^{-1}

Table 38. Degradation of 1 in 0.870M sodium hydroxide at 195.0°C.

Time, minutes	*cis*-Cinnamic acid (1), M
0.0	0.00890
179.3	0.00661
360.0	0.00450

$k_r = 3.16 \pm 2.88 \times 10^{-5}$ sec^{-1}

Table 39. Degradation of 1 in 0.870M sodium hydroxide and 0.0881M sodium sulfite at 195.0°C.

Time, minutes	*cis*-Cinnamic acid (1), M
0.0	0.00890
179.3	0.00447
360.0	0.00254

$k_r = 5.81 \pm 0.11 \times 10^{-5}$ sec^{-1}

Table 40. Degradation of 1 in 0.869M sodium hydroxide and 0.0890M sodium thiosulfate at 195.0°C.

Time, minutes	*cis*-Cinnamic acid (1), M
0.0	0.00890
179.3	0.00542
360.0	0.00324

$k_r = 4.68 \pm 0.51 \times 10^{-5}$ sec^{-1}

Table 41. Degradation of 1 in 0.399M sodium hydroxide and 0.391M sodium hydrosulfide at 194.5°C.

Time, minutes	*cis*-Cinnamic acid (1), M
0.0	0.00885
59.6	0.00803
119.9	0.00747

$k_r = 2.35 \pm 2.66 \times 10^{-5}$ sec^{-1}

Table 42. Degradation of 1 in 0.793M sodium hydroxide and 0.785M sodium hydrosulfide at 194.5°C.

Time, minutes	*cis*-Cinnamic acid (1), M
0.0	0.00885
59.6	0.00688
119.9	0.00546

$k_r = 6.70 \pm 2.53 \times 10^{-5}$ sec^{-1}

Table 43. Degradation of 1 in 0.401M sodium hydroxide and 0.0873M sodium sulfite at 194.5°C.

Time, minutes	*cis*-Cinnamic acid (1), M
0.0	0.00885
59.6	0.00777
119.9	0.00687

$k_r = 3.53 \pm 0.91 \times 10^{-5}$ sec^{-1}

Table 44. Degradation of 1 in 0.401M sodium hydroxide and 0.175M sodium sulfite at 194.5°C.

Time, minutes	*cis*-Cinnamic acid (1), M
0.0	0.00885
59.6	0.00719
119.9	0.00584

$k_r = 5.78 \pm 1.56 \times 10^{-5}$ sec^{-1}

Table 45. Degradation of 1 in 0.399M sodium hydroxide, 0.391M sodium hydrosulfide, and 0.175M sodium sulfite at 194.5°C.

Time, minutes	*cis*-Cinnamic acid (1), M
0.0	0.00885
59.6	0.00718
119.9	0.00559

$k_r = 6.38 \pm 3.93 \times 10^{-5}$ sec^{-1}

Table 46. Degradation of 1 in 0.440M sodium hydroxide and 0.116M anthrahydroquinone at 195.0°C.

Time, minutes	*cis*-Cinnamic acid (1), M	*trans*-Cinnamic acid (6), M	Benzoic acid, M
0.3	0.00757	0.00086	0.00000
0.3	0.00715	0.00140	0.00000
89.9	0.00621	0.00174	0.00005
89.9	0.00556	0.00234	0.00005
180.1	0.00514	0.00251	0.00014
180.1	0.00503	0.00276	0.00014
270.1	0.00452	0.00288	0.00025
270.1	0.00443	0.00302	0.00026
360.0	0.00406	0.00324	0.00039
360.0	0.00341	0.00385	0.00038
479.8	0.00292	0.00378	0.00056
479.8	0.00302	0.00382	0.00055

$k_r = 3.05 \pm 0.36 \times 10^{-5}$ sec^{-1}

Table 47. Degradation of 1 in 0.437M sodium hydroxide and 0.116M anthrahydroquinone at 195.1°C.

Time, minutes	*cis*-Cinnamic acid (1), M	*trans*-Cinnamic acid (6), M	Benzoic acid, M
0.2	0.00766	0.00076	0.00000
0.2	0.00755	0.00089	0.00000
89.9	0.00639	0.00174	0.00005
89.9	0.00604	0.00183	0.00004
180.1	0.00530	0.00248	0.00013
180.1	0.00513	0.00266	0.00013
269.9	0.00480	0.00281	0.00024
269.9	0.00453	0.00305	0.00025
360.0	0.00411	0.00320	0.00038
360.0	0.00394	0.00341	0.00037
479.9	0.00345	0.00330	0.00056
479.9	0.00335	0.00344	0.00056

$k_r = 2.74 \pm 0.24 \times 10^{-5}$ sec^{-1}

Table 48. Degradation of 1 in 0.435M sodium hydroxide and 0.118M anthrahydroquinone at 194.9°C.

Time, minutes	*cis*-Cinnamic acid (1), M	*trans*-Cinnamic acid (6), M	Benzoic acid, M
0.2	0.00835	0.00054	0.00000
0.2	0.00837	0.00059	0.00000
90.0	0.00668	0.00178	0.00005
90.0	0.00659	0.00185	0.00005
179.9	0.00579	0.00246	0.00013
179.9	0.00556	0.00272	0.00013
270.1	0.00499	0.00297	0.00023
270.1	0.00464	0.00329	
360.0	0.00412	0.00356	0.00036
360.0	0.00394	0.00380	0.00036
479.9	0.00348	0.00386	0.00053
479.9	0.00310	0.00410	0.00051

$k_r = 3.20 \pm 0.26 \times 10^{-5}$ sec^{-1}

Table 49. Degradation of 1 in 0.451M sodium hydroxide and 0.110M anthrahydroquinone at 195.1°C.

Time, minutes	*cis*-Cinnamic acid (1), M	*trans*-Cinnamic acid (6), M	Benzoic acid, M
0.1	0.00866	0.00059	0.00000
0.1	0.00872	0.00070	0.00000
90.1	0.00705	0.00192	0.00005
90.1	0.00649	0.00246	0.00005
179.9	0.00603	0.00271	0.00014
179.9	0.00563	0.00298	0.00016
270.1	0.00540	0.00309	0.00027
270.1	0.00502	0.00341	0.00027
360.0	0.00478	0.00352	0.00042
360.0	0.00460	0.00362	0.00042
479.7	0.00379	0.00398	0.00065
479.7	0.00363	0.00408	0.00064

$k_r = 2.76 \pm 0.35 \times 10^{-5}$ sec^{-1}

Table 50. Degradation of 1 in 0.807M sodium hydroxide at 170.8°C.

Time, minutes	*cis*-Cinnamic acid (1), M	*trans*-Cinnamic acid (6), M	Benzoic acid, M
0.3	0.00982	0.00001	0.00000
960.2	0.00681	0.00272	0.00000
1919.3	0.00498	0.00469	0.00000
2879.9	0.00338	0.00582	0.00000

$k_r = 6.10 \pm 0.71 \times 10^{-6}$ sec^{-1}

Table 51. Degradation of 1 in 0.395M sodium hydroxide and 0.404M sodium hydrosulfide at 170.8°C.

Time, minutes	*cis*-Cinnamic acid (1), M	*trans*-Cinnamic acid (6), M	Benzoic acid, M
0.3	0.00859	0.00013	0.00000
960.2	0.00623	0.00243	0.00000
1919.3	0.00471	0.00433	0.00000
2879.9	0.00314	0.00489	0.00000

$k_r = 5.72 \pm 1.30 \times 10^{-6}$ sec^{-1}

Table 52. Degradation of 1 in 0.481M sodium hydroxide and 0.110M anthrahydroquinone at 170.8°C.

Time, minutes	*cis*-Cinnamic acid (1), M	*trans*-Cinnamic acid (6), M	Benzoic acid, M
0.3	0.00790	0.00046	0.00000
960.2	0.00493	0.00257	0.00000
1919.3	0.00367	0.00342	0.00000
2879.9	0.00268	0.00379	0.00000

$k_r = 6.15 \pm 2.12 \times 10^{-6}$ sec^{-1}

Table 53. Degradation of 1 in 0.348M sodium hydroxide and 0.105M anthrahydroquinone at 194.2°C.

Time, minutes	*cis*-Cinnamic acid (1), M
0.0	0.00883
59.8	0.00772
59.8	0.00780
122.9	0.00704
122.9	0.00698

$k_r = 3.07 \pm 0.61 \times 10^{-5}$ sec^{-1}

Table 54. Degradation of 1 in 0.654M sodium hydroxide and 0.105M anthrahydroquinone at 194.2°C.

Time, minutes	*cis*-Cinnamic acid (1), M
0.0	0.00883
59.8	0.00712
59.8	0.00716
122.9	0.00594
122.9	0.00573

$k_r = 5.59 \pm 0.83 \times 10^{-5}$ sec^{-1}

Table 55. Degradation of 1 in 0.348M sodium hydroxide and 0.0526M anthrahydroquinone at 194.2°C.

Time, minutes	*cis*-Cinnamic acid (1), M
0.0	0.00883
59.8	0.00781
59.8	0.00776
122.9	0.00716
122.9	0.00755

$k_r = 2.34 \pm 1.62 \times 10^{-5}$ sec^{-1}

DEGRADATIONS OF 3-[3'-(α,α,α-TRIFLUOROMETHYL)PHENOXYMETHYL]BENZOIC ACID AND RELATED COMPOUNDS

Table 56. Degradation of 3-[3'-(α,α,α-trifluoromethyl)phenoxymethyl]benzoic acid (2) in 1.23M sodium hydroxide at 196.0°C.

Time, minutes	3-[3'-(α,α,α-Trifluoromethyl)-phenoxymethyl]benzoic acid (2), M	3-(α,α,α-Trifluoromethyl)-phenol (10), M
0.0	0.00608	0.00111
180.0	0.00296	0.00449
365.0	0.00145	0.00615

$k_r = 6.56 \pm 0.74 \times 10^{-5}$ sec^{-1}

Table 57. Degradation of 2 in 1.04M sodium hydroxide at 195.3°C.

Time, minutes	Compound 2, M	Compound 10, M	3-(α-Hydroxymethyl)-benzoic acid (7), M
59.6	0.00622	0.00264	0.00296
120.5	0.00479	0.00408	0.00445
240.2	0.00298	0.00550	0.00686
359.8	0.00183	0.00566	0.00761

$k_r = 6.76 \pm 0.21 \times 10^{-5}$ sec^{-1}

Table 58. Degradation of 2 in 0.515M sodium hydroxide and 0.524M sodium iodide at 195.3°C.

Time, minutes	Compound 2, M	Compound 10, M	Compound 7, M
0.0	0.00825	0.00092	0.00064
59.6	0.00711	0.00219	0.00221
120.5	0.00577	0.00295	0.00332
240.2	0.00406	0.00473	0.00543
359.8	0.00284	0.00452	0.00656

$k_r = 4.98 \pm 0.25 \times 10^{-5}$ sec^{-1}

Table 59. Degradation of 3-(α,α,α-trifluoromethyl)phenol (**10**) in 1.04M sodium hydroxide and 0.174M sodium 4-toluenesulfonate at 195.6°C.

Time, minutes	Compound **10**, M
0.0	0.00918
120.0	0.00733
180.5	0.00709
240.0	0.00626
300.0	0.00619
360.0	0.00558

$k_r = 2.20 \pm 0.54 \times 10^{-5}$ sec^{-1}

Table 60. Degradation of **10** in 1.04M sodium hydroxide and 0.176M sodium hydrosulfide at 195.6°C.

Time, minutes	Compound **10**, M
0.0	0.00918
60.0	0.00832
120.0	0.00746
180.5	0.00720
240.0	0.00635
300.0	0.00478
360.0	0.00431

$k_r = 3.51 \pm 0.96 \times 10^{-5}$ sec^{-1}

Table 61. Degradation of resorcinol in 0.967M sodium hydroxide at 195.5°C.

Time, minutes	Resorcinol, M
0.1	0.00872
119.6	0.00798
239.9	0.00729

$k_r = 1.24 \pm 0.09 \times 10^{-5}$ sec^{-1}

Table 62. Degradation of 2 in 0.955M sodium hydroxide and 0.0895M sodium hydrosulfide at 193.6°C.

Time, minutes	Compound 2, M	Compound 10, M	Dimer 13, M	Isophthalic acid (17), M
0.2	0.00805	0.00101	0.00000	0.00000
15.8	0.00718	0.00204	0.00011	0.00046
30.8	0.00626	0.00276	0.00018	0.00065
45.6	0.00570	0.00358	0.00026	0.00087
60.1	0.00498	0.00421	0.00037	0.00109
120.5	0.00299	0.00481	0.00066	0.00141

$k_r = 13.7 \pm 0.6 \times 10^{-5}$ sec^{-1}

Table 63. Degradation of 2 in 0.862M sodium hydroxide and 0.0878M sodium 3-(α-mercaptomethyl)benzoate (8) at 193.6°C.

Time, minutes	Compound 2, M	Compound 10, M
0.2	0.00407	0.00536
15.8	0.00177	0.00786
30.8	0.00098	0.00818
45.6	0.00063	0.00869
60.1	0.00048	0.00840

$k_r = 59.3 \pm 20.9 \times 10^{-5}$ sec^{-1}

Table 64. Degradation of dimer 13 in 1.04M sodium hydroxide at 193.5°C.

Time, minutes	Dimer 13, M	3-Toluic acid (16), M
0.2	0.00799	0.00003
31.0	0.00879	0.00020
59.9	0.00871	0.00029
119.8	0.00863	0.00061
180.4	0.00837	0.00102
239.4	0.00811	0.00128

Table 65. Degradation of dimer 13 in 0.954M sodium hydroxide and 0.0882M sodium hydrosulfide at 193.5°C.

Time, minutes	Dimer 13, M	3-Toluic acid (16), M
0.2	0.00909	0.00003
31.0	0.00909	0.00012
59.9	0.00850	0.00020
119.8	0.00904	0.00022
180.4	0.00939	0.00028
239.4	0.00869	0.00044

Table 66. Degradation of 2 in 1.05M sodium hydroxide at 193.6°C.

Time, minutes	Compound 2, M
0.1	0.00839
119.9	0.00591
239.8	0.00398

$k_r = 5.19 \pm 2.29 \times 10^{-5}$ sec^{-1}

Table 67. Degradation of 2 in 1.03M sodium hydroxide and 0.00899M dimer 13 at 193.6°C.

Time, minutes	Compound 2, M
0.1	0.00863
119.9	0.00589
239.8	0.00376

$k_r = 5.78 \pm 3.40 \times 10^{-5}$ sec^{-1}

Table 68. Degradation of 2 in 0.519M sodium hydroxide at 194.7°C.

Time, minutes	Compound 2, M
0.5	0.00845
0.5	0.00881
60.1	0.00796
60.1	0.00805
119.8	0.00734
119.8	0.00735
179.8	0.00680
179.8	0.00673
240.1	0.00624
240.1	0.00618
360.4	0.00517
360.4	0.00515

$k_r = 2.38 \pm 0.11 \times 10^{-5}$ sec^{-1}

Table 69. Degradation of 2 in 1.05M sodium hydroxide at 194.7°C.

Time, minutes	Compound 2, M	Compound 10, M
0.3	0.00857	0.00059
0.3	0.00846	0.00059
89.8	0.00637	0.00274
89.8	0.00640	0.00273
180.0	0.00476	0.00405
180.0	0.00475	0.00405
268.8	0.00352	0.00462
268.8	0.00352	0.00465
359.8	0.00262	0.00497
359.8	0.00259	0.00496
480.0	0.00179	0.00511
480.0	0.00180	0.00502

$k_r = 5.45 \pm 0.06 \times 10^{-5}$ sec^{-1}

Table 70. Degradation of 2 in 1.05M sodium hydroxide at 195.0°C.

Time, minutes	Compound 2, M
0.2	0.00888
0.2	0.00865
90.1	0.00659
180.0	0.00492
180.0	0.00491
270.0	0.00364
270.0	0.00365
360.1	0.00262
360.1	0.00269
479.9	0.00182
479.9	0.00183

$k_r = 5.48 \pm 0.09 \times 10^{-5}$ sec^{-1}

Table 71. Degradation of 2 in 1.05M sodium hydroxide at 194.6°C.

Time, minutes	Compound 2, M
0.1	0.00857
0.1	0.00859
89.9	0.00642
89.9	0.00647
180.0	0.00492
180.0	0.00487
270.4	0.00353
270.4	0.00354
359.9	0.00264
359.9	0.00267
480.1	0.00185
480.1	0.00183

$k_r = 5.39 \pm 0.09 \times 10^{-5}$ sec^{-1}

Table 72. Degradation of 2 in 0.958M sodium hydroxide and 0.0872M sodium hydrosulfide at 195.0°C.

Time, minutes	Compound 2, M	Dimer 13, M
0.2	0.00830	0.00000
0.2	0.00841	0.00000
29.8	0.00626	
29.8	0.00631	
60.0	0.00481	
60.0	0.00476	0.00040
89.9	0.00359	0.00065
89.9	0.00347	0.00066
119.9	0.00265	0.00071
119.9	0.00264	
150.1	0.00199	0.00081
150.1	0.00192	0.00079

$$k_r = 16.1 \pm 0.3 \times 10^{-5}\ sec^{-1}$$

$$d[2]/dt = (-1.17 \pm 0.06 \times 10^{-6}) + (5.21 \pm 0.64 \times 10^{-11})t$$
$$d[13]/dt = (1.53 \pm 0.23 \times 10^{-7}) + (-7.10 \pm 2.90 \times 10^{-12})t$$

Table 73. Degradation of 2 in 0.958M sodium hydroxide and 0.0873M sodium hydrosulfide at 194.6°C.

Time, minutes	Compound 2, M	Dimer 13, M
0.1	0.00799	0.00000
0.1	0.00806	0.00000
30.0	0.00626	0.00024
30.0	0.00613	0.00024
60.0	0.00462	
60.0	0.00464	
89.9	0.00345	0.00056
89.9	0.00347	0.00058
119.9	0.00268	0.00065
119.9	0.00265	0.00064
149.9	0.00185	
149.9	0.00192	0.00068

$$k_r = 16.0 \pm 0.5 \times 10^{-5}\ sec^{-1}$$

$$d[2]/dt = (-1.09 \pm 0.06 \times 10^{-6}) + (4.61 \pm 0.61 \times 10^{-11})t$$
$$d[13]/dt = (1.49 \pm 0.05 \times 10^{-7}) + (-8.22 \pm 0.63 \times 10^{-12})t$$

Table 74. Degradation of 2 in 0.958M sodium hydroxide and 0.0874M sodium hydrosulfide at 194.3°C.

Time, minutes	Compound 2, M	Compound 10, M
0.1	0.00764	0.00110
0.1	0.00794	0.00112
30.0	0.00606	0.00300
30.0	0.00616	0.00302
60.0	0.00461	0.00447
60.0	0.00461	0.00442
90.0	0.00337	0.00536
90.0	0.00339	0.00537
120.0	0.00258	0.00601
120.0	0.00260	0.00594
149.9	0.00199	0.00640
149.9	0.00197	0.00630

$k_r = 15.4 \pm 0.4 \times 10^{-5}\ sec^{-1}$

Table 75. Degradation of 2 in 0.869M sodium hydroxide at 195.0°C.

Time, minutes	Compound 2, M
0.0	0.00924
360.0	0.00324

$k_r = 4.85 \times 10^{-5}$ sec^{-1}

Table 76. Degradation of 2 in 0.869M sodium hydroxide and 0.0881M sodium sulfite at 195.0°C.

Time, minutes	Compound 2, M
0.0	0.00924
179.3	0.00384
360.0	0.00153

$k_r = 8.31 \pm 1.02 \times 10^{-5}$ sec^{-1}

Table 77. Degradation of 2 in 0.869M sodium hydroxide and 0.0890M sodium thiosulfate at 195.0°C.

Time, minutes	Compound 2, M
0.0	0.00924
179.3	0.00372
360.0	0.00140

$k_r = 8.72 \pm 2.00 \times 10^{-5}$ sec^{-1}

Table 78. Degradation of 2 in 0.786M sodium hydroxide and 0.0872M anthrahydroquinone at 194.9°C.

Time, minutes	Compound 2, M
0.2	0.00745
0.2	0.00730
30.0	0.00582
30.0	0.00569
60.2	0.00478
60.2	0.00474
90.1	0.00391
90.1	0.00380
120.0	0.00310
120.0	0.00304
179.9	0.00208
179.9	0.00219

$k_r = 11.5 \pm 0.5 \times 10^{-5}$ sec^{-1}

Table 79. Degradation of 2 in 0.776M sodium hydroxide and 0.0802M anthrahydroquinone at 195.0°C.

Time, minutes	Compound 2, M
0.1	0.00730
0.1	0.00722
30.0	0.00567
30.0	0.00551
59.9	0.00452
59.9	0.00440
89.9	0.00345
89.9	0.00365
120.0	0.00284
120.0	0.00292
180.1	0.00194
180.1	0.00194

$k_r = 12.2 \pm 0.5 \times 10^{-5}$ sec^{-1}

Table 80. Degradation of **2** in 0.785M sodium hydroxide and 0.0872M anthrahydroquinone at 194.7°C.

Time, minutes	Compound **2**, M	Compound **10**, M
0.2	0.00766	0.00156
0.2	0.00750	0.00151
29.9	0.00551	0.00314
29.9	0.00572	0.00321
60.7	0.00440	0.00431
60.7	0.00425	0.00426
90.0	0.00377	0.00502
90.0	0.00394	0.00505
120.1	0.00308	0.00562
120.1	0.00312	0.00556
180.7	0.00217	0.00612
180.7	0.00206	0.00598

$k_r = 11.4 \pm 1.0 \times 10^{-5}\ sec^{-1}$